DISSERTATION

THE ROLE OF PHYSICAL AND CHEMICAL PROPERTIES OF SINGLE AND MULTICOMPONENT LIQUID FUELS ON SPRAY PROCESSES, FLAME STABILITY, AND EMISSIONS

Submitted by

Radi Abdulmonem Alsulami

Department of Mechanical Engineering

In partial fulfillment of the requirements

For the Degree of Doctor of Philosophy

Colorado State University

Fort Collins, Colorado

Fall 2019

Doctoral Committee:

Advisor: Bret Windom

Anthony Marchese
Daniel Olsen
Karan Venayagamoorthy

ABSTRACT

THE ROLE OF PHYSICAL AND CHEMICAL PROPERTIES OF SINGLE AND MULTICOMPONENT LIQUID FUELS ON SPRAY PROCESSES, FLAME STABILITY AND EMISSIONS

Ensuring reliable and clean combustion performance of IC engines, such as liquid-fueled gas turbines, is associated to our understanding of the impact of fuel composition and properties, as well as the processes that the liquid fuel experiences, e.g., atomization, vaporization, turbulent mixing, and chemical kinetics, on the combustion efficiency, stability, and emissions. This understanding is a key prerequisite to the development of fuel surrogates and the deployment of alternative jet fuels. Most of the surrogate formulation activities, especially with regard to aviation fuels, have targeted only the gas-phase behavior of the real fuels, often neglecting properties responsible for atomization, vaporization, and fuel/air mixing (i.e., physical properties). In addition, much research has been done to understand the flame stability (e.g., lean blowout limit and flame liftoff height) of gaseous and pre-vaporized fuels. Thus, the optimization of the fuels and the liquid fueled combustion devices, e.g., gas turbines, requires the consideration of the two-phase process and the coupling between the complex physical and chemical processes. This will improve the understanding of the mechanisms that controls flame lean blowout limit and liftoff height of liquid fuels. Therefore, an appropriate surrogates will be formulated and a faster processes to certify the alternative fuels will be achieved.

In this work, the flame stability in spray burner, quantified by flame lean blowout liftoff height, for different single, binary, alternative, and conventional fuels were experimentally measured. The flame behavior from the spray burner was compared to the results which was done using gaseous

flame platform, e.g., counterflow flame burner, to clearly demonstrate the significant importance of two-phase spray processes (i.e., atomization, vaporization, and turbulent mixing) on flame stability. It was found that the atomization process, which can lead to the variation of the droplet size and distribution, has significant impact on flame stability. This is because any change in the droplet size can enhance/diminish the vaporization and mixing processes, and therefore influence the clean and efficient energy conversion process.

In addition, the sensitivity of the fuels properties on flame stability was evaluated to provide an explanation for why certain fuel properties govern flame stability, such as lean blowout and liftoff height. Thus, flame stability mechanisms can be developed. A number of approaches were used in this work to address these issues, such as multiple linear regression analysis, and previously developed correlations. The results indicate the importance of the atomization process (i.e. droplet size) on the vaporization rate and suggest that the liquid fuel fraction entering the flame plays a dominant role in controlling lean blowout limits. Thus, the large droplet and less volatile fuel was the most resistance fuel to flame blowout. The differences in liftoff height was shown to be a result of two-phase flame speed, which accounts for both pre-vaporized fuel reactivity defined by laminar flame speed (SL) and time scales associated with droplet evaporation.

The influence of the physical and chemical properties of different jet fuels on spray process and thus on emissions is also investigated. This is done by measuring soot formation using Laser-Induced Incandescence (LII). The trends in spray flame soot formation are compared to the gas-phase Yield Sooting Index (YSI). Results indicate differences in planar soot distributions amongst the fuels and suggest a significant influence of the atomization and the vaporization processes on mixing and the soot formation.

ACKNOWLEDGEMENTS

I remember the first day I walked to Dr. Windom's office to talk with him about my PhD plan and research. I was worried to start the new degree and afraid to disappoint the people who gave me this opportunity including Dr. Windom. However, I left his office with confidence, as a result of his great attitude and his friendly behavior and therefore I accepted the challenge. This first impression made me excited to start this adventure, and the excitement has only grown as I progressed through my research. For this, I am deeply thankful for my advisor Dr. Bret Windom and for his indispensable guidance, encouragement and support. He has a contagious passion for his work that has been very influential in helping me to find so much fulfillment in combustion research.

I would also like to directly thank my committee members, Dr. Anthony Marchese, Dr. Daniel Olsen, and Dr. Karan Venayagamoorthy, for their time and guidance in this process. Special thanks to Dr. Sang Hee Won at the University of South Carolina for hosting me in his lab to characterize our spray burner using his PDPA laser system, for sharing his knowledge, and for the lessons that I have learned from him about studying problems deeply and explaining the results. I would also like to extend my thanks to his students, Stuart Nates and Dr. Weijing Wang, for their assistance with spray characterization measurements.

I would like to thank King Abdulaziz University, Jeddah 21589, Saudi Arabia and the Saudi Arabian Cultural Mission (SACM) for the scholarship and supporting my studies in the USA.

I also gratefully acknowledge the help, ideas and insights of numerous colleagues at the Chemical Energy Conversion Laboratory and at the Powerhouse, including Stephen Burke, Anish Jadhav, Carson Belknap, Danielle Bartholet, Brye Windell, Stephen Lucas, Saeid Aghahossein Shirazi, Diego Bernardi Bestel, Geet Mohan Padhi, Siddhesh Bhoite, Elizabeth Browne, Jesse

Schulthess, Miguel Valles Castro, and Frank Chan. Special thanks to Brye Windell for his assistance during the experimental measurements.

I would like to thank my American host family “parents”, Bob and Barbara Sample, for hosting me in their house in Denver for a period of 4.5 years, before I moved to Fort Collins. Living with them was fun and life changing experience; I have learned a lot from them.

Above all, I would like to convey my deep gratitude to my parents, wife, sisters, brothers, and friends for their support and unlimited love every day throughout this journey. My parents taught me that with hard work everything is possible. They call me every week or two to encourage me to work harder to accomplish my goal and make them proud. I am also grateful to my wife, Malak Alsulami, for her love and support, and I only can say that I love you and I look forward to the many years to come together. Since my parents are illiterate, my sister, Jawaher Alsulami, was in charge of teaching me at home, when I was in primary school. For this, I would like to express my appreciation and love to her. Without you and the supervision of our parents, I would not be the person I am today.

DEDICATION

To my beloved parents

Abdulmonem Soqaer Alsulami & Nahar Hudhairm Alsulami

TABLE OF CONTENTS

LIST OF FIGURES

CHAPTER 1: Introduction

1.1 Motivation

Around 85% of the world's energy is generated from combustion. In the United States, most of the combustion sources come from burning petroleum, natural gas, and coal [1]. In 2016, the US transportation sectors consumed approximately 29% of the country's energy with 92% of the energy consumed by transportation devices coming from the chemical energy conversion of petroleum with internal combustion engines. This equates to ~13.9 million barrels per day [2]. In the aviation sector, the demand on petroleum is expected to continue. It was predicted that the demand on jet fuels would grow worldwide by 38% from 2008 to 2025 with an average growth rate of 1.9%/year [3]. The reason for the high demand on petroleum is due to the high energy density found in these fuels. For example, a simple calculation can show that the energy released upon the complete combustion of a single teaspoon of gasoline, diesel, or jet fuel is nearly equivalent to the kinetic energy of a 1.5 ton car traveling at 60 MPH [4].

Although fossil fuels have an enormous amount of energy, they contribute to environmental problems, e.g. global climate change, ozone depletion, and subsequent health/ecosystem consequences. Global warming is a result of the accumulation of greenhouse gasses, including methane (CH_4), carbon dioxide (CO_2), nitrous oxide (N_2O), etc., in the atmosphere arising from the combustion of fossil fuels [5, 6]. Furthermore, emissions from the combustion of fossil fuels, e.g. CO, SO_2, NO_X, particulate matter and soot, can be hazardous to human health and harmful to the natural environment.

Because petroleum is not a sustainable source of energy combined with the fact that it is harming our planet, it is desirable to develop new technologies and engine strategies that can reduce fuel consumption and reduce pollutant emissions. This is achieved by converting the

enormous amounts of energy tied to the chemical bonds of the fuel into as much mechanical power as possible. In this light, it becomes important to understand the complex interaction between the processes inside engines and the fuel's properties, as well as the mechanisms inside the engines that can impact the chemical energy conversion processes and emissions. This understanding will ultimately lead to the development of high fidelity simulations capable of predicting the energy conversion process inside an engine, which will be critical in the development of optimal fuel/engine combinations. However, this process is extremely complicated because of the nature of the extreme environment inside these heat engines and the coupling of complex combustion chemistry that results from real fuels.

Recently, special focus has been implemented on optimizing the fuel and the engine in concert with one another to achieve high efficiency low polluting chemical energy conversion, i.e., a DOE sponsored program called Co-optimization of Fuels and Engines (Co-Optima). Along the same line, Saudi Aramco and King Abdullah University of Science and Technology (KAUST) are also cooperating in project called FUELCOM to optimize fuels and engines to achieve the highest efficiency, lowest harmful emissions, and lowest well-to-wheel greenhouse gas emissions.

In addition, a main program called the National Jet Fuels Combustion Program (NJFCP), led by number of agencies and laboratories in the US, focuses on the development of alternative (non-petroleum) jet fuels (AJFs), which are produced from renewable and cleaner sources, such as bio-derived feedstock, and can deliver identical performance to that from petroleum jet fuels [7, 8]. The certification process of AJFs requires the testing of the combustion operability limits (i.e., figures of merit (FOM)) of the fuel, which include lean blowout (LBO) limit, high-altitude relight, and cold-start ignition [7].

To contribute in this effort, my research is focused on answering number of questions including the following: First, what is the role of the atomization and the evaporation processes (spray process) on the energy conversion? This includes the understanding of the impact of preferential vaporization phenomena of multicomponent fuels on the energy conversion and flame stability. Second, what are the properties that we need to emulate in a surrogate or new bio-derived fuel to enable their use in design and practice? The results and knowledge gained from this work will provide critical data required to develop high efficiency, low polluting fuels and energy conversion devices.

1.2 Literature Review

1.2.1 Complex Liquid Fuels

Understanding the effects of fuel composition is one of the key challenges towards the development of new more efficient and less polluting advanced engines. Commercial fuels often

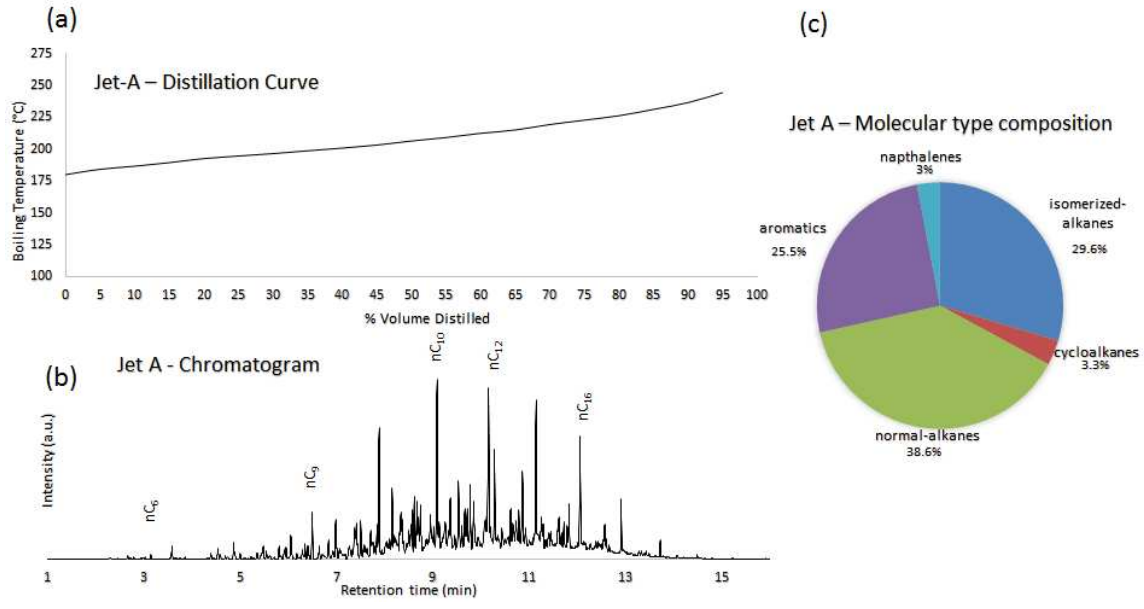

Figure 1.1. Jet-A distillation curve, fuel chromatogram, and hydrocarbon type distribution [10].

utilized in engines, e.g. Jet A, are mixtures that consist of hundreds to thousands of hydrocarbons spanning a wide range of molecular weights and different hydrocarbon families. These differences in molecular weights lead to different effects on the fuel properties, e.g. density, volatility, energy content, and combustion characteristics [9]. For example, a typical jet fuel may span boiling temperatures from 175 to 275 °C (Fig. 1.1a) and contain a high concentration of n-paraffins (e.g. ranging from n-heptane – n-hexadecane, see (Fig. 1.1b)), iso-paraffins, and aromatic species (Fig. 1.1c) [10]. The physical properties, such as density, viscosity and surface tension can be different from one fuel to another, which can impact the atomization and vaporization processes, as will be discussed in the next section.

Moreover, species from different hydrocarbon families have markedly different ignition tendencies, especially at low temperatures (i.e. less than 1000 K) as can be seen in Fig. 1.2a. Normal alkane species demonstrate much faster ignition kinetics (by multiple orders of magnitude) in these low to moderate temperature ranges than aromatics and even iso-paraffin hydrocarbons. Furthermore, the n-alkane species exhibit a strong low temperature ignition phenomenon, which can occur on time scales less than 1 ms at elevated pressures (Fig. 1.2b) and can result in significant change to the reactant composition (Fig. 1.2c), which can influence subsequent combustion phenomenon including flame speeds and flame stability [11].

In addition, the individual components, which make up the complex fuels, can have different soot formation tendencies. For instance, aromatics (e.g. toluene) produces significantly higher soot than n-paraffin fuels (e.g. n-heptane) which can be observed from the difference in the flame luminosity in Fig. 1.3. The reason for this is due to the chemistry and the aromatic ring structure that more easily leads to polycyclic aromatic hydrocarbons (PAHs). The effect of molecular

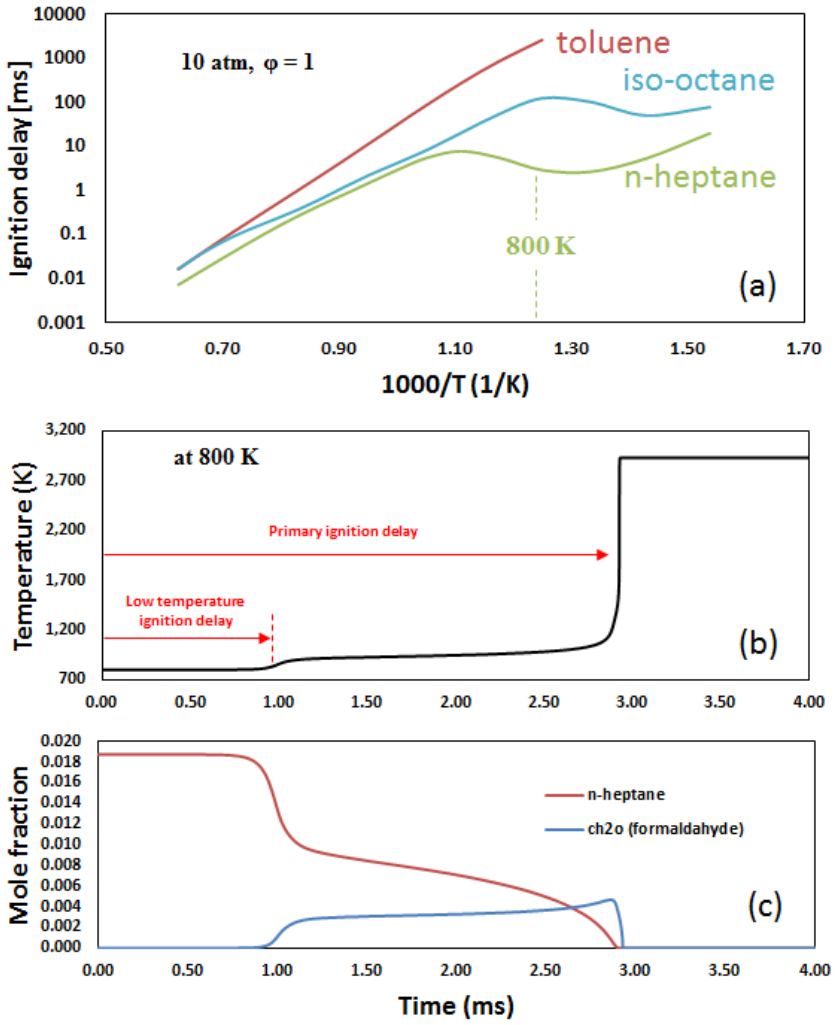

Figure 1.2. Ignition delays for select hydrocarbon types (a), time dependent ignition of n-alkane (b), and the influence of low temperature ignition on reactant species composition (c).

structure on soot formation has been characterized by researchers from Yale University (i.e., yield sooting index (YSI)) and others, e.g. [12-14].

1.2.2 Processes inside IC Engines

In many heat engines, the complex energy conversion process begins with the injection of a liquid petroleum fuel followed by the atomization and vaporization of the fuel, which then must mix with air before finally reacting via combustion converting the chemical energy of the reactants into heat and then work. Each step in this thermodynamic process plays an important role in

Figure 1.3. Flame images of n-heptane and toluene at 50 mL/min and 200 L/min fuel and air flow rates, respectively.

ensuring that the chemical energy is converted to work efficiently with minimal emission of harmful pollutants. The phase change process (i.e. the thermophysical properties of the fuel) can influence the engine's performance just as much as the chemical activity of the fuel. Real application fuels (gasoline, diesel, jet fuel, etc.) contain hundreds of compounds, all with very different thermophysical and chemical properties as discussed above. The importance of phase change process on the energy conversion of a fuel can be seen by looking at a couple applications, namely, a direct injection spark ignition (DISI) engine and a jet turbine.

In DISI engines, the fuel is injected directly into an air-filled combustion chamber rather than in a manifold prior to entering the engine cylinder. DISI has advantages stemming from evaporative cooling effects that can allow for higher mass loading of reactants into the cylinder leading to higher compression ratio and lower risk of knocking [15]. As a result, the fuel efficiency is increased compared to that in port fuel injection (PFI) engines [16]. However, it is critical for the fuel and air to mix prior to the initiation of the spark which commences combustion as a uniform mixture is less likely to auto-ignite (i.e. engine knock) and generate NOx and particulate matter (PM, i.e. soot and unburned hydrocarbons). To ensure a high degree of mixing between the reactants prior to combustion, the fuel needs to be finely atomized promoting vaporization and

preventing impingement of the spray on wall surface interactions. For this reason, gasoline fuels typically are highly volatile. However, modern DISI engines, where time for the air and fuel to mix is reduced compared to port injection strategies, tend to exhibit higher PM emissions [15]. Furthermore, it has been shown that fuels which have a high C/H ratio (e.g. high aromatic content), especially at the tail end of the distillation curve, have a greater tendency to produce PM [15]. Stemming from these results, it is clear that the vaporization process plays a large role in the subsequent combustion process suggesting a fuel with lower volatility and a composition such that the heavier fractions are comprised of compounds with a higher C/H ratio are more likely to produce PM.

In liquid fueled-gas turbines, the complex interaction between atomization, vaporization, turbulent mixing, and chemical kinetics of the fuel impact the combustion/flame stability and therefore the engine efficiency as suggested in previous studies [17-19]. These processes can be

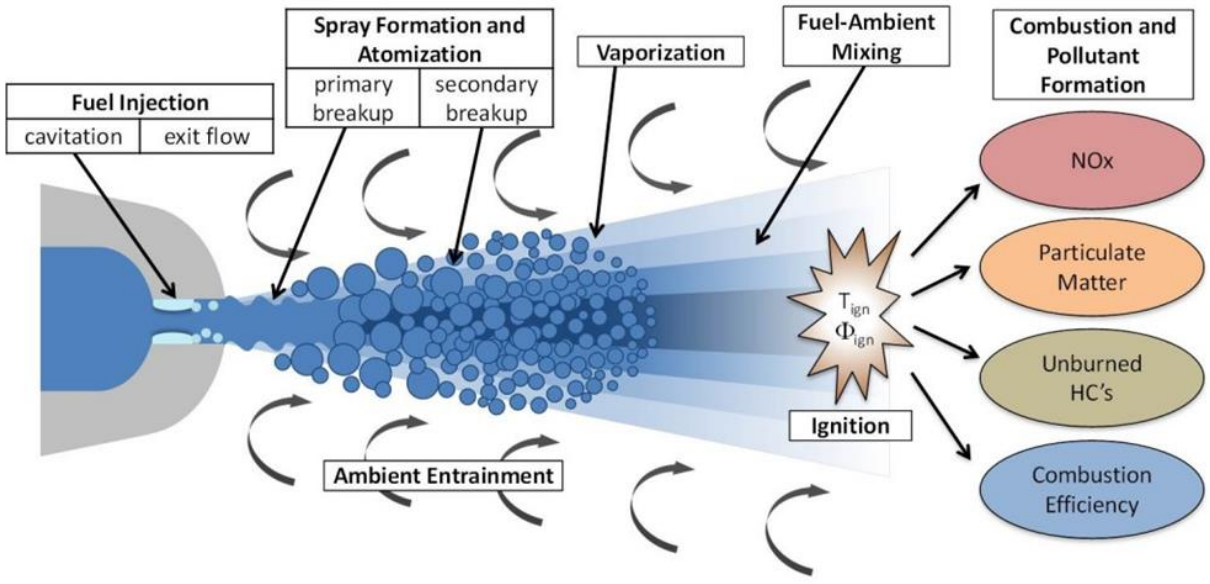

Figure 1.4. Energy conversion process in a liquid fueled turbine combustor. Reprinted from https://www.archie-west.ac.uk/projects/computational-fluid-dynamics/the-cfd-development-of-non-premixed-dual-fuel-combustion-diesel-engine-injected-by-high-pressure-gas-in-the-cylinder-chamber/.

examined by looking at Fig. 1.4. In these engines, the fuel is injected in a compressed high temperature and pressure (e.g. up to 1200 K and pressures up to 40x the ambient pressure [20]) air stream prior to reacting in a highly turbulent stabilized flame.

As such, this requires the evaporation of the fuel and mixing of the reactants prior to the main heat releasing flame [21]. The liquid atomization is a major process in a gas turbine combustion system. Since the liquid fuel that is used in these engines is less volatile than gasoline, e.g. Jet A, it is important that the liquid fuel is atomized to form small droplet sizes to enhance evaporation and ensure efficient energy conversion [20, 21]. Moreover, finer droplet sizes of jet fuel lead to noticeable reductions in CO emissions, unburned hydrocarbons (UHC), and soot formation as mentioned in many works, e.g. [21, 22]. Poor atomization, which can result from a high fuel viscosity, can lead to larger droplet sizes, slower fuel vaporization and thus poorer ignition performance [23].

1.2.3 Fuel atomization process and technology

Fuel atomization, being the first step in the energy conversion process is responsible for the fuel droplet size distribution, trajectories, and velocities and thus can control the degree of fuel/air mixing ahead of the chemical energy conversion step (e.g. stabilized flame, forced ignition, or auto-ignition). Slight differences in the spray and the liquid fuel loading can greatly impact the combustion dynamics/emissions and thus becomes a key component of the process in liquid fuel combustion [24, 25].

The quality of the atomization process is often described using the droplet diameters inside the spray, i.e., the Sauter mean diameter (SMD) [26]. In most cases, it is important that the liquid fuel be atomized to form small SMDs, which enhance evaporation, better mixing between the fuel and the air, and as a result, ensure efficient energy conversion [20, 21]. The spray droplet distribution

(SDD) - a statistical quantity describing the variability of the number of droplets detected by phase doppler particle analyzer (PDPA) in a spray - is another indication of the atomization quality and can also influence the combustion of liquid fuels. For example, Bossard and Peck have shown experimentally that the SDD has a direct influence on the flame structure, burning rates, and emission [27]. They found that narrower SDDs enhanced the efficiency of combustion and heat release.

There are a number of injection technologies, e.g., pressure, rotary, air-assist, and airblast injectors that are generally used to form a spray, which have varying degrees of performance. In general, the atomization/spray process occurs when a bulk liquid transforms into ligaments and then into small droplets in gaseous environment as a result of the pressure drop across the injector. As such, the design and the internal geometry of the atomizer can affect the spray properties (e.g., droplet sizes, velocity, distribution, and penetration). However, for a given injector type, the fuel's physical properties, such as density, viscosity and surface tension, will play an important role in determining the spray properties. These differences in physical properties can be significantly large especially in surrogate fuels when a small number of components are used.

The sensitivity of the spray and atomization properties to a fuel's physical properties can be affected by the nozzle technology that is used, and thus make fundamental studies of two-phase combustion systems difficult. When identical hardware is used to compare two-phase flame behaviors of multiple fuels, it can be difficult to isolate the impacts stemming from differences in the atomization between the fuels from other influences including differences in the vapor liquid equilibrium and chemical activity.

1.2.4 Vaporization Process

The resultant spray properties produced by the atomization process influences the vaporization process by enhancing or worsening the spray droplets vaporization rate. For example, considering initial droplet sizes of n-heptane fuel of 5 and 20 µm at T=1200 K and P = 0.84 atm, using the simple d^2 law, the evaporation times can be estimated as 2.3 and 37 ms, respectively, as illustrated in Fig. 1.5. The sensitivity on evaporation times to initial droplet diameter is attributed to the differences in the surface area:volume ratio and points to the influence of the atomization process (i.e. SMD) on subsequent evaporation and air/fuel mixing steps.

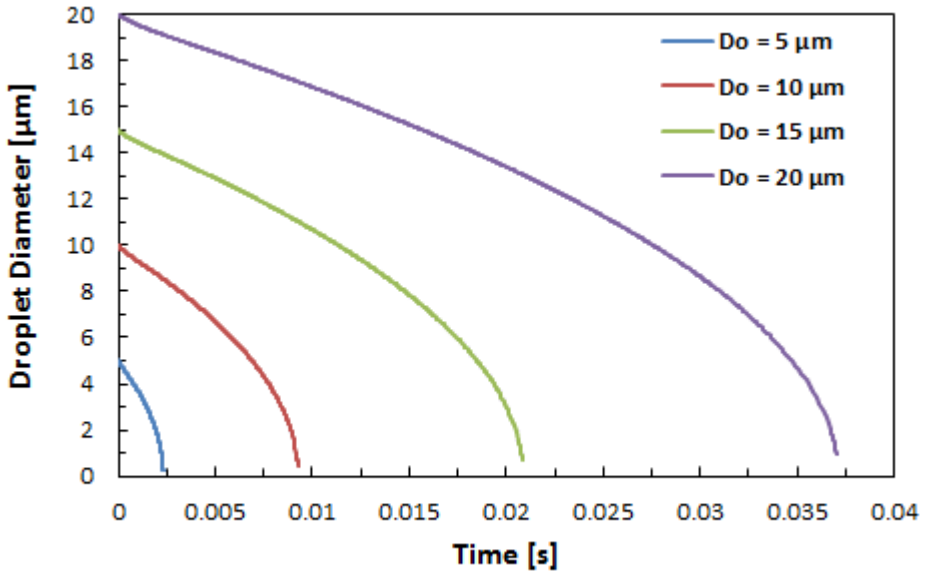

Figure 1.5. Life times for four different droplet sizes calculated using d^2 law.

For single fuels, the amount of fuel vapor produced by the vaporization process can influence the mixing process, and thus the energy conversion process. In multicomponent fuels, e.g., jet fuels, preferential vaporization can occur resulting in vapor composition different from that of the liquid due to the differences in volatility of the multiple species which makeup the fuel [28]. It is important to recognize that the pre-vaporization of liquid fuels for a diffusion flame eliminates the

effect of significant physical phenomena on the energy conversion process, namely atomization and vaporization, including the potential of preferential vaporization for multicomponent fuels. This preferential droplet evaporation can affect the fuel composition distribution within the engine and potentially control the ignition timing, flame phenomenon and pollutant formation [28-32]. As such, ignition may occur much faster or slower than that of the global gas phase ignition delay (of the entire complex fuel), depending on the fuel composition and the relative volatility distribution of the reactive species (e.g. the n-alkanes). The preferential evaporation of the reactive species may undergo low temperature ignition and produce a reactant composition comprised of partially oxidized species, which can affect the flame speed and stability of the turbulent flame [33]. Thus, these phenomena should be considered, in practically, when surrogates or alternative fuels are formulated. In fact, many current surrogate fuels are derived from gas phase flame phenomenon, and they may not emulate the target fuel in a real combustion application.

1.2.5 Surrogate Formation

Conventional fuels are complex and consist of hundreds to thousands hydrocarbon species [34]. As a result, it is challenging to understand the fundamental combustion. Moreover, simulating the combustion aspects of real fuel using detailed numerical simulation is impossible [35]. Therefore, using a small number of single fuels as candidates of the real fuels (also called surrogate fuels) is desirable. Surrogate fuels must emulate both the physical and chemical characteristics of the target real fuel, as well as, injection, vaporization, mixing processes and the combustion behavior [34, 36]. The surrogate fuels should target a number of physical properties, including density, distillation curves, viscosity, and surface tension, as well as, properties describing the chemical reactivity of the real fuel, including, C/H ratio, ignition delay, flame speed, adiabatic

flame temperature, sooting tendency, RON and MON (i.e. for gasoline engines), derived cetane number (DCN), and extinction strain rates (i.e. for gas turbine engines).

Most of the surrogate formulation activities, especially with regard to aviation fuels, have targeted mainly the gas- phase behavior of the real fuels, often neglecting properties responsible for atomization, vaporization, and fuel/air mixing, e.g. [10, 35, 37-45]. For example, a three component surrogate fuel for jet-A POSF-4658, comprised of n-decane, iso-octane, and toluene were chosen by Dooley et al. to reproduce the H/C ratio, and the DCN of the real fuel [35]. Specific combustion properties of the surrogate fuel, e.g. chemical reactivity (low, intermediate temperature and hot ignition kinetic behavior), diffusion flame extinction strain rate, and ignition delays were evaluated using experimental measurements. Dooley et al. emulated the gas-phase combustion of the non-aromatic synthetic S-8 fuel using two components surrogates (e.g. n-dodecane and iso-octane, 51.9/48.1 mole%, respectively) [41]. The surrogated fuel was formulated using certain chemical properties, e.g. C/H molar ratio, DCN, threshold sooting index (TSI), and average molecular weight, and was meant to target number of combustion characteristics, such as ignition delay, laminar flame speed, and extinction strain rate. Dagaut et al. used a jet stirred reactor, a shock tube, and a burner to match the species profiles, ignition delay, and laminar burning velocity of a pre-vaporized surrogate fuel of a Gas-to-Liquid (GtL) Fischer–Tropsch Synthetic kerosene fuel at wide range of temperatures, pressures, and equivalence ratios [44]. The surrogate fuel consisted of n-decane, iso-octane (2,2,4-trimethylpentane), and n-propylcyclohexane. Similarly, Naik et al. emulated GtL fuel by evaluating the gas-phase flame propagation, flame extinction, and NOx emissions of their surrogate fuels, i.e. iso-octane, n-decane, and n-dodecane [45].

Other limited works have used physical surrogate, only targeting the physical properties of the real fuel, e.g. [46-48]. For instance, Huber et al. suggested a seven-component surrogate fuel to

represent the physical properties of the synthetic S-8 fuel [47]. The surrogate fuel was derived from distillation curve, density, viscosity, speed of sound, and thermal conductivity properties of the S-8 fuel. Furthermore, Huber et al. developed, in a later work, a surrogate fuel consisting of five-components based on the equation of state (EOS) approach to emulate the distillation curve of S-8 fuel [46].

However, there have been only a few studies which have targeted both physical and chemical properties in the development of surrogate fuels (called comprehensive surrogates), e.g. [49, 50]. Edwards and Maurice developed two surrogates, e.g. physical surrogate and chemical surrogate, for JP-8 fuel [49]. The physical surrogate targeted density, viscosity, surface tension, thermal conductivity, distillation curve, and phase diagram of the real fuel, while the chemical surrogate was developed to have similar chemical composition and the average molecular weight of the target fuel to emulate selected combustion characteristics.

1.2.6 Counterflow Flame

The counterflow burner is a common experimental combustion platform that allows one to measure a number of important flame/combustion properties including the laminar flame extinction and ignition limits [9], laminar flame speeds [51], and flame temperatures and species profiles [51, 52]. Laminar flame extinction in counterflow burner is governed by chemical kinetics, as well as, thermal and mass transport [53]. Thus, extinction occurs when the rate of heat loss from the flame (thermal diffusion) exceeds the rate of heat generation. When the convective mass transport rate is much larger than the reaction rate, the flame destabilizes and extinguishes [54, 55]. In addition to being one of the main tools used in surrogate formulation, the counterflow burner has played a significant role in developing chemical kinetic mechanisms of previous works, e.g. [56-58].

Flame behavior and extinction of pre-vaporized liquid fuels has been studied extensively using counterflow burners to develop fuel surrogates in many works, e.g. [35, 38, 40, 41, 45, 59]. For example, Dooley et al. developed a surrogate fuel for Jet-A POSF-4658 by matching several combustion properties, including the extinction strain rate of both fuels at 500 K and 298 K fuel and oxidizer (air) temperatures, respectively [35]. Later, Dooley et al. used the same experimental approach to formulate a surrogate for S-8 POSF-4734 fuel [41].

1.2.7 Spray Flame Stability

As previously discussed, variety of practical combustion devices, such as gas turbines, DISI and CI engines, and boilers, require the injection of a liquid fuel into a heated environment requiring the fuel to vaporize and mix with the air prior to stabilizing a flame. The heated environment, especially in gas turbine engines, makes the mixing region vulnerable to preferential evaporation and pre-flame reactions, which can affect the downstream turbulent flame. Since gas turbine engine is a continuous-flow machine unlike other IC engines, which work in a cycle, one of the main requirements is that combustion must be stabilize and sustained over a wide range of conditions, such as fuel/air ratios, temperatures, and pressures [21]. Depending on the engine design, the combustion process and flame stabilization technologies vary. However, a common flame stabilization approach is usually implemented in gas turbine engines using a fuel injector coupled with air co-flow [15]. Several techniques are used to enhance the mixing and flame stabilization by using swirl and a bluff body to provide a recirculation region of hot combustion products [15, 21]. As a result, the flame becomes more stable and difficult to blowout.

Recently, a large focus has been implemented on spray flame combustion to understand the processes that real fuels undergo in practical IC engines. Understanding the flame stability and extinction limits, in addition to the factors that influence them, e.g. physical and chemical

properties of the fuel, is desirable and significantly important in determining the combustion efficiency and pollutant emissions in gas turbine engine [20]. Thus, lean blowout limit of conventional and alternative fuels can be determined and tested in spray burners, which can serve as a model for realistic gas turbine or simple laboratory burner. Understanding these limits is important since lean combustion is a key strategy for emission reduction [60]. The lean blowout behavior for spray flames at different air preheated temperature was experimentally predicted by Grohmann et al. for multiple single component fuels, including n-hexane, iso-octane, and n-dodecane [17, 18]. Rock et al. investigated the lean blowout limits of eight liquid fuels, including Jet-A, JP-5, and JP-8 fuels, using a swirl stabilized combustor [19]. O'Loughlin and Masri studied the liftoff height of single component fuels including alcohol and n-alkane fuels [61]. For many of these studies, conclusions were drawn that the processes of atomization, mixing, turbulence, evaporation, and flame chemistry could all influence flame stability limits, and that the effect of different physical and chemical properties of the fuel, such as boiling temperature, enthalpy of vaporization and ignition temperature influence flame liftoff height. Esclapez et al. experimentally investigated the influence of the physico-chemical processes (e.g. evaporation-ignition) of Jet-A (Cat-A2) and two alternative fuel candidates (e.g. Cat-C5 and Cat-C1) on spray formation, droplet evaporation, and lean blowout/flame stability and compared these results using large-eddy simulations (LES) [60]. Their investigation showed that the Cat-C5 differs from Cat-A2 mainly because its physical properties, while the difference for Cat-C1 comes from its chemical properties. Two flame regions were indicated near blowout condition, namely (i) very lean premixed flame that was sustained by the recirculation of hot gases from the diffusion flame, and (ii) diffusion flame around very dense droplet clouds. Their simulation showed that the reduction of the

recirculation temperature slows the evaporation process, which leads to reduced availability of the gaseous fuel, eventually leading to the flame blowout.

Other works have focused on studying the influence of spray burner configuration on flame stability. For example, Liu et al. used a swirl-cup combustor to investigate the effect of the spray characteristics (e.g. orifice diameter) on combustion stability [62]. This work concluded with a relation between the spray characteristic and ignition and flame stabilization. Experimental and simulation characterization of turbulent ethanol spray was done by Düwel et al. by measuring droplet sizes, droplet temperature, liquid phase temperature, and gas phase temperature [63]. The spray burner, which was used in their work, was able to stabilize the flame without the use of a bluff-body or a pilot flame.

The complex flame structure in spray burners is coming from the interaction between the fuel droplet dispersion, evaporation, turbulent flow, and finally the heat released by the flame [58, 64]. Many studies in the literature characterize their burner by measuring and predicting the complex structure of the flame using optical and laser techniques and CFD simulations. For example, a combined experimental and numerical study of a spray jet burner at ambient temperature was performed by Shum-Kivan et al. [65]. In this work, the flame structure and stabilization mechanism where discussed based on results from OH-PLIF and LES. The droplet size distribution and aerodynamics as well as the flame structure of an open burner was investigated using Phase Doppler Anemometry (PDA) and OH-PLIF images by Verdier et al. [66]. Similar investigation was done by Mansour et al. [67]. Many of the studies mentioned above have absorbed a similar flame structure, with an inner wrinkled partially premixed flame front, which enhance the stabilization of the flame, and an outer diffusion flame front. For the droplet distribution, most of works noticed that the bigger droplets are located at the boarder of the spray and the smaller

droplets located in the center. The smaller droplets are responsible for the premixed flame behavior.

Finally, flame stability, e.g. flame liftoff height and blowout limit, using a spray flame can be a powerful tool in fuel surrogate formulation. Thus, to the best of our knowledge, this approach has not been used effectively in surrogate formulation activities. In contrast, the extinction strain rate approach of pre-vaporized liquid fuels has been used extensively, even though it does not reflect the real two-phase energy conversion process that practical fuels experience.

1.2.8 Objective of the Research

The goals of the research are to answer the following questions which will help in the effort of co-optimizing fuels and engines, and thus designing the next generation of high efficiency less pollutant power plants that operate on liquid fuels;

I. **What is the role of the atomization and the evaporation processes (spray process) on the energy conversion?**

This includes the understanding of the impact of droplet size distribution, evaporation, and chemical kinetics on flame stability. For fuel mixtures, the impact of preferential vaporization phenomenon on flame stability will also be included in the investigation.

II. **What are the properties that we need to emulate in the surrogate fuels to make sure that we capture the coupled physical/chemical behaviors of the real fuel?**

This understanding will ultimately lead to higher fidelity simulations that can be used toward the co-development of advanced engines and the fuels, with optimal combustion and physical properties, to maximize energy conversion efficiency and minimize associated emissions. Thus, the research goals are to be achieved by implementing the following steps:

1. **Designing and constructing a spray burner to simulate the multi-step energy conversion process experienced by liquid fuels in steady fueled IC engines (e.g. gas turbines).**

The final burner design leveraged previous research [63, 66-68], CFD simulation, and a prototype burner to optimize the design. This allowed us to investigate the optimal exit area of air co-flow with respect to the fuel flow rates provided by available commercial spray nozzles, which can help in stabilizing the flame without excess recirculation.

2. **Investigating the influence of the different physical and chemical properties of multiple single liquid fuels on the combustion/flame behavior and stability.**

Prior to studying the impact of preferential fuel evaporation effects on the energy conversion of multi component fuels. It is desirable to conduct experimental measurements of single component fuels to provide the baseline understanding regarding the role of fuel physical and chemical properties on ignition and flame stability. That is done in this task by using different hydrocarbon fuels from different families, including iso-octane, n-heptane, n-dodecane, toluene, and 1,2,4-trimethylbenzene (TMB). These selected fuels exhibit a wide range of physical and chemical properties.

3. **Investigating the influence of varying fuel and air flow rates on the spray properties and the flow field turbulence.**

This is explored by measuring the droplet sizes and velocities of the spray at different radial and axial positions of n-heptane fuel under nonreacting conditions (i.e. a cold spray). In addition, the turbulence intensity and the liquid spray droplet distribution are quantified for different fuel and air flow rate conditions. The measurements are obtained by using Phase Doppler Particle Analyzer/Laser Doppler Velocimetry (TSI PDPA/LDV) at P = 1 atm and T = 298 K.

4. **Understanding the influence of the atomization (i.e., SMD and SDD) on flame stability.**

This is achieved by measuring the liftoff height and blowout limit for n-heptane using different spray nozzle sizes. The use of different nozzle sizes results in variations of droplet sizes and as a result, the atomization effect on flame stability can be noticed.

5. **Understanding the Influence of the spray process including vaporization (preferential vaporization of multicomponent fuels) and the variation in fuels' properties on the combustion/flame behavior and stability of multicomponent, alternative, and conventional fuels.**

   This is to be investigated using two approaches:

   I. By comparing the flame stability and behavior of two binary mixtures in two apparatus, the gas phase Counterflow Burner and the Spray Flame Burner.

   II. By investigating the relative influence of the fuel's properties on flame lean blowout (LBO) and liftoff height (LOH)

6. **Exploring the influence of two-phase spray process on soot formation of liquid jet fuels.**

This aims to highlight the importance of accounting for the influence of the two-phase spray process on the soot development of jet fuels. The soot formation was determined using Laser-Induced Incandescence technique (LII). The results from the two-phase combustion system are compared to the gas-phase Yield Sooting Index (YSI) to highlight the influences from the spray/vaporization process on soot formation.

The dissertation is organized in eight chapters based on published, submitted, and under preparation manuscripts. These works (from Chapter 2 to Chapter 7) share much of the same methods and introductory materials and thus the reader may find some repetition in the text. The dissertation is organized such that each new chapter relies on the outcomes of the previous section and targets an added layer of complexity.

Chapter 1 provides a motivation for this work and covers the existing literature on the topics of spray flame stability of liquid fuels. Chapter 2 presents the development and designing of the ACS burner. It also discusses the flame stability of different single fuels. In addition, a Fuel Ignition Tester (FIT) was used to investigate the impact of volatility and local enrichment on ignition delay. Results indicate a strong influence of fuel volatility and atomization on the flame stability. The less volatile/heavier fuels have higher liftoff heights, while the fuels with smaller droplet sizes and higher volatility blowout easier than less volatile fuels which and those which atomize into larger droplets. In the FIT, it was noticed that the local equivalence ratio defined by the fuel's volatility has more effect on the ignition delay than the global air fuel ratio. This work was presented and published in the 2018 AIAA SciTech Conference and Exposition. Chapter 3 focuses on characterizing the ACS Burner by investigating the impact of varying the fuel and air flow rates on the spray atomization (e.g. droplet size distribution). This was explored by measuring droplet sizes and velocities of the spray at different radial and axial positions of n-heptane fuel under nonreacting conditions. In addition, the turbulence intensity and the liquid spray droplet distribution were quantified for different fuel and air flow rate conditions. The measurements were obtained by using a Phase Doppler Particle Analyzer/Laser Doppler Velocimeter (PDPA/LDV) at P = 1 atm and T = 298 K. Moreover, the Sauter Mean Diameters for different flow conditions are predicted, using established correlations, and compared to PDPA/LDV measurements. This study provides a fair understanding of the influence of varying the fuel and air flow rates on the droplet sizes, velocity, and turbulent intensity. This work was was presented and published in the 2019 ASME TurboExpo Conference. After the spray characterization, it was desired to focus on unraveling the role of phase change on flame stability. This is achieved by investigating the influence of the variation in the properties of different fuels on the spray properties (atomization

process), and thus on the flame stability as presented in Chapter 4. In this chapter, two approaches are used. First, the flame stabilities of three single fuels, e.g., n-heptane, n-dodecane, and toluene, are measured using a single nozzle size. Second, the flame stabilities are also measured while the atomization process was controlled by minimizing the differences in spray properties of the tested fuels, e.g., SMD, and SDD. This was achieved by using different nozzle sizes with the different fuels. The comparison of the results from the two approaches shows a significant influence of the atomization process on the flame stability. When the atomization process controlled, more similar liftoff heights and blowout limits for the set fuels where observed as compared to the results from the common nozzle approach. Chapter 5 builds upon these findings and proposes a novel approach to investigate the influence of spray processes (atomization and vaporization) on flame stability. Using a derived correlation capable of predicting the gas phase global extinction behavior of simple hydrocarbon blends, the compositions of two mixtures were formulated to match gas phase extinction performance with differences in the relative volatility of the reactive species. Despite having similar gas phase extinction limits, when utilized in the spray burner while maintaining a constant droplet size, the mixtures exhibited different stability behaviors marked by variation in flame liftoff height and blowout limits. Chapters 6 and 7 present results which correlate the properties of jet fuels with the flame stability and soot formation. It is shown that the liquid droplet penetrating to the flame and the fuel's volatility have greater impact on the flame stability (flame LOH and LBO) and soot formation compared to that from chemical properties. The dissertation concludes with Chapter 8 in which the main findings are summarized. Finally, several recommendations for future work are presented.

References

[1] U.S.E.I. Administration, U.S. primary energy consumption by source and sector, 2016.
[2] U.S.E.I.A. (EIA), U.S. petroleum flow, 2016,
[3] B. Chèze, P. Gastineau, J. Chevallier, Forecasting world and regional aviation jet fuel demands to the mid-term (2025), Energy Policy 39 (2011) 5147-5158.
[4] R.D. Reitz, Directions in internal combustion engine research, Combustion and Flame 160 (2013) 1-8.
[5] A. Haines, R.S. Kovats, D. Campbell-Lendrum, C. Corvalán, Climate change and human health: impacts, vulnerability and public health, Public health 120 (2006) 585-596.
[6] N. Panwar, S. Kaushik, S. Kothari, Role of renewable energy sources in environmental protection: a review, Renewable and Sustainable Energy Reviews 15 (2011) 1513-1524.
[7] M. Colket, J. Heyne, M. Rumizen, M. Gupta, T. Edwards, W.M. Roquemore, G. Andac, R. Boehm, J. Lovett, R. Williams, Overview of the national jet fuels combustion program, AiAA Journal (2017) 1087-1104.
[8] T.M. Lovestead, J.L. Burger, N. Schneider, T.J. Bruno, Comprehensive assessment of composition and thermochemical variability by high resolution GC/QToF-MS and the advanced distillation-curve method as a basis of comparison for reference fuel development, Energy & Fuels 30 (2016) 10029-10044.
[9] C. Zhang, X. Hui, Y. Lin, C.-J. Sung, Recent development in studies of alternative jet fuel combustion: Progress, challenges, and opportunities, Renewable and Sustainable Energy Reviews 54 (2016) 120-138.
[10] S. Dooley, S.H. Won, J. Heyne, T.I. Farouk, Y. Ju, F.L. Dryer, K. Kumar, X. Hui, C.-J. Sung, H. Wang, The experimental evaluation of a methodology for surrogate fuel formulation to emulate gas phase combustion kinetic phenomena, Combustion and Flame 159 (2012) 1444-1466.
[11] S.H. Won, B. Windom, B. Jiang, Y. Ju, The role of low temperature fuel chemistry on turbulent flame propagation, Combustion and Flame 161 (2014) 475-483.
[12] D.D. Das, C.S. McEnally, L.D. Pfefferle, Sooting tendencies of unsaturated esters in nonpremixed flames, Combustion and Flame 162 (2015) 1489-1497.
[13] D.D. Das, W.J. Cannella, C.S. McEnally, C.J. Mueller, L.D. Pfefferle, Two-dimensional soot volume fraction measurements in flames doped with large hydrocarbons, Proceedings of the Combustion Institute 36 (2017) 871-879.
[14] Y. Xuan, G. Blanquart, Numerical modeling of sooting tendencies in a laminar co-flow diffusion flame, Combustion and Flame 160 (2013) 1657-1666.
[15] J.M. Bergthorson, M.J. Thomson, A review of the combustion and emissions properties of advanced transportation biofuels and their impact on existing and future engines, Renewable and Sustainable Energy Reviews 42 (2015) 1393-1417.
[16] A.C. Alkidas, Combustion advancements in gasoline engines, Energy Conversion and Management 48 (2007) 2751-2761.
[17] J. Grohmann, W. O'Loughlin, W. Meier, M. Aigner. Comparison of the Combustion Characteristics of Liquid Single-Component Fuels in a Gas Turbine Model Combustor. ASME Turbo Expo 2016: p. V04AT04A010-V004AT004A010.
[18] J. Grohmann, B. Rauch, T. Kathrotia, W. Meier, M. Aigner, Influence of Single-Component Fuels on Gas-Turbine Model Combustor Lean Blowout, Journal of Propulsion and Power (2017) 1-11.

[19] N. Rock, I. Chterev, T. Smith, H. Ek, B. Emerson, D. Noble, J. Seitzman, T. Lieuwen. Reacting Pressurized Spray Combustor Dynamics: Part 1—Fuel Sensitivities and Blowoff Characterization. In: editor^editors. ASME Turbo Expo 2016: Turbomachinery Technical Conference and Exposition; 2016: American Society of Mechanical Engineers. p. V04AT04A021-V004AT004A021.
[20] A. Lefebvre, Atomization and sprays, combustion: an international series, Hemisphere Pub. Corp (1989).
[21] A.H. Lefebvre, Gas turbine combustion: alternative fuels and emissions, CRC press2010.
[22] R. Williams, Final Report Evaluation of Sasol Fully Synthetic Jet Fuel for Approval for Use as Jet A-1 Fuel, Honeywell Aerospace, Report (2007).
[23] Y. Lin, Y. Lin, C. Zhang, Q. Xu, C.-J. Sung, G. Liu, Evaluation of Combustion Performance of a Coal-Derived Synthetic Jet Fuel, (2012) 569-576.
[24] J.-S. Gong, W.-B. Fu, The experimental study on the flow characteristics for a swirling gas–liquid spray atomizer, Applied Thermal Engineering 27 (2007) 2886-2892.
[25] H.G. Wagner, Soot formation in combustion, Symposium (International) on Combustion 17 (1979) 3-19.
[26] J. Jedelsky, M. Jicha, Energy considerations in spraying process of a spill-return pressure-swirl atomizer, Applied Energy 132 (2014) 485-495.
[27] J.A. Bossard, R.E. Peck, Droplet sie distribution effects in spray combustion, Symposium (International) on Combustion 26 (1996) 1671-1677.
[28] A. Stagni, L. Esclapez, P. Govindaraju, A. Cuoci, T. Faravelli, M. Ihme, The role of preferential evaporation on the ignition of multicomponent fuels in a homogeneous spray/air mixture, Proceedings of the Combustion Institute 36 (2017) 2483-2491.
[29] S.C. Burke, M. Ratcliff, R. McCormick, R. Rhoads, B. Windom, Distillation-based Droplet Modeling of Non-Ideal Oxygenated Gasoline Blends: Investigating the Role of Droplet Evaporation on PM Emissions, SAE International Journal of Fuels and Lubricants 10 (2017) 69-81.
[30] N. Kurimoto, N. Watanabe, S. Hoshi, S. Sasaki, M. Matsumoto, Numerical Modeling of International Variations in Diesel Spray Combustion with Evaporation Surrogate and Virtual Species Conversion, SAE International, 2017.
[31] L.M. Itani, G. Bruneaux, A. Di Lella, C. Schulz, Two-tracer LIF imaging of preferential evaporation of multi-component gasoline fuel sprays under engine conditions, Proceedings of the Combustion Institute 35 (2015) 2915-2922.
[32] J.E. Madero, R.L. Axelbaum, Spray breakup and structure of spray flames for low-volatility wet fuels, Combustion and Flame 180 (2017) 102-109.
[33] B. Windom, S.H. Won, C.B. Reuter, B. Jiang, Y. Ju, S. Hammack, T. Ombrello, C. Carter, Study of ignition chemistry on turbulent premixed flames of n-heptane/air by using a reactor assisted turbulent slot burner, Combustion and Flame 169 (2016) 19-29.
[34] M. Mehl, W.J. Pitz, C.K. Westbrook, H.J. Curran, Kinetic modeling of gasoline surrogate components and mixtures under engine conditions, Proceedings of the Combustion Institute 33 (2011) 193-200.
[35] S. Dooley, S.H. Won, M. Chaos, J. Heyne, Y. Ju, F.L. Dryer, K. Kumar, C.-J. Sung, H. Wang, M.A. Oehlschlaeger, A jet fuel surrogate formulated by real fuel properties, Combustion and Flame 157 (2010) 2333-2339.

[36] A. Ahmed, G. Goteng, V.S.B. Shankar, K. Al-Qurashi, W.L. Roberts, S.M. Sarathy, A computational methodology for formulating gasoline surrogate fuels with accurate physical and chemical kinetic properties, Fuel 143 (2015) 290-300.
[37] A. Agosta, N.P. Cernansky, D.L. Miller, T. Faravelli, E. Ranzi, Reference components of jet fuels: kinetic modeling and experimental results, Experimental Thermal and Fluid Science 28 (2004) 701-708.
[38] S. Humer, A. Frassoldati, S. Granata, T. Faravelli, E. Ranzi, R. Seiser, K. Seshadri, Experimental and kinetic modeling study of combustion of JP-8, its surrogates and reference components in laminar nonpremixed flows, Proceedings of the Combustion Institute 31 (2007) 393-400.
[39] S.S. Vasu, D.F. Davidson, R.K. Hanson, Jet fuel ignition delay times: Shock tube experiments over wide conditions and surrogate model predictions, Combustion and Flame 152 (2008) 125-143.
[40] S. Honnet, K. Seshadri, U. Niemann, N. Peters, A surrogate fuel for kerosene, Proceedings of the Combustion Institute 32 (2009) 485-492.
[41] S. Dooley, S.H. Won, S. Jahangirian, Y. Ju, F.L. Dryer, H. Wang, M.A. Oehlschlaeger, The combustion kinetics of a synthetic paraffinic jet aviation fuel and a fundamentally formulated, experimentally validated surrogate fuel, Combustion and Flame 159 (2012) 3014-3020.
[42] M. Mawid, Development of a Detailed Chemical Kinetic Mechanism for Mixtures of JP-8 Fuel and Fischer-Tropsch-Based Synthetic Jet Fuel, 43rd AIAA/ASME/SAE/ASEE Joint Propulsion Conference & Exhibit, American Institute of Aeronautics and Astronautics2007.
[43] A. Mzé-Ahmed, K. Hadj-Ali, P. Diévart, P. Dagaut, Kinetics of oxidation of a synthetic jet fuel in a jet-stirred reactor: experimental and modeling study, Energy & Fuels 24 (2010) 4904-4911.
[44] P. Dagaut, F. Karsenty, G. Dayma, P. Diévart, K. Hadj-Ali, A. Mzé-Ahmed, M. Braun-Unkhoff, J. Herzler, T. Kathrotia, T. Kick, C. Naumann, U. Riedel, L. Thomas, Experimental and detailed kinetic model for the oxidation of a Gas to Liquid (GtL) jet fuel, Combustion and Flame 161 (2014) 835-847.
[45] C.V. Naik, K.V. Puduppakkam, A. Modak, E. Meeks, Y.L. Wang, Q. Feng, T.T. Tsotsis, Detailed chemical kinetic mechanism for surrogates of alternative jet fuels, Combustion and Flame 158 (2011) 434-445.
[46] M.L. Huber, T.J. Bruno, R.D. Chirico, V. Diky, A.F. Kazakov, E.W. Lemmon, C.D. Muzny, M. Frenkel, Equations of state on demand: Application for surrogate fuel development, International Journal of Thermophysics 32 (2011) 596-613.
[47] M.L. Huber, B.L. Smith, L.S. Ott, T.J. Bruno, Surrogate mixture model for the thermophysical properties of synthetic aviation fuel S-8: Explicit application of the advanced distillation curve, Energy & Fuels 22 (2008) 1104-1114.
[48] N.A. Slavinskaya, A. Zizin, M. Aigner, On Model Design of a Surrogate Fuel Formulation, Journal of Engineering for Gas Turbines and Power 132 (2010) 111501-111501-111511.
[49] T. Edwards, L.Q. Maurice, Surrogate mixtures to represent complex aviation and rocket fuels, Journal of Propulsion and Power 17 (2001) 461-466.
[50] A. Violi, S. Yan, E. Eddings, A. Sarofim, S. Granata, T. Faravelli, E. Ranzi, Experimental formulation and kinetic model for JP-8 surrogate mixtures, Combustion Science and Technology 174 (2002) 399-417.

[51] E. Ranzi, A. Frassoldati, R. Grana, A. Cuoci, T. Faravelli, A.P. Kelley, C.K. Law, Hierarchical and comparative kinetic modeling of laminar flame speeds of hydrocarbon and oxygenated fuels, Progress in Energy and Combustion Science 38 (2012) 468-501.
[52] H. Tsuji, Counterflow diffusion flames, Progress in energy and combustion science 8 (1982) 93-119.
[53] S.H. Won, S. Dooley, F.L. Dryer, Y. Ju, A radical index for the determination of the chemical kinetic contribution to diffusion flame extinction of large hydrocarbon fuels, Combustion and Flame 159 (2012) 541-551.
[54] P.S. Veloo, Studies of combustion characteristics of alcohols, aldehydes, and ketones, University of Southern California2011.
[55] C.W. Curtis, Combustion characteristics of thermally stressed hydrocarbon fuels, University of Colorado at Colorado Springs2016.
[56] P. Saxena, F.A. Williams, Testing a small detailed chemical-kinetic mechanism for the combustion of hydrogen and carbon monoxide, Combustion and Flame 145 (2006) 316-323.
[57] Y. Wang, A. Raj, S.H. Chung, A PAH growth mechanism and synergistic effect on PAH formation in counterflow diffusion flames, Combustion and Flame 160 (2013) 1667-1676.
[58] Z. Luo, S. Som, S.M. Sarathy, M. Plomer, W.J. Pitz, D.E. Longman, T. Lu, Development and validation of an n-dodecane skeletal mechanism for spray combustion applications, Combustion theory and modelling 18 (2014) 187-203.
[59] J.A. Cooke, M. Bellucci, M.D. Smooke, A. Gomez, A. Violi, T. Faravelli, E. Ranzi, Computational and experimental study of JP-8, a surrogate, and its components in counterflow diffusion flames, Proceedings of the Combustion Institute 30 (2005) 439-446.
[60] L. Esclapez, P.C. Ma, E. Mayhew, R. Xu, S. Stouffer, T. Lee, H. Wang, M. Ihme, Fuel effects on lean blow-out in a realistic gas turbine combustor, Combustion and Flame 181 (2017) 82-99.
[61] W. O'Loughlin, A. Masri, A new burner for studying auto-ignition in turbulent dilute sprays, Combustion and Flame 158 (2011) 1577-1590.
[62] C. Liu, F. Liu, J. Yang, Y. Mu, G. Xu, Investigations of the effects of spray characteristics on the flame pattern and combustion stability of a swirl-cup combustor, Fuel 139 (2015) 529-536.
[63] I. Düwel, H.W. Ge, H. Kronemayer, R. Dibble, E. Gutheil, C. Schulz, J. Wolfrum, Experimental and numerical characterization of a turbulent spray flame, Proceedings of the Combustion Institute 31 (2007) 2247-2255.
[64] J. Reveillon, L. Vervisch, Analysis of weakly turbulent dilute-spray flames and spray combustion regimes, Journal of Fluid Mechanics 537 (2005) 317-347.
[65] F. Shum-Kivan, J. Marrero Santiago, A. Verdier, E. Riber, B. Renou, G. Cabot, B. Cuenot, Experimental and numerical analysis of a turbulent spray flame structure, Proceedings of the Combustion Institute 36 (2017) 2567-2575.
[66] A. Verdier, J. Marrero Santiago, A. Vandel, S. Saengkaew, G. Cabot, G. Grehan, B. Renou, Experimental study of local flame structures and fuel droplet properties of a spray jet flame, Proceedings of the Combustion Institute 36 (2017) 2595-2602.
[67] M.S. Mansour, I. Alkhesho, S.H. Chung, Stabilization and structure of n-heptane flame on CWJ-spray burner with kHZ SPIV and OH-PLIF, Experimental Thermal and Fluid Science 73 (2016) 18-26.
[68] S. Marley, E. Welle, K. Lyons, W. Roberts, Effects of leading edge entrainment on the double flame structure in lifted ethanol spray flames, Experimental thermal and fluid science 29 (2004) 23-31.

CHAPTER 2: Spray Flame Stability and Ignition of Single Fuels[1]

2.1 Summary

Liquid fuels have different physical and chemical properties which can affect the atomization, evaporation and mixing processes inside heat engines, including turbine and reciprocating internal combustion engines. In this work, the relationship between the fuel's properties and its ignition/flame stability is investigated. A spray burner was designed and manufactured to simulate the mixing dynamics experienced in a turbine engine combustor capable of delivering high fuel and air co-flow rates. The flame behavior and stability have been studied by measuring the flame liftoff heights and blowout limits for different single component fuels at different fuel and air flow conditions. In addition, a Fuel Ignition Tester (FIT) was used to investigate the impact of volatility and local enrichment on ignition delay. Results indicate a strong influence of fuel volatility and atomization on the flame stability. The less volatile/heavier fuels have higher liftoff heights, while the fuels with smaller droplet sizes and higher volatility blowout easier than less volatile fuels which and those which atomize into larger droplets. In the FIT, it was noticed that the local equivalence ratio defined by the fuel's volatility has more effect on the ignition delay than the global air fuel ratio. As a result, n-dodecane ignites faster than n-heptane, despite having a lowered measured global equivalence ratio.

[1] This chapter is largely based on a published manuscript: Alsulami, Radi A., et al. "Exploring the Role of Physical and Chemical Properties on the Ignition and Flame Stability of Liquid Fuels with a Spray Burner and Fuel Ignition Tester (FIT)." *2018 AIAA Aerospace Sciences Meeting*. 2018

2.2 Introduction

In IC engine (i.e., liquid-fueled gas turbine), the dynamic of spray processes can influence the turbulent flame stability [1, 2]. Recent numerical works have shown that in the conditions for gas turbine engines (as well as other engine configurations), distillation vaporization phenomenon (i.e. preferential evaporation) can occur resulting in a vapor composition different from that of the liquid fuel droplet [3, 4]. This preferential droplet evaporation can impact the fuel composition distribution within the engine and potentially control the ignition timing, flame phenomenon and pollutant formation [3-7]. For example, ignition may occur much faster or slower than that of the global gas phase ignition delay (of the entire complex fuel), depending on the fuel composition and the relative volatility distribution of the reactive species (e.g. the n-alkanes). To illustrate this, two mixtures have been chosen (described in Table 2.1) and simulated using CHEMKIN constant volume adiabatic ignition simulation to demonstrate the potential impact of preferential evaporation on the ignition of a complex fuel [8, 9]. The ignition delays of the two mixtures in the gas phase are nearly identical (Fig. 2.1a), however when considering the differences in phase composition resulting from preferential evaporation of the liquid fuel mixtures (Fig. 2.1b,

Table 2.1. Selected mixtures to demonstrate the impact of preferential vaporization on the ignition of complex fuels.

Mix 1		**Mix 2**	
Species	Mole Fraction	Species	Mole Fraction
n-heptane	33.3%	toluene	33.3%
toluene	33.3%	m-xylene	33.3%
m-xylene	33.3%	i-dodecane	23.3%
		n-dodecane	10%

predicted by a multicomponent droplet evaporation model [3]), significantly different ignition delays can be seen (Fig. 2.1c). In this case, much shorter initial ignition delays (~two orders of magnitude) for mixture 1 is observed early in the droplet lifetime with the trend reversed as the final liquid fractions of the droplet are evaporated.

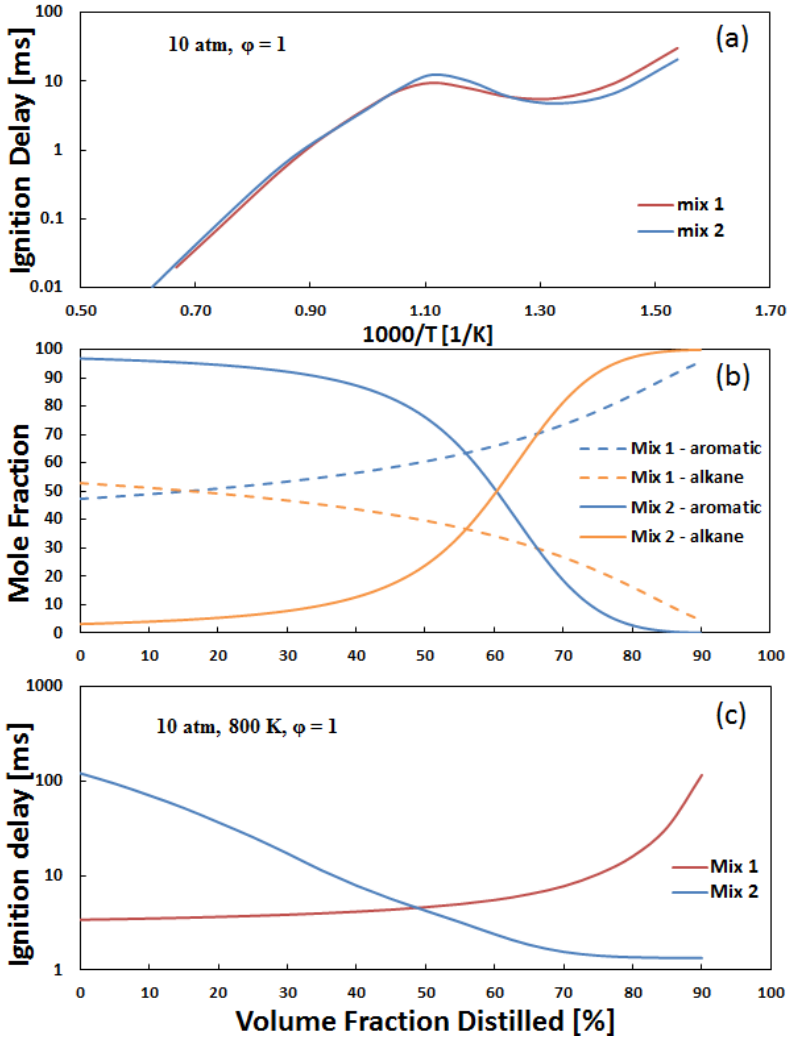

Figure 2.1. Preferential vaporization impact on ignition timing. Ignition delay of complete fuel blends (a), composition evolution during droplet evaporation (b), and the vaporization dependent ignition delay (c).

Prior to studying the impact of preferential fuel evaporation effects on the energy conversion of multi component fuels, experimental measurements of single component fuels must be conducted to provide the baseline understanding regarding the role of fuel vaporization and

atomization along with chemical properties on ignition and flame stability. In light of this, experiments have been conducted using a newly designed turbulent spray burner to explore the impact of fuel properties on flame dynamics/stability and a Fuel Ignition Tester (FIT) to determine the role of properties on the ignition delay of liquid single hydrocarbon fuels experiencing a wide range of volatilities and gas phase reactivity, including n-heptane, n-dodecane, iso-octane, toluene, and 1,2,4-trimethylbenzene (1,2,4-TMB). The impact of vaporization and atomization on the local enrichment and subsequent effect on the ignition delay and blowout limits are discussed.

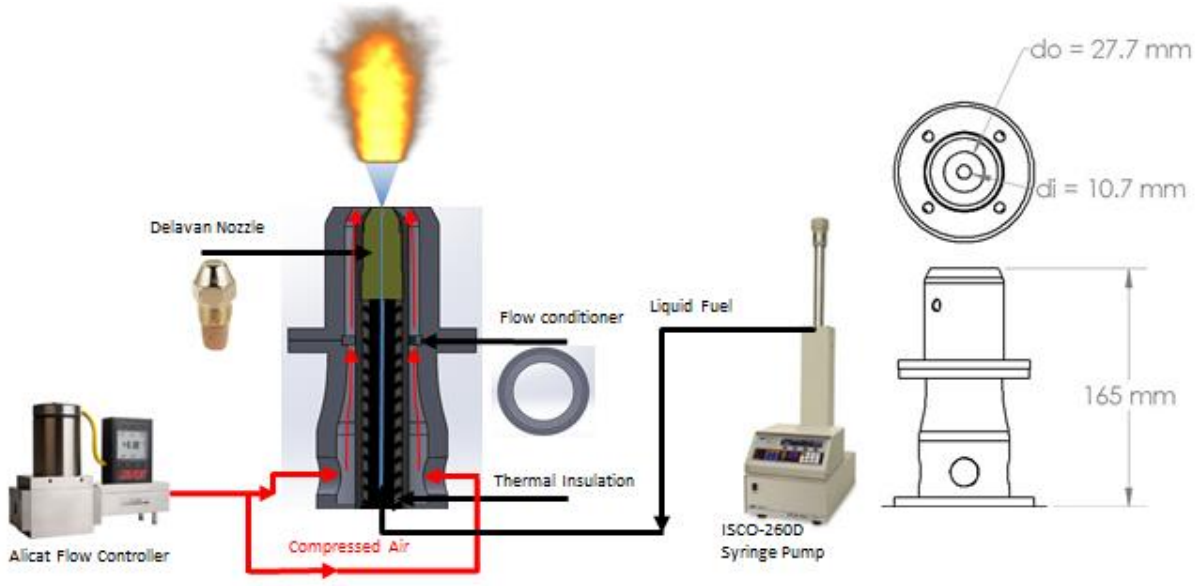

Figure 2.2. Schematic of the experiment set up, including the PDPA system, details of the burner geometries.

2.3 Annular Co-flow Spray (ACS) Burner

To investigate the link between the thermodynamic properties of liquid hydrocarbon fuels and flame stability, an Annular Co-flow Spray Burner (ACS Burner) was constructed with the ability to accurately deliver large flow rates of fuel and air. The cross section schematic of the spray burner is shown in Fig. 2.2. It consists of a solid cone spray injector (DELAVAN .40 GPH 80° B SOLID NOZZLE) at the center, surrounded by an unconfined annular air co-flow. The injector concentricity is maintained by a flow straightener, which has 240 circular slots evenly distributed over the ring's area. The burner is made of stainless steel and it is 165 mm tall with converging shape toward the outlet. The nozzle position can be adjusted to achieve a stabilized flame. The exit area of the co-flow is kept constant throughout this study at $512.64\ \text{mm}^2$. The burner is connected to flow controller system that has the ability to deliver high air flow rates, i.e. up to 3000 L/min (Alicat, MCR-3000SLPM-D-PAR) with a stated accuracy of ±0.8% of reading, and 0.2% of full-scale. High pressure syringe pump (ISCO, Model 260D) was used to supply the liquid fuel. It is capable of delivering up to 107 ml/min of liquid fuel.

Table 2.2. Flame liftoff height measurement conditions at the burner exit (outlet area of 512.64 mm^2).

Fuel Flow Rate [mL/min]	Air Flow Rate [SLPM]	Air Velocity @ the burner exit [m/s]	Reynolds Number of the co-flow
50	200	6.5	5762
50	300	9.8	8643
50	400	13	11523
50	500	16.3	14404
50	600	19.5	17285

Spray flame experiments were carried out in the atmospheric environment of Fort Collins, CO, i.e. T = 298 K $\pm$ 5 K & P = 0.84 atm. Fuel and air flow rates were carefully controlled to maintain desired global equivalence ratios. To investigate the role of evaporation on flame stability, flame liftoff heights (LOH) and flame lean blowout limits (LBO) for the selected liquid fuels were measured. Flame liftoff height is measured by collecting 50 images of the spray flame for each condition as listed in Table 2.2. The set of images are averaged, and the liftoff height is defined as the distance between the nozzle tip and the base of the flame, identified by the location of the maximum intensity gradient in the image as illustrated in Fig. 2.3.

Figure 2.3. Liftoff height measurement procedure.

Blowout limit was determined by slowly increasing the air flow rate while keeping the selected fuel flow rate constant until the flame extinguishes. Air flow rates and global equivalence ratios at time of blowout were identified. The blowout measurements were repeated at least twice for each of the six fuel flow rates, i.e. $\dot{V}_F = 40, 45, 50, 55, 60, \text{and } 65 \text{ mL/min}$. The repeatability of the blowout limit measurements was good with relative standard deviation from the mean value between 0.8-2%, 1.3-3.1%, 0.72-4.2%, 0-3.4% and 0.5-2.6% for n-heptane, n-dodecane, iso-octane, toluene, and 1,2,4-trimethylbenzene, respectively. To evaluate the role of turbulence on the blowout limit measurements, a second experimental approach was also applied in which the air flow rates were held constant and the fuel flow rate slowly decreased until the flame extinguished.

2.4 Fuel Selection

To investigate the effect of physical (vaporization) and chemical properties of liquid fuels on the flame stability and ignition, five single fuels were chosen from three different hydrocarbon families, e.g. n-alkane, iso-paraffin and aromatic, with a wide range of volatilities and reactivity, including n-heptane, n-dodecane, iso-octane, toluene, and 1,2,4-trimethylbenzene. The fuels were chosen because of the differences and similarities in their properties as listed in Table 2.3 [10]. For example, n-heptane and iso-octane have similar physical and volatility properties, but different reactivity stimming from the variation in chemical structure of these two fuels. Thus, this allows investigating the influence of fuel reactivity on flame stability, e.g., LOH and LBO. In the other hand, n-heptane and n-dodecane are n-alkane fuels and thus they have similar reactivity, which provides a good opportunity to examine the impact of fuels volatility and physical properties. Similar behavior is expected for the aromatic fuels, e.g., toluene, and 1,2,4-trimethylbenzene, but with lower reactivity compared to the n-alkanes. Fuel physical properties, such as viscosity, surface tension, and density effect the spray atomization. Therefore, Sauter Mean Diameter (SMD) is calculated using Lefebvre correlation [11, 12]:

$$\mathrm{SMD}_{Lefebvre} = 2.25\sigma_l^{0.25}\mu_l^{0.25}\dot{m}_l^{0.25}\Delta P^{-0.5}\rho_{air}^{-0.25} \tag{2.1}$$

where σ_l is the liquid surface tension, μ_l is the liquid viscosity, $\dot{m}_l$ is the liquid mass flow rate, ΔP is the pressure drop across the spray nozzle and ρ_{air} is the surrounding air density.

2.5 Fuel Ignition Tester (FIT)

To study the role of fuel volatility and local enrichment on ignition, a Waukesha FIT was used to measure ignition delays of multiple n-alkane fuels, including n-heptane and n-dodecane, at multiple pressures and temperatures. The FIT injects a liquid fuel into a reacting environment requiring the fuel to evaporate and mix with the air before igniting. Similar to an engine there is a

Table 2.3. Selected thermodynamic properties and calculated Sauter mean diameter for the hydrocarbon fuels at temperature of 298 K, excluding the normal boiling temperature (NBT) and the derived cetane number (DCN).

Fuel	NBT [K]	P_V [kPa]	$\boldsymbol{\rho_F}$ [kg/m^3]	$\boldsymbol{\mu_l}$ [kg/m.s]	$\boldsymbol{\sigma_l}$ [N/m]	SMD [µm] at $\dot{\mathbf{V}}_{\mathbf{fuel}} = \mathbf{50\ mL/min}$	DCN
iso-octane	372.388	6.529	690.42	0.00048	0.0184	9.67	17.4
n-heptane	371.58	6.021	681.66	0.00039	0.0198	9.02	53.8
n-dodecane	489.473	0.018	746.39	0.0014	0.0249	14.22	74
toluene	383.78	3.775	864.05	0.00056	0.0279	10.31	6
1,2,4-TMB	442.53	0.284	872.31	0.00089	0.0292	12.4	8.9

complex interaction between the evaporation of the fuel and the subsequent ignition. Furthermore, the FIT provides flexibility to adjust the chamber temperature, pressure, and injection timing (between 3 to 8 ms) allowing for limited control of the air fuel ratio, making it an ideal platform to study the impact of evaporation on the ignition dynamics of a liquid fuel. Twenty five ignition delays were measured for each temperature and pressure used (i.e. 753 and 828 K; 10, 15, and 24 bar). Figure 2.4, shows the average pressure trace of 25 injections of n-heptane (at $P_{air} = 24$ bar and $T_{air} = 753$ K). The FIT reads the ignition delay time when the pressure rises above the chamber initial pressure by 0.2 bar, however, as a result of varying pressure rise rates for the multiple fuels tested, ignition delays were also calculated using the point of maximum slope, as demonstrated in Fig. 2.4 [13, 14]. The assembled average ignition delay for each fuel at each temperature/pressure condition is calculated and reported. It should be noted, the measured

ignition delay of the n-heptane reference fuel with the FIT was repeated daily and agreed with ASTM standard (D6890) [13].

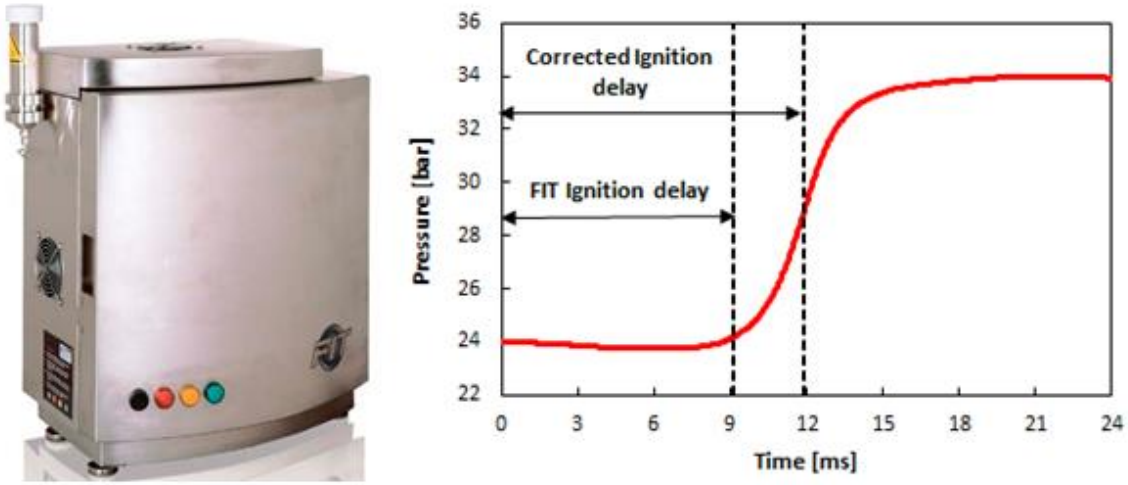

Figure 2.4. Image and average pressure trace of n-heptane at a pressure of 24 bar and air temperature of 753 K taken from CSU's Fuel Ignition Tester (FIT).

2.6 Results and Discussion

2.6.1 The role of Physical and Chemical Properties on Flame Stability of Single Fuels

Prior to studying the impact of preferential fuel evaporation effects on the energy conversion of multi component fuels, experimental measurements of single component fuels must be conducted to provide the baseline understanding regarding the role of fuel vaporization and atomization along with chemical properties on ignition and flame stability. In light of this, experiments have been conducted using the spray burner to explore the impact of fuel properties on flame dynamics/stability. The liquid single hydrocarbon fuels used in this section were selected to cover a wide range of volatilities and gas phase reactivity, including n-heptane, n-dodecane, iso-octane, toluene, and 1,2,4-trimethylbenzene (1,2,4-TMB).

2.6.1.1 Flame Behavior (Structure)

Single hydrocarbon fuels were used to investigate the link between their physical (vaporization) and chemical properties and flame dynamics/stability. Consistent with previous works, e.g. [15-17], a double flame structure appears in the flames of n-heptane, n-dodecane and iso-octane fuels as shown in Fig. 2.5. A blue color (partially premixed) flame is observed in the

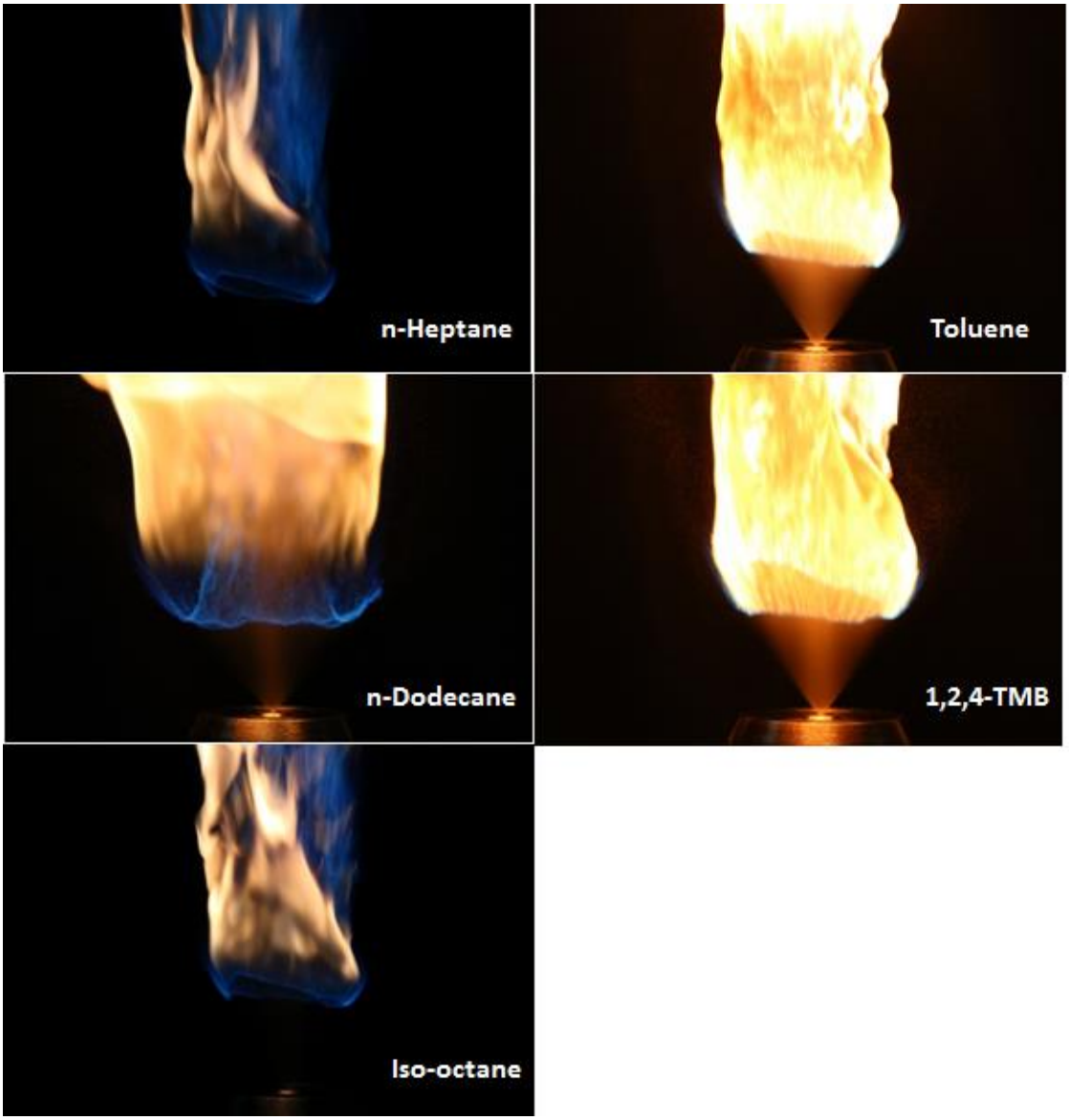

Figure 2.5. Flame images of the five fuels at VF = 50 mL/min, Vair = 200 mL/min, using the same nozzle, e.g. nozzle# 0.4 GPH.

upstream near the burner tip, which is established by the small droplets, followed by soot rich yellow flame. The flames of n-heptane and iso-octane have similar structure because of their similarity in physical properties and droplet size as listed in Table 2.3. For aromatic fuels, e.g. toluene and 1,2,4-trimythelbenzene, the entire flame is sooty yellow with high luminosity resulting from their chemical structures. For n-dodecane and 1,2,4-trimethylbenzene unburned droplets were seen passing through the flame which is caused by their larger droplet sizes and low vapor pressure (PV). The same nozzle was used for all fuels (e.g. nozzle# 0.4 GPH).

2.6.1.2 Liftoff Height

In general, increasing the air flow rate increases the liftoff height. As illustrated in Fig. 2.6, the heavier/less volatile fuels which generate bigger droplets experience larger flame liftoff distances. These results are explained due to the heavier fuels requiring more time to evaporate than the lighter fuels before being capable of sustaining a flame. The flame is sustained and stabilized at location where the flame speed is in balance with the local velocity of incoming air and fuel flows and at which the mixture is at around stoichiometric. n-Heptane and iso-octane have similar liftoff

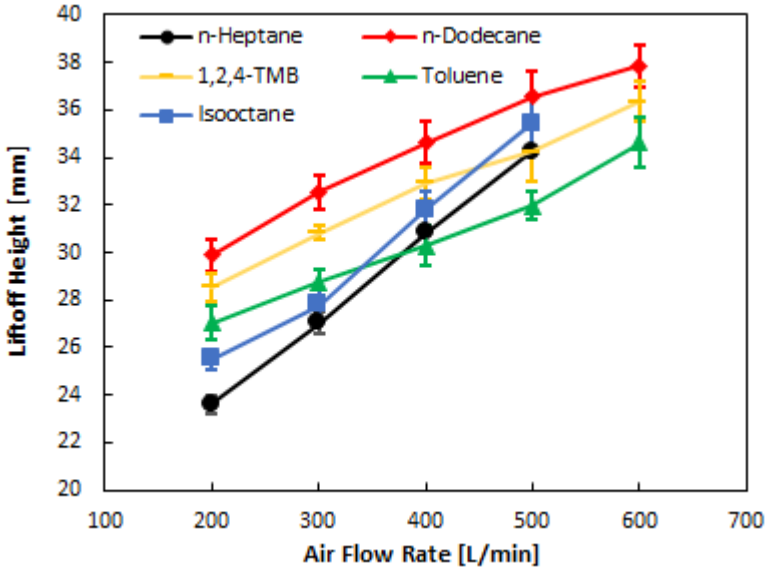

Figure 2.6. Liftoff heights of all single component fuels at 50 mL/min fuel flow rate and using 0.4 GPH nozzle size.

height trends again because their droplets sizes and volatility are similar. The difference in their liftoff height is most likely resulting from reactivity differences. As the fuel and/or air flow rates increase, the droplet sizes, especially for the lighter fuels, e.g. n-heptane and iso-octane, become significantly small resulting in locally and globally fuel lean conditions and flame behaviors similar to a premixed flame. As a result, the liftoff height trends of these two fuels experience a sharp increase relative to the heavier fuels. The droplet sizes of the different fuels are shown in Table 2.3.

2.6.1.3 Blowout limit

Figure 2.7 shows the calculated global equivalence ratio at blowout for different fuel flow rates. The larger hydrocarbon fuels were the most difficult to achieve blowout requiring the use of large air flow rates (up to 1070 L/min and Re = 28500). The lighter fuels experienced blowout at much lower air flow rates (e.g. as low as 383 L/min and Re = 10220). The reason for this is believed to be caused by the local enrichment. For the most volatile fuels, those producing the smallest

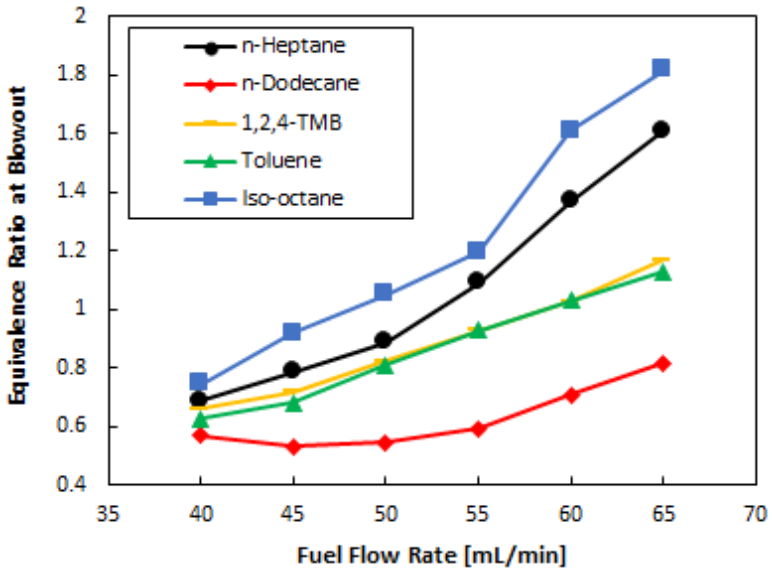

Figure 2.7. Global equivalence ratio at blowout limits of all single component fuels using 0.4 GPH nozzle size for all fuels.

droplets, e.g. n-heptane, the liquid fuel transfers fast to the gas phase improving the fuel and air mixing and resulting in a leaner local equivalence ratio closer to the nozzle exit than the less volatile fuels under the same flow conditions. On the other hand, the heavy fuels, e.g. n-dodecane, have a lower vapor pressure and higher viscosity, density and surface tension, which slows vaporization and produces larger droplets [18-20]. As a result, more droplets enter the flame zone generating more regions, which have higher local equivalence ratios helping sustain and stabilize the flame. The general trend of increasing blowout limits with increased fuel flow rate experienced by all fuels can be attributed to the increased velocity of the droplets as fuel flow rate is increased shortening the resident time of the droplets inside the flame preheat zone impacting the localized droplet evaporation and burning. More explanation for the local enrichment effect on flame ignition/stability will be discussed in the FIT results section.

The larger fuels require higher air flow rates (or higher Reynolds numbers) to achieve blowout generating more turbulence which can enhance the atomization and mixing as well as flame

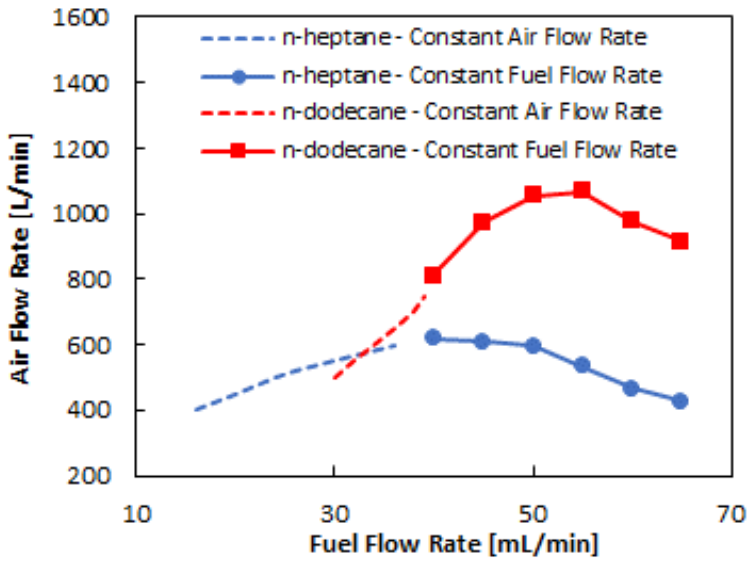

Figure 2.8. Global equivalence ratio at blow out limits of n-heptane and n-dodecane for constant fuel flow rates (solid lines) and constant air flow rates (dashed lines) using same nozzle size.

stabilization. In contrast with the previous method used in Fig. 2.7, Figure 2.8 illustrates the blowout limits of n-heptane and n-dodecane when the air flow rate was kept constant while slowly

Table 2.4. FIT ignition delays (measured and corrected) for multiple temperature and pressures, $T_{air} = 753$ & $828\ K$ and $P_{air} = 24, 15$ & $10\ bar$, for n-heptane and n-dodecane.

Fuel	Temperature [K]	Pressure [bar]	FIT Ignition Delay [ms]	Corrected Ignition Delay [ms]	Equivalence Ratio
n-heptane	753	24	9.14	11.85	1.14
		15	9.95	14	1.26
		10	11.23	17.4	2.18
	828	24	3.32	3.65	0.58
		15	4.35	5.4	1.53
		10	5.1	7.3	2.18
n-dodecane	753	24	6.25	8.2	0.25
		15	7.27	8.8	0.49
		10	7.88	10.25	0.61
	828	24	2.23	2.65	0.49
		15	3.07	3.85	0.43
		10	4.01	5.15	0.65

decreasing the fuel flow rate. This method eliminates the influence of flow turbulence when comparing flame blowout limits between two fuels. It is clear that the flow turbulence has no major effect on the blowout limits as measurements for each method (i.e. constant fuel flow rate vs. constant air flow rate) follow similar trends. It was noticed that the poor atomization at lower fuel flow rate has significant effect on n-dodecane causing its lean blow out limit to increase with reduced fuel flow. The influence of air flow turbulence on spray characteristics, such as droplet sizes and velocities will be investigated in more detailed in Chapter 3

2.6.2 The Role of Local Enrichment on Ignition Delay of Single Fuels in FIT

Many ignition delay measurement equipment, *e.g.* RCM and shock tube, measure a fuel's gas phase ignition behaviors, which is not often representative of ignition in real liquid fuel engines. The FIT provides an ideal/simple environment (compared to a real engine) to investigate the role of evaporation on ignition delays of liquid fuels. The FIT's ignition delay is influenced by the chemical kinetics and the mixing/evaporation of the liquid fuel. It is also influenced by the locally fuel rich environment immediately surrounding the droplet/spray as previously suggested [21-25].

The measured and corrected ignition delays from the FIT are provided in Table 2.4 for n-heptane and n-dodecane at multiple gas temperatures and pressures. For clarification, the results in Table 2.4 are plotted in Fig. 2.9. When the pressure and temperature were decreased the ignition delay for both fuels increased as expected. It should also be noted that measurements carried out at lower pressures resulted in the injection of more fuel resulting in higher global equivalence ratios. In each case tested, n-dodecane ignites faster than n-heptane, despite repeatedly exhibiting a leaner global equivalence ratio than that of n-heptane. The reason is believed to be due to the significant effect that local enrichment has on the ignition delay, i.e., more so than the global

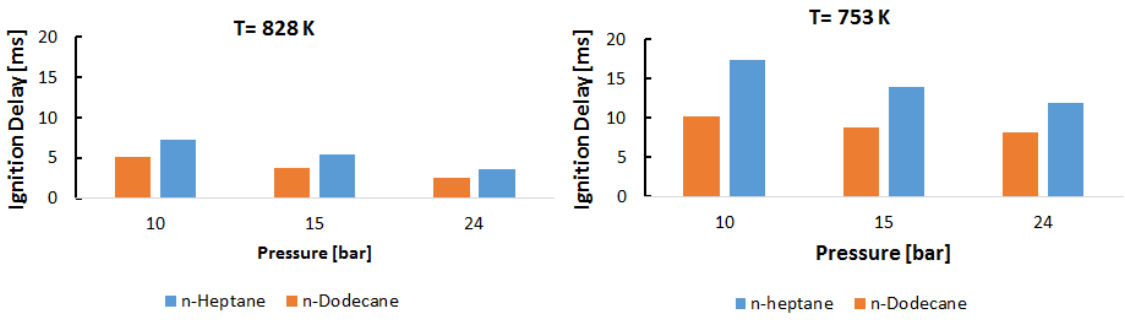

Figure 2.9. FIT ignition delays at different temperature and pressures, e.g. T_air=753 & 828 K and P_air=24,15 & 10 bar, for n-heptane and n-dodecane.

equivalence ratio. This represents the same phenomenon/impact noticed in the blowout limit measurements.

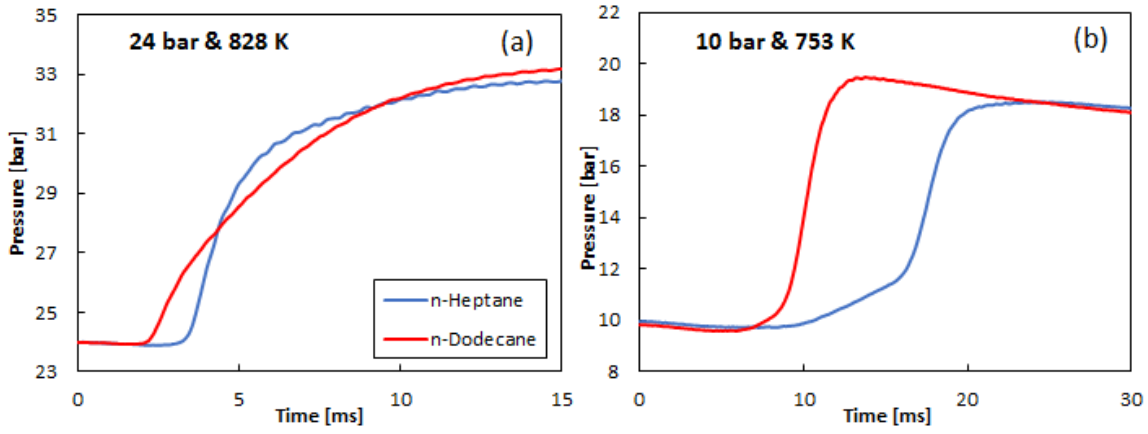

Figure 2.10. FIT Pressure traces at two different conditions: a) at 24 bar and 828 K, b) at 10 bar and 753 K, for n-heptane and n-dodecane.

Figure 2.10 illustrates measured pressure traces for each fuel at two different conditions, e.g. the first condition is at 24 bar & 828 K, where the second is at 10 bar & 753 K, for pressure and temperature, respectively. In Fig. 2.10a, at conditions of high pressure and temperature, e.g. 24 bar and 828 K, the n-dodecane pressure trace experiences a slower rise than that of n-heptane. This can be attributed to the difference in the fuel's volatility. This means that the vaporization time of n-dodecane fuel takes longer time compared with n-heptane, and thus the heat release experiences a delay. However, as the pressure and temperature were decreased, the pressure traces for both fuels experience rapid rise rates as demonstrated in Fig. 2.10b. This stems from the fact that within the less extreme environment, lower pressure and temperatures, ignition is delayed allowing more time for the reactants to mix and a homogeneous mixture to exist. This explains the increased difference in the ignition delays between the two fuels, as n-heptane evaporates and mixes with the air faster than n-dodecane (stemming from differences in volatility), generating a leaner charge

and extending ignition timing. It is noticed that the pressure trace of n-heptane exhibited a resemblance of a two-stage ignition. Thus, it will be a source of a future investigation.

2.7 Conclusions

Volatility of single liquid fuels plays a significant role in the flame stability. The less volatile fuels showed higher liftoff height because of the need for more time for the liquid droplets to evaporate before ignition. They also were the most difficult fuels to blowout. The fuel's reactivity has impact on flame liftoff heights responsible for differences in liftoff heights for n-heptane and iso-octane. In addition, the fuel atomization process (droplet size) has a major role in flame stability (in both liftoff height and blowout limits) and will be investigated in details in Chapter 3 and 4 by first looking into the role of varying fuel and/or air flow rates on the spray characteristics, including droplet size (SMD). Then, the influence of atomization and vaporization processes on flame stability will be investigated in Chapter 4.

It was noticed that the local enrichment can impact the fuel ignition delay more significantly than the global equivalence ratio in the FIT. Even though n-heptane has an overall larger global equivalence ratio than n-dodecane, n-dodecane consistently ignites faster than n-heptane. The impact of local enrichment was noticed to have also a major effect on the blowout out limit of single fuels. Again, this will be discussed later (Chapter 4) by looking into the spatial spray distribution of the different fuels and how this phenomena can influence flame stability.

Several unanswered questions have been raised, after completing this first step, and thus they need to be addressed before any further investigations:

(1) How accurate is the Lefebvre correlation in predicting the SMD of the different fuels and conditions using ACS burner?

(2) What are the influences of the operation conditions that we are using in this work, such as varying fuel and air flow rates, on the spray properties (spray droplet sizes, velocity, and distribution, as well as the turbulence intensity)?

(3) If we need to study the influence of vaporization (even preferential vaporization for multicomponent fuels) and chemical reactivity for number of fuels with different physical properties (density, viscosity, surface tension), how can we control the atomization process (e.g., SMD) to provide a fair comparison?

References

[1] A.H. Lefebvre, Gas turbine combustion, CRC press1998.
[2] A.H. Lefebvre, Gas turbine combustion: alternative fuels and emissions, CRC press2010.
[3] S.C. Burke, M. Ratcliff, R. McCormick, R. Rhoads, B. Windom, Distillation-based Droplet Modeling of Non-Ideal Oxygenated Gasoline Blends: Investigating the Role of Droplet Evaporation on PM Emissions, SAE International Journal of Fuels and Lubricants 10 (2017) 69-81.
[4] A. Stagni, L. Esclapez, P. Govindaraju, A. Cuoci, T. Faravelli, M. Ihme, The role of preferential evaporation on the ignition of multicomponent fuels in a homogeneous spray/air mixture, Proceedings of the Combustion Institute 36 (2017) 2483-2491.
[5] N. Kurimoto, N. Watanabe, S. Hoshi, S. Sasaki, M. Matsumoto, Numerical Modeling of International Variations in Diesel Spray Combustion with Evaporation Surrogate and Virtual Species Conversion, SAE International, 2017.
[6] L.M. Itani, G. Bruneaux, A. Di Lella, C. Schulz, Two-tracer LIF imaging of preferential evaporation of multi-component gasoline fuel sprays under engine conditions, Proceedings of the Combustion Institute 35 (2015) 2915-2922.
[7] J.E. Madero, R.L. Axelbaum, Spray breakup and structure of spray flames for low-volatility wet fuels, Combustion and Flame 180 (2017) 102-109.
[8] Y. Pei, M. Mehl, W. Liu, T. Lu, W.J. Pitz, S. Som, A multicomponent blend as a diesel fuel surrogate for compression ignition engine applications, Journal of Engineering for Gas Turbines and Power 137 (2015) 111502.
[9] M. Mehl, W.J. Pitz, C.K. Westbrook, H.J. Curran, Kinetic modeling of gasoline surrogate components and mixtures under engine conditions, Proceedings of the Combustion Institute 33 (2011) 193-200.
[10] D. Diadem, DIPPR information and data evaluation manager for the design institute for physical properties. 2006, BYU.
[11] A. Lefebvre, Atomization and sprays, combustion: an international series, Hemisphere Pub. Corp (1989).
[12] L. Esclapez, P.C. Ma, E. Mayhew, R. Xu, S. Stouffer, T. Lee, H. Wang, M. Ihme, Fuel effects on lean blow-out in a realistic gas turbine combustor, Combustion and Flame 181 (2017) 82-99.
[13] D. ASTM, 6890 Standard Test Method for Determination of Ignition Delay and Derived Cetane Number (DCN) of Diesel Fuel Oils by Combustion in a Constant Vol, Chamber, 2011.
[14] M.E. Baumgardner, S.M. Sarathy, A.J. Marchese, Autoignition characterization of primary reference fuels and n-heptane/n-butanol mixtures in a constant volume combustion device and homogeneous charge compression ignition engine, Energy & Fuels 27 (2013) 7778-7789.
[15] M.S. Mansour, I. Alkhesho, S.H. Chung, Stabilization and structure of n-heptane flame on CWJ-spray burner with kHZ SPIV and OH-PLIF, Experimental Thermal and Fluid Science 73 (2016) 18-26.
[16] A. Verdier, J. Marrero Santiago, A. Vandel, S. Saengkaew, G. Cabot, G. Grehan, B. Renou, Experimental study of local flame structures and fuel droplet properties of a spray jet flame, Proceedings of the Combustion Institute 36 (2017) 2595-2602.
[17] S. Marley, E. Welle, K. Lyons, W. Roberts, Effects of leading edge entrainment on the double flame structure in lifted ethanol spray flames, Experimental thermal and fluid science 29 (2004) 23-31.

[18] I. Düwel, H.W. Ge, H. Kronemayer, R. Dibble, E. Gutheil, C. Schulz, J. Wolfrum, Experimental and numerical characterization of a turbulent spray flame, Proceedings of the Combustion Institute 31 (2007) 2247-2255.
[19] J. Grohmann, W. O'Loughlin, W. Meier, M. Aigner. Comparison of the Combustion Characteristics of Liquid Single-Component Fuels in a Gas Turbine Model Combustor. In: editor^editors. ASME Turbo Expo 2016: Turbomachinery Technical Conference and Exposition; 2016: American Society of Mechanical Engineers. p. V04AT04A010-V004AT004A010.
[20] J. Grohmann, B. Rauch, T. Kathrotia, W. Meier, M. Aigner, Influence of Single-Component Fuels on Gas-Turbine Model Combustor Lean Blowout, Journal of Propulsion and Power (2017) 1-11.
[21] V.Y. Basevich, A. Belyaev, V. Brandshteter, M. Neigauz, R. Tashl, S. Frolov, Simulation of auto-ignition of iso-octane and n-heptane in an internal combustion engine, Combustion, Explosion, and Shock Waves 30 (1994) 737-745.
[22] G.E. Bogin Jr, E. Osecky, J. Chen, M.A. Ratcliff, J. Luecke, B.T. Zigler, A.M. Dean, Experiments and computational fluid dynamics modeling analysis of large n-alkane ignition kinetics in the ignition quality tester, Energy & Fuels 28 (2014) 4781-4794.
[23] G.E. Bogin Jr, E. Osecky, M.A. Ratcliff, J. Luecke, X. He, B.T. Zigler, A.M. Dean, Ignition quality tester (IQT) investigation of the negative temperature coefficient region of alkane autoignition, Energy & Fuels 27 (2013) 1632-1642.
[24] G.E. Bogin Jr, A. DeFilippo, J.Y. Chen, G. Chin, J. Luecke, M.A. Ratcliff, B.T. Zigler, A.M. Dean, Numerical and experimental investigation of n-heptane autoignition in the ignition quality tester (IQT), Energy & Fuels 25 (2011) 5562-5572.
[25] Y. Ra, R.D. Reitz, J. McFarlane, C.S. Daw, Effects of Fuel Physical Properties on Diesel Engine Combustion using Diesel and Bio-diesel Fuels, SAE International Journal of Fuels and Lubricants 1 (2008) 703-718.

CHAPTER 3: Effects of Varying Liquid Fuel and Air Co-flow Rates on Spray Characterization of ACS Burner[2]

3.1 Summary

The processes, which real liquid fuels experience in IC engines, are interconnected; the atomization process, which leads to various droplet sizes can enhance or diminish the vaporization rate of the liquid fuel and consequently impact the energy conversion process. Furthermore, the combustion/flame stability of liquid-fueled gas turbine can be influenced by the fuel and the air co-flow rates delivered in the engine. Increasing the fuel and/or air flow rates can enhance droplet breakup and the turbulence of the flow, and as a result sway the droplet size distribution of the spray. This work focuses on investigating the impact of varying the fuel and air flow rates on the spray atomization (e.g. droplet size distribution) of an Annular Co-Flow Spray Burner. This was explored by measuring droplet sizes and velocities of the spray at different radial and axial positions of n-heptane fuel under nonreacting conditions. In addition, the turbulence intensity and the liquid spray droplet distribution were quantified for different fuel and air flow rate conditions. The measurements were obtained by using a Phase Doppler Particle Analyzer/Laser Doppler Velocimeter (PDPA/LDV) at P = 1 atm and T = 298 K. Moreover, the Sauter Mean Diameters for different flow conditions are predicted, using an established correlations, and compared to PDPA/LDV measurements. The results provided a fair understanding of the influence of varying the fuel and air flow rates on the droplet sizes, velocity, and turbulent intensity. Furthermore, the

[2] This chapter is largely based on a published manuscript: Alsulami, Radi A., et al. "Effects of Varying Liquid Fuel and Air Co-floe Rates on Spray Characterization of an Annular Co-flow Spray Burner." *ASME Turbo Expo 2019: Turbomachinery Technical Conference and Exposition.*

results presented here will support future work that will focus on unraveling the role of phase change on flame stability.

3.2 Introduction

The optimization of combustion systems is essential, as a result of the current environmental and energy requirements. Therefore, the complex interaction between the processes which govern the combustion of liquid fuel, including atomization, fuel/air loading and mixing, and chemical reactions in multi-phase and turbulent environment, should be understood to achieve optimal performance. This understanding can be achieved by studying each process that liquid fuels experience in a combustion engine individually before any further complex investigation. For example, when the role of atomization, volatility and reactivity of different fuels on flame stability of combustion system is meant to be studied, it is desirable to begin with the atomization process (e.g. characterization of the spray distribution and the factors that can influence it) for a single fuel. Thus, the complexity of the problem can be broken down and a full understanding can be reached.

The atomization process and the dynamics of liquid fuel spray are important in determining flame stability at varying load, safe and efficient energy conversion, and pollutant formation for spray combustion as it becomes a main part of many energy conversion devices [1]. As such, the spray droplet distribution (SDD), velocity, and the penetration of the spray, as well as the flow turbulence, play a significant role in the cleaner energy conversion process as suggested in many previous works, including [2-4], and therefore it is desirable to be investigated.

There has been a substantial amount of work investigating the influence of fuel properties, such as viscosity and surface tension, and fuel injection pressure on the atomization behavior of liquid fuel for different nozzle types, e.g., [5-9]. In particular, Fisher et al. [5], examined fundamental spray characteristics under nonreacting conditions of flow-blurring (FB) atomizer for

fluids with different physical properties. Other works have implemented similar efforts on understanding the turbulent two-phase combustion of spray burner, such as [10-13], as it remains a challenge for experiments and numerical simulations because of the complex interaction of the different mechanisms that govern spray combustion. Although many researchers have carried out extensive experiments to study the relationships between the atomization process (i.e. droplet size and velocity) and flame stability mechanism using a spray burner, the factors (e.g. air co-flow and fuel flow rates), which can influence the spatial SDD, velocity, and turbulence need more investigation. The impacts of these factors are essential when, for instance, the flame stability limits are investigated. Moreover, the ability to maintain combustion inside a gas turbine combustor over a wide range of operating conditions (e.g. fuel/air ratio, temperature, and pressure) is one of the primary requirements, especially for aircraft engines [14, 15].

Detailed experimental works of spray surrounded by co-flowing turbulent air stream were performed to measure droplet sizes and distributions by limited number of studies, such as [16, 17]. Sommerfeld et al. [16], measured droplet sizes, distributions, velocities, and droplet mass fluxes using PDPA for hollow cone spray with co-flow heated airstream. This is was done for different flow conditions, i.e., varying air and liquid flow rates and air temperatures. The results showed that low air injection velocities as compared to the droplet initial velocity increase the evaporation rate as a result of the larger droplet interaction time (resident time) with the surrounding heated air. In addition, the decreasing of air injection velocity allows for a wider radial spray.

The experimental study of Yule et al. [17], focused on the development and testing of a Laser Doppler Velocimeter (LDV) with top-hat intensity profile in the probe volume to measure the droplet size distributions and droplet velocities for kerosene spray surrounded by heated co-flow.

The measurements showed increasing droplet sizes, as one moves downstream away from spray tip. This was argued to be caused by the preferential vaporization of the smaller droplets. Similar arguments were listed in Sinha et al. study using a spray in a crossflow configuration, where droplet sizes and velocities are measured at different locations along the crossflow direction to estimate droplet evaporation [18]. In each of these previous works, however, limited air and fuel flow rates have been investigated and a comprehensive mapping of the 2-D spray/droplet parameters is not presented for a spray with an annular co-flow.

This work focuses on investigating the impact of varying the fuel and air flow rates on the spray atomization (e.g. droplet size distribution) of an Annular Co-Flow Spray Burner (ACF-Spray Burner). This is explored by measuring the droplet sizes and velocities of the spray at different radial and axial positions of n-heptane fuel under nonreacting conditions (i.e. a cold spray). In addition, the turbulence intensity and the liquid spray droplet distribution are quantified for different fuel and air flow rate conditions. The measurements are obtained by using Phase Doppler Particle Analyzer/Laser Doppler Velocimetry (TSI PDPA/LDV) at P = 1 atm and T = 298 K. Moreover, the Sauter Mean Diameters (SMD) for different flow conditions are calculated, using established correlations, and compared to the PDPA measurements. The results provide a fair understanding of the influence of varying the fuel and air flow rates on the droplet sizes, velocity, and turbulent intensity and demonstrate the large spatial variation in these parameters that can be expected. In addition, a comparison between estimated and measured SMD is carried out and a discussion regarding when one can use previously derived correlations to predict droplet diameters is provided. These results provide the necessary baseline for future studies that will focus on further understanding the role of phase change on flame stability and dynamics.

3.3 Experimental Setup

3.3.1 Facility

An Annular Co-flow Spray Burner (ACS Burner) was used to investigate the impact of varying the fuel and air flow rates on the spatial SDD, velocity, and turbulence experienced by a nonreacting n-heptane fuel spray. The experimental setup and the burner description are provided in Chapter 2. The general pattern of the nonreacting cold spray is also illustrated by way of a light scattering spray image seen in Fig. 3.1. The fuel and the air are delivered to the spray burner at room temperature of 298 K.

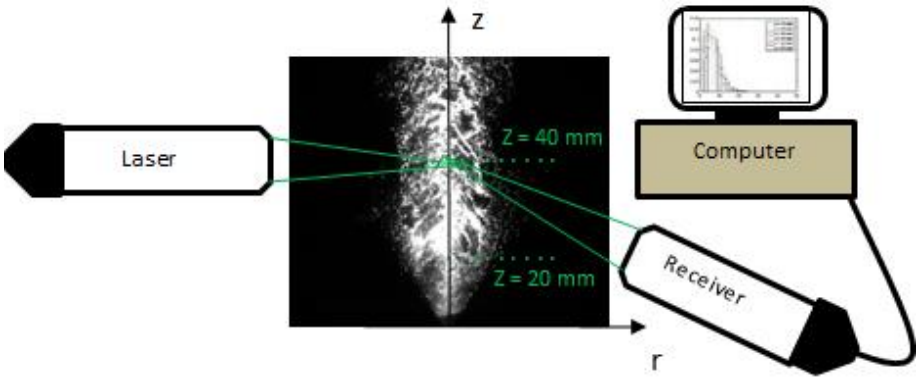

Figure 3.1. The nonreacting cold spray pattern of n-heptane fuel and schematic of the PDPA/LDV laser system.

3.3.2 Phase Doppler Particle Analyzer (TSI PDPD)

A schematic of the PDPA/LDV laser used in this study is illustrated in Fig. 3.1. Laser Doppler Velocimeter (LDV) and Phase Doppler Particle Analyzer (PDPA) systems measure the velocity and diameter of small droplets in a fluid. These systems use two crossing laser beams, specifically the interaction of these two beams to calculate the velocity and diameters of these droplets. At the location, which the two laser beams meet, they interact with each other causing both constructive and destructive interference and creating a fringe pattern. Because the wavelength, distance from

the laser lens, and the frequency of these beams are known, this fringe pattern of light and dark regions can be calculated. When a droplet enters this fringe pattern it obscures the light from reaching the receiver, which detects a sinusoidal profile with both high and low frequency. The velocity of the droplet can be calculated from this sinusoidal profile using the known values of the laser beams. In the case of PDPA, two receivers are offset from each other by a known distance and high frequency in these sinusoidal profiles that are detected have a phase shift. Using the known offset between the receivers allows for the calculation of the droplet diameters from this phase shift.

The system used in the current study consisted of a TSI Powersight laser (Model No. TR-SS-1D-532) and a receiver (Model No. 450300). One single 300-mW, 532 nm laser beam is split using a Bragg Cell into two crossing beams that form an intersection and sample volume in the vertical plane where droplets pass and get measured. The receiver was placed 40 degrees off axis of the laser. The receiver is equipped with two lenses, front and back, with focal lengths of 300 mm and 250 mm, respectively. Signals coming out of the receiver feed into the Photo-detector Module PDM1000-1PSS through photomultiplier tubes (PMTs). Signals are then transferred to a Flow and Size Analyzer (FSA3500-1P) which communicates with a PC using the FlowSizer64 software and provides measurements of size and velocity. For all measurements the detection limits in terms of diameter range from 0.5 μm to 161.1 μm.

For the validity of the measurement's time, data was first collected for 5 seconds (i.e. an average of ~30000 drops/location) and then compared to that of 1 second data (i.e. an average of ~5000 drops/location) for one condition, and they showed similar results. Thus, the PDPA/LDV system was setup to collect data for 1 second for all the specified locations and flow conditions. The droplet mean diameter and velocities were determined by averaging over the entire droplet

size spectrum. In addition, standard deviations were calculated for the different conditions and locations to illustrate the influence of varying fuel and air flow rates on the flow turbulence (RMS velocities). It is worth noting that all the velocities measured in this study are for the axial component.

The uncertainty for the PDPA measurements is investigated in many previous works by calculating the ratio of one standard deviation to the mean of multiple repeated measurements at the same condition [19-21]. The measurement uncertainty is estimated to be 5.9 and 2.9% for mean droplet diameter and mean droplet velocity, respectively [19].

Table 3.1. Summary of the measurement conditions, where $\dot{V}_F$ and $\dot{V}_a$ represent the fuel and air flow rates, respectively.

Constant Conditions	**Variable Conditions**	**Axial Measurements Positions**	**Radial Measurements Positions**
$\dot{V}_F = 40$ mL/min	$\dot{V}_a = 0$, 200, and 600 L/min	20 and 40 mm	0 , 2.5, 5, 7.5, 10, 12.5, 15, 17.5, and 20 mm
$\dot{V}_a = 200$ L/min	$\dot{V}_F = 40$, 50, and 65 mL/min	20 and 40 mm	0 , 2.5, 5, 7.5, 10, 12.5, 15, 17.5, and 20 mm
$\dot{V}_F = 50$ mL/min, $\dot{V}_a =$ 200 L/min	-	5, 10, 15, 20, 25, 30, 35, 40, 45, 50, 55, and 60 mm	0 (at the spray's centerline)

3.3.3 Experimental Conditions and Parameters

Experiments were carried out at T = 298 K & P = 1 atm with n-heptane as the fuel. The spray burner was kept stationary, while the PDPA system was setup to take measurements in a 2-D plane (z-dir and r-dir) above the spray burner scanned over. The primary focus of this study was to examine the influence of varying the fuel and/or the air flow rates on the spray characterization. Thus, the droplet size profile, SDD, velocity, and turbulence generated by the two flows were obtained for different radial positions and at multiple heights for all the conditions identified in

Table 3.1. In addition, the droplet size and velocity were obtained along the axial positions (e.g. at z = 5 - 60 mm with increments of 5 mm) for 50 mL/min and 200 L/min fuel and air flow rates, respectively. Below 5 mm there was an issue with taking data because of significant scattering due to high spray density and the possibility of the spray not being fully atomized.

3.4 Results and Discussion

3.4.1 Constant Fuel Flow Rate

Initial tests focused on understanding the influence of different air flow rates on the spray atomization by varying the air flow rates while maintaining a constant fuel flow rate of 40 mL/min. As illustrated by the radial profiles in Fig. 3.2a, the mean droplet velocities experience a dramatic rise, as the rate of air co-flow was increased. In general, the droplets decelerate with increasing height, which is expected due to the co-flow momentum reduction, especially at radial locations away from the spray centerline. However, opposite behavior is noticed as the air flow rate increased (e.g. 600 L/min) at the centerline, which is believed to be caused by turbulent secondary breakup, leading to the generation of smaller droplets with higher velocities. In general, it was noticed that the root mean square (RMS) velocities (i.e. turbulence intensity) is higher for large air flow rates over the radial positions, as illustrated in Fig. 3.2b. For all conditions, the velocity fluctuation is minimum along the axial centerline of the spray and peaks at the outer edge of the measurement's region. This indicates the presence of a higher mixing in the shear layer at the edge of the spray compared to the centerline region. Similar behavior was reported in a previous study [5]. With increasing the axial height, peak RMS velocity decays and profiles appears to flatten, as expected. However, opposite behavior was noticed with the case of 600 L/min air co-flow, where the peak velocity fluctuation was measured at location downstream, e.g., z= 40 mm. This can be interpreted that in the case of extreme co-flow (e.g. 600 L/min) the flow experiences a less wrinkle

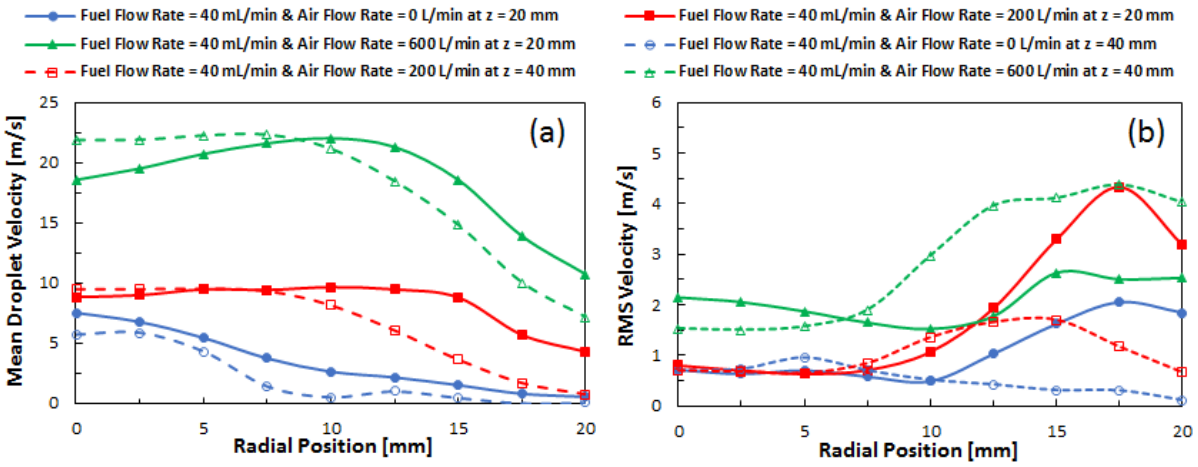

Figure 3.2. Mean velocity radial profiles (a) and RMS velocity profiles (b) at constant fuel flow rate and three different air flow rates at two axial positions, i.e., 20 mm (solid lines) and 40 mm (dashed lines). The uncertainty of the droplet velocity measurement is 2.9%.

region especially close to the tip of the burner before the development of a turbulent flow downstream and the spray droplets follow the stream line of the co-flow (low Stokes number). This behavior was noticed with other fuels that were tested at the same condition.

The droplet size profiles plotted versus the radial positions at two different heights are shown in Fig. 3.3. Droplet size is presented as the mean droplet diameter. For all conditions, the mean droplet diameter is smaller at the spray axis and increases with increasing radial distances. Surprisingly, the mean droplet size increases as higher air flow rates are delivered, especially at a height of 20 mm from the burner. In addition, it was noticed that for the air flow rates of 0, 200, and 600 L/min, the average number of droplets over the radial profile are 5083, 4863, and 1412, respectively for the same data collection time of 1 sec. This means that in the case of 600 L/min, ~72% of the droplets are below detection limits of the sensor and/or that some droplets are completely vaporized, likely caused by enhancement of the vaporization process as a result of increasing the air co-flow rate and the flow turbulence.

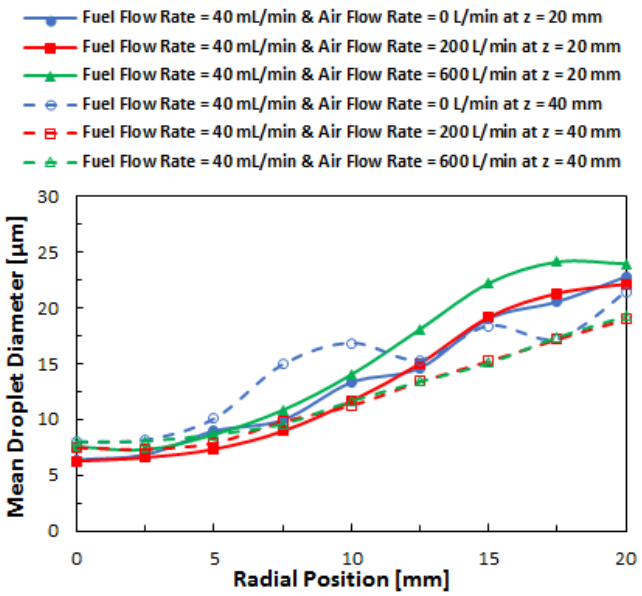

Figure 3.3. Mean radial droplet diameter profiles at constant fuel flow rate and three different air flow rates at two axial positions, i.e., 20 mm (solid lines) and 40 mm (dashed lines). The uncertainty of droplet diameter measurement is 5.9%.

To explain more clearly the reason of increasing the droplet sizes as the co-flow rate is increased, the SDDs (i.e., droplet sizes histograms or PDFs) for the axial position of 20 mm and at five radial positions are illustrated in Fig. 3.4. As a result of vaporization of smaller droplets, the mean droplet size increases as the co-flow rates rise. In addition, the number of droplets decrease at the outer edge of the measurement's region, as a result of exceeding the spray width region at z= 20 mm. In addition, the co-flow velocity enhances droplet breakup and evaporation near the spray edge. This can be seen by the reduction of the SDD counts at smaller diameters as the co-flow rate is increased. The histograms of the 40 mm axial location are provided in Appendix.

3.4.2 Constant Air Co-flow Rate

The influence of varying fuel flow rates on the spray characteristics was studied at a constant air co-flow rate of 200 L/min. As shown in Fig. 3.5a, the mean droplet velocities increase at the centerline of the spray as the fuel flow rates are increased. The mean droplet velocities converge

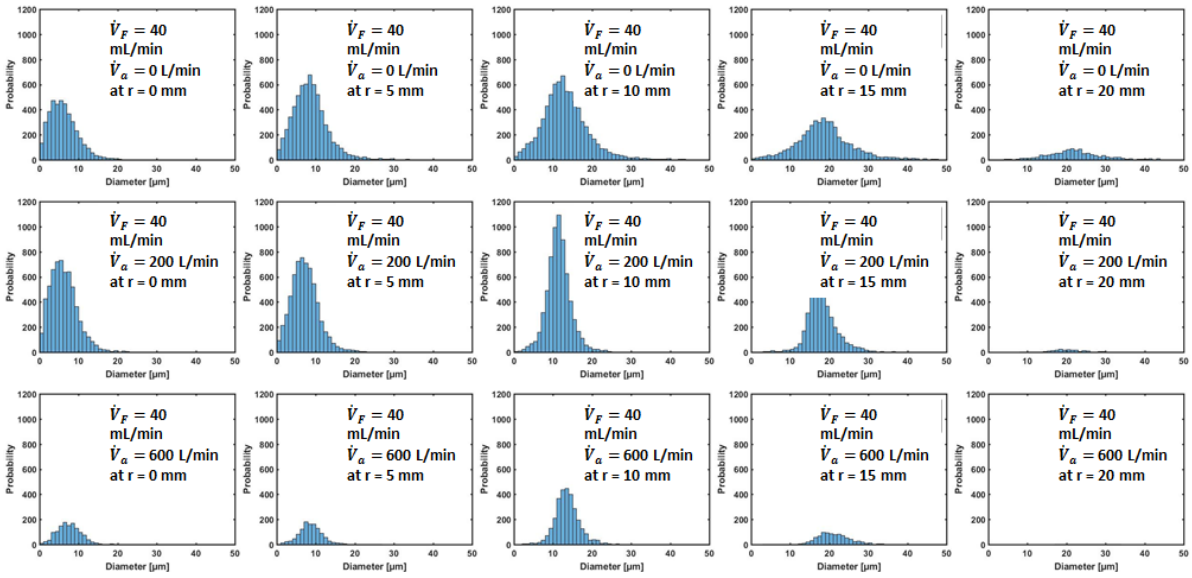

Figure 3.5. Histograms of spray droplet size distributions of constant fuel flow rate of $\dot{V}_F = 40$ mL/min and at three different air co-flow rates, i.e., $\dot{V}_a = 0, 200,$ and 600 L/min and at axial position of 20 mm. The histograms from left to right represent PDF of different radial positions, i.e., r = 0, 5, 10, 15, and 20 mm.

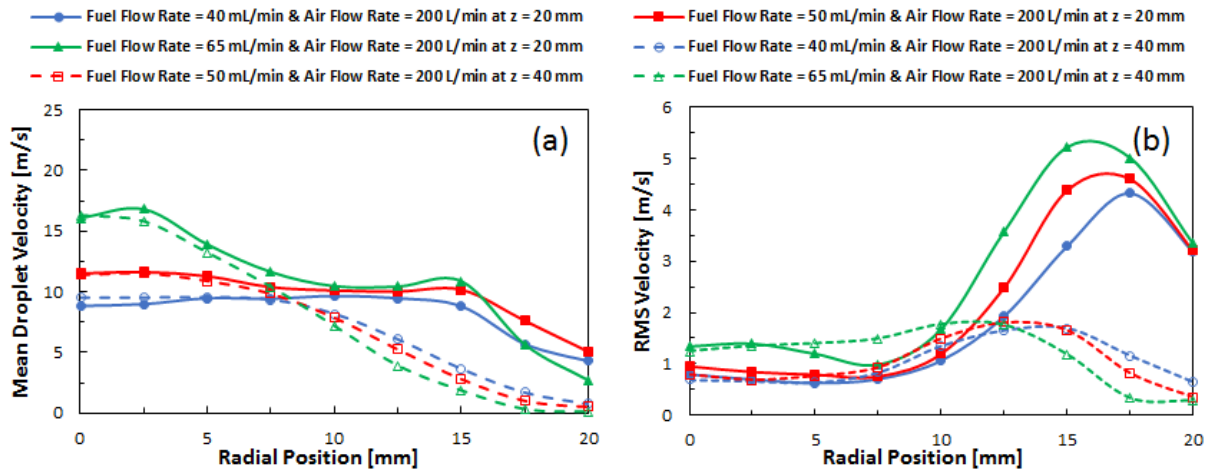

Figure 3.4. Mean radial profiles of droplet velocities (a) and RMS velocities (b) of constant air co-flow rate and three different fuel flow rates at two axial positions, i.e., 20 mm (solid lines) and 40 mm (dashed lines). The uncertainty of droplet velocity measurement is 2.9%.

to similar values for all conditions and follow the velocity pattern of the co-flow outside of the radial location of ~ 7.5 mm. The mean velocity profiles fall off after passing the location of the co-flow region (e.g., after a radial position of 15 mm). Similar trends were noticed farther downstream

(e.g. at z = 40 mm) at location close to the spray's centerline. However, the velocity profiles of each of the fuel flow rate conditions drop and become nearly quiescent at radial locations between 7.5 mm and the outer edge of the measurement's region. This is caused by the reduction of the co-flow momentum as the co-flow travels farther from the burner tip. In general, the turbulent intensity represented by RMS velocities in Fig. 3.5b increases as the fuel flow rates rise. All the conditions experience higher velocity fluctuation as the radial location increases, similar to behaviors noticed in previous studies [5, 22]. The peak of RMS velocities at axial location of 20 mm decays and all the different conditions' profiles become flatter.

In general, mean droplet sizes decrease, as the fuel flow rates increase, as shown in Fig. 3.6. This is caused by the pressure rise across the nozzle orifice, which improves the atomization process of the liquid fuel and generates smaller droplets. The influence of increasing fuel flow rate on reducing droplet size is more obvious at the edge of the spray for the axial position close to the

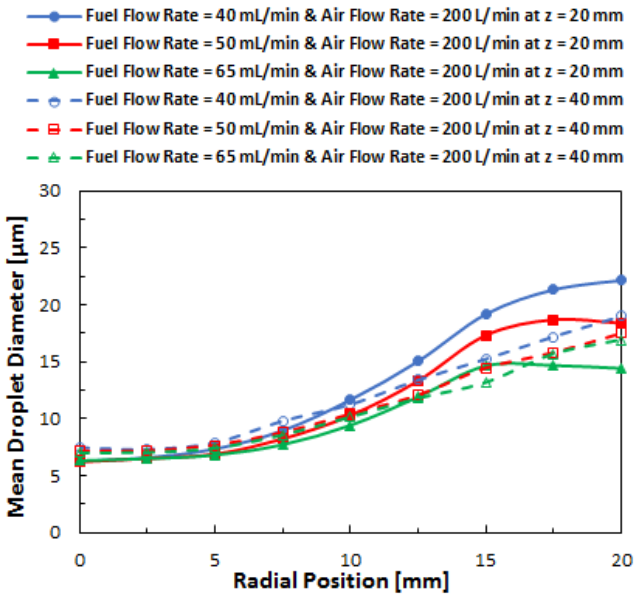

Figure 3.6. Mean radial droplet diameter profiles at constant air flow rate of 200 L/min and three different fuel flow rates at two axial positions, i.e., 20 mm (solid lines) and 40 mm (dashed lines). The uncertainty of droplet diameter measurement is 5.9%.

nozzle outlet (i.e. at z = 20 mm). Similar mean droplet sizes for all fuel flow rates is noticed at the downstream location (z = 40 mm), however the droplet size differences drop.

3.4.3 Spray Characterization along the Axial Centerline

The spray evolution and the effects of droplet vaporization and coalescence on the droplet diameter, velocity, and the flow turbulence are studied in this section for a fuel flow rate of 50 mL/min and an air co-flow rate of 200 L/min. This is done along the spray axial centerline as mentioned in Table 3.1.

Figure 3.7 shows the axial profiles of the mean droplet velocity, turbulent intensity, and droplet mean diameter along the spray centerline (i.e. at r = 0). The mean droplet velocity is affected by the turbulence generated by liquid spray and the air co-flow close to the nozzle and burner tips, which causes the drop in the velocity profile, as illustrated in Fig. 3.5a. Between the axial positions of 5 and 10 mm (i.e. near the nozzle tip), the droplet velocity decreases, which is believed to be caused by destruction of the air co-flow by the nozzle, which can cause a similar to stagnation region. However, as the air co-flow merges with the spray (i.e. between the axial positions of 10 mm and 25 mm), the mean droplet velocity increases. Thus, this is which believed to cause turbulent secondary breakup leading to the generation of smaller droplets with higher velocity. Then, as a result of the reduction of spray and co-flow momentums, the droplets decelerate at higher than 25mm axial positions. As expected, the turbulent intensity is at its peak close to the injector tip, before it reduces and levels out farther downstream away from the nozzle, Fig. 3.7b. Interestingly, the mean diameter of the droplets increases linearly with height above the burner, as shown in Fig 3.7c.

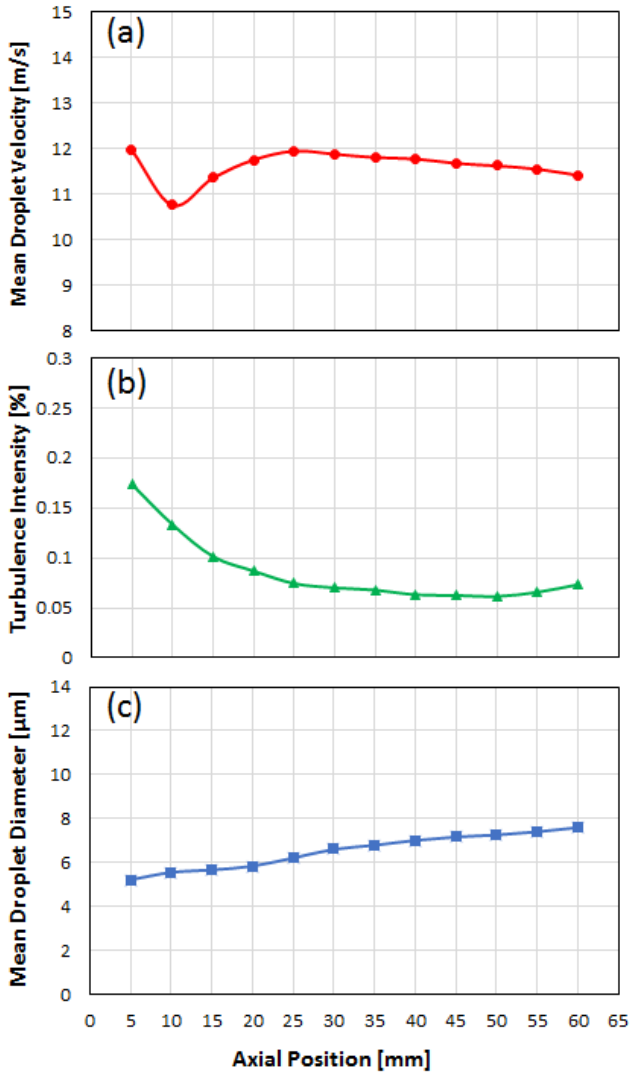

Figure 3.7. The axial droplet velocity, turbulence intensity, and droplets sizes profiles at r = 0. The uncertainty of droplet velocity and size measurements are 2.9% and 5.9%, respectively.

The normalized SDD at multiple axial locations (i.e. z = 5, 30, and 60 mm) along the centerline of the spray is illustrated in Fig. 3.8 It is clear that the SDD shifts to larger droplet sizes as the droplets travel away from the burner tip. This is believed to be caused by combined effects of droplet evaporation and coalescence. Smaller droplets evaporate faster, which leads to an increase in mean droplet size. To explain this, the droplet life time is calculated using d^2 law for different initial droplet diameters, as shown in Fig. 3.9. Here it is clear that the smaller droplets (e.g. 5 µm) take noticeably less time to evaporate compared to the larger droplet (e.g. 20 µm) as a result of the

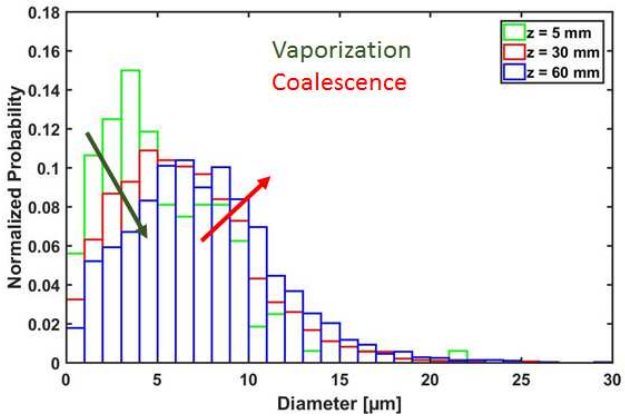

Figure 3.8. Normalized DSD probability at r = 0 and different axial positions.

differences in the surface area:volume ratio. For instance, as the droplet reach the axial position of 5 mm (i.e. the left edge of the shaded box in Fig. 3.9), smaller and bigger droplets have not completely evaporated. In contrast, at the axial position of 60 mm (i.e. the right edge of the shaded box in Fig. 3.9), only the smaller droplets have evaporated causing a shift in the droplet size distribution and an increase in the mean droplet sizes as illustrated previously in Fig. 3.8. It is worth noting that the lifetime of the droplets presented in Fig. 3.9 does not account for the influence of convection and thus should not be used to represent the absolute dynamics of the droplets here, but rather serves the primary purpose of highlighting the non-linear time scales that govern droplet

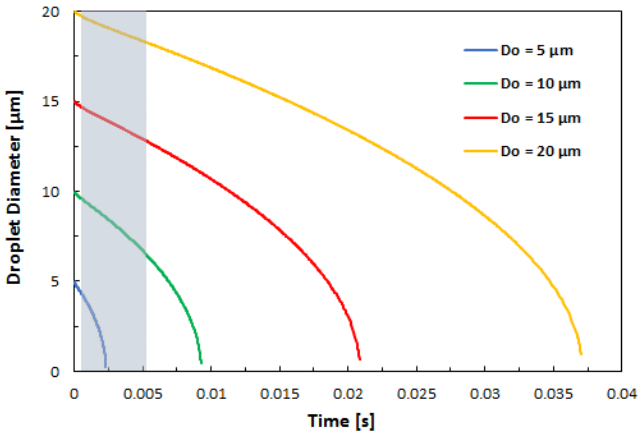

Figure 3. 9. Life times for four different droplet sizes calculated using d^2 law.

evaporation. In addition, because of the deceleration of the liquid and air momentums, droplets undergo slight deceleration, which can induce coalescence as mentioned by previous experimental and numerical works [5, 23-26] .

3.4.4 Comparison Between Measured and Predicted SMD

For the sake of comparison between the measured and calculated SMD results, a global Sauter Mean Diameter (SMD_{global}) is defined as a single parameter to represent the overall spray droplet size. Note that some studies use the same term, while others refer to different terms, such as integral, or overall SMD [27-29]. The simplified equation for the calculation of SMD_{global} over the complete radial cross section at a set axial location (i.e. 20 mm from the nozzle tip in this study) is given as the following:

$$\mathrm{SMD}_{\mathrm{global}} = \sum_{i=2}^{m}(r_i D_{30,i}^3 N_i) / \sum_{i=2}^{m}(r_i D_{20,i}^2 N_i) \tag{3.1}$$

where $D_{30,i}$ and $D_{20,i}$ are the volumetric and surface diameters of fuel droplets measured at the radial position r_i. N_i represents the number of droplets detected at the radial position r_i.

The measured SMD_{global} using PDPA is then compared to the SMD calculated by three well-known correlations, e.g. Radcliffe [30], Jasuja [31], and Lefebvre [32] given in order as the following :

$$\mathrm{SMD}_{Radcliffe} = 7.3\sigma_l^{0.6}\nu_l^{0.2}\dot{m}_l^{0.25}\Delta P^{-0.4} \tag{3.2}$$

$$\mathrm{SMD}_{Jasuja} = 4.4\sigma_l^{0.6}\nu_l^{0.16}\dot{m}_l^{0.22}\Delta P^{-0.43} \tag{3.3}$$

$$\mathrm{SMD}_{Lefebvre} = 2.25\sigma_l^{0.25}\mu_l^{0.25}\dot{m}_l^{0.25}\Delta P^{-0.5}\rho_{air}^{-0.25} \tag{3.4}$$

where σ_l is the liquid surface tension. μ_l and ν_l are the dynamic and kinematic liquid viscosities, respectively. $\dot{m}_l$ is the liquid mass flow rate, ΔP is the pressure drop across the spray nozzle and ρ_{air} is the surrounding air density. Notice that Eq. (3.4) was also used in Chapter 2, as Eq. (2.1).

The measured SMD_{global} for three different air flow rates is compared to the predicted SMD in Fig. 3.10a. When the air co-flow rate is zero, the correlations predicted the measured SMD_{global} well. However, because the influence of air co-flow is not included in the correlations, the predicted SMDs remain the same as the air flow rates increased. As discussed before, increasing the air co-flow rate increases the measured SMD_{global}. This can be attributed to faster evaporation of the smaller droplets causing the mean SMD to increase as highlighted in Fig. 3.8. To study the influence and the correlation's ability to predict the SMD_{global} while varying fuel flow rate, a constant air co-flow rate of 200 L/min were used. The results of this study are illustrated in Fig. 3.10b. Despite the global value of the measurements being larger than the predicted diameters, the predicted SMD does follows the measurement trend. The difference between the measured and predicted SMDs reduces as the fuel flow rate (i.e., ΔP) increases. This indicates that the correlations are more accurate for higher ΔP (~2 MPa). Consistently, the SMD predicted by Radcliffe's correlation is closest to the measured values, follow by Jasuja's correlation. It is

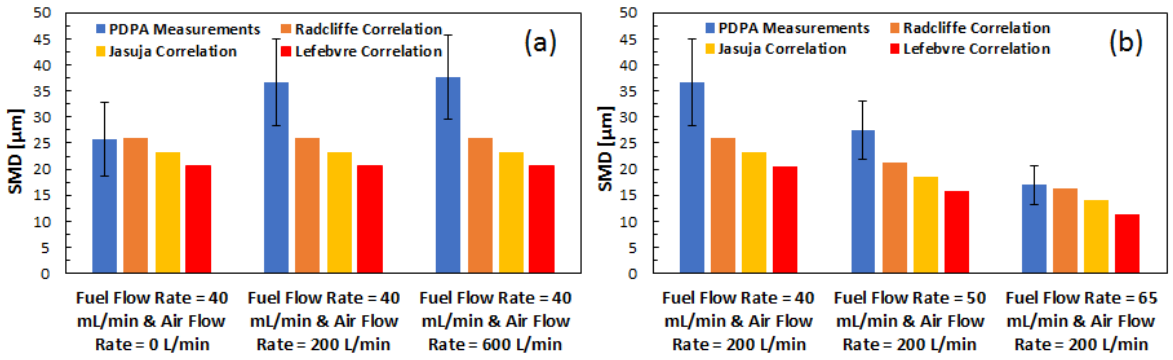

Figure 3.10. Comparison between the measured and estimated SMD for constant fuel flow rates and different air flow rates (a) and for constant air flow rates and different fuel flow rates (b).

noticed that the droplet sizes for both measured and predicted SMD decrease as the fuel flow rate increases. As expected and discussed previously, this is due to the increase in fuel pressure and increase in fuel flow rate described by the correlations (i.e., Eq. (3.2), Eq. (3.3), and Eq. (3.4)). The bars in Fig. 3.10 represent the droplet size distribution collected by the PDPA system for each condition.

3.5 Conclusions

The purpose of this work was to examine the effects of varying liquid fuel and air co-flow rates on spray characterization of ACS Burner under nonreacting conditions (i.e. cold spray). Droplet sizes and velocities were measured for n-heptane fuel at different radial and axial positions using PDPA system. In general, droplet velocities are at maximum around the centerline of the spray and decrease as radial and/or axial positions increase. The turbulence intensity (i.e. RMS velocity) is at a minimum along the axial centerline of the spray and peaks at the outer edge of the measurement's region (i.e. shear layer region). The solid cone spray generates smaller droplets close to the centerline and larger droplets for large radial distances from the spray axis with maximum diameters of ~ 25 μm. Based on the results and observations, the following conclusions can be drawn:

(1) The spatially dependent spray characteristics including droplet sizes, velocities, turbulence, and SDDs is highly influenced by the air co-flow rate and thus, influence droplet dissipation and vaporization.

(2) The spray characteristics is also influenced by the variation of liquid fuel flow rate. This influence is more obvious along the outer edge of the spray.

(3) The interaction between evaporation and coalescence phenomena of droplets in a spray has a major influence on the measured droplet sizes, velocities, turbulence, and SDDs. It is

shown that the evaporation of smaller droplets can increase the mean droplet size as one moves farther away from the nozzle tip.

(4) The correlations do well at predicting the relative change of the SMD with varying fuel flow rates, especially at higher ΔP. However, since the correlations do not account for the influence from a co-flow, the current formulas do not predict the increase in the global SMD when the air co-flow is raised.

References

[1] X. Jiang, G.A. Siamas, K. Jagus, T.G. Karayiannis, Physical modelling and advanced simulations of gas–liquid two-phase jet flows in atomization and sprays, Progress in Energy and Combustion Science 36 (2010) 131-167.

[2] R.P. Probert, XV. The influence of spray particle size and distribution in the combustion of oil droplets, The London, Edinburgh, and Dublin Philosophical Magazine and Journal of Science 37 (1946) 94-105.

[3] J.A. Bossard, R.E. Peck, Droplet sie distribution effects in spray combustion, Symposium (International) on Combustion 26 (1996) 1671-1677.

[4] H.G. Wagner, Soot formation in combustion, Symposium (International) on Combustion 17 (1979) 3-19.

[5] B.T. Fisher, M.R. Weismiller, S.G. Tuttle, K.M. Hinnant, Effects of Fluid Properties on Spray Characteristics of a Flow-Blurring Atomizer, Journal of Engineering for Gas Turbines and Power 140 (2017) 041511-041511-041518.

[6] A. Davanlou, J.D. Lee, S. Basu, R. Kumar, Effect of viscosity and surface tension on breakup and coalescence of bicomponent sprays, Chemical Engineering Science 131 (2015) 243-255.

[7] D. Sivakumar, S.K. Vankeswaram, R. Sakthikumar, B.N. Raghunandan, Analysis on the atomization characteristics of aviation biofuel discharging from simplex swirl atomizer, International Journal of Multiphase Flow 72 (2015) 88-96.

[8] J.E. Madero, R.L. Axelbaum, Spray breakup and structure of spray flames for low-volatility wet fuels, Combustion and Flame 180 (2017) 102-109.

[9] B. Abdollahipoor, S.A. Shirazi, K.F. Reardon, B.C. Windom, Near-azeotropic volatility behavior of hydrous and anhydrous ethanol gasoline mixtures and impact on droplet evaporation dynamics, Fuel Processing Technology 181 (2018) 166-174.

[10] F. Shum-Kivan, J. Marrero Santiago, A. Verdier, E. Riber, B. Renou, G. Cabot, B. Cuenot, Experimental and numerical analysis of a turbulent spray flame structure, Proceedings of the Combustion Institute 36 (2017) 2567-2575.

[11] A. Verdier, J. Marrero Santiago, A. Vandel, S. Saengkaew, G. Cabot, G. Grehan, B. Renou, Experimental study of local flame structures and fuel droplet properties of a spray jet flame, Proceedings of the Combustion Institute 36 (2017) 2595-2602.

[12] H. Correia Rodrigues, M.J. Tummers, E.H. van Veen, D.J.E.M. Roekaerts, Spray flame structure in conventional and hot-diluted combustion regime, Combustion and Flame 162 (2015) 759-773.

[13] S.H. Stårner, J. Gounder, A.R. Masri, Effects of turbulence and carrier fluid on simple, turbulent spray jet flames, Combustion and Flame 143 (2005) 420-432.

[14] C. Liu, F. Liu, J. Yang, Y. Mu, G. Xu, Investigations of the effects of spray characteristics on the flame pattern and combustion stability of a swirl-cup combustor, Fuel 139 (2015) 529-536.

[15] A.H. Lefebvre, Gas turbine combustion, CRC press1998.

[16] M. Sommerfeld, H.H. Qiu, Experimental studies of spray evaporation in turbulent flow, International Journal of Heat and Fluid Flow 19 (1998) 10-22.

[17] A.J. Yule, P.R. Ereaut, A. Ungut, Droplet sizes and velocities in vaporizing sprays, Combustion and Flame 54 (1983) 15-22.

[18] A. Sinha, R. Surya Prakash, A. Madan Mohan, R.V. Ravikrishna, Experimental studies on evaporation of fuel droplets under forced convection using spray in crossflow methodology, Fuel 164 (2016) 374-385.
[19] N.S. Rodrigues, V. Kulkarni, J. Gao, J. Chen, P.E. Sojka, An experimental and theoretical investigation of spray characteristics of impinging jets in impact wave regime, Experiments in Fluids 56 (2015) 50.
[20] N.S. Rodrigues, P.E. Sojka. A parametric investigation of gelled propellant spray characteristics utilizing impinging jet geometry. In: editor^editors. 52nd Aerospace Sciences Meeting; 2014. p. 1184.
[21] S.J. Kline, Describing uncertainty in single sample experiments, Mech. Engineering 75 (1953) 3-8.
[22] J.D. Gounder, A. Kourmatzis, A.R. Masri, Turbulent piloted dilute spray flames: Flow fields and droplet dynamics, Combustion and Flame 159 (2012) 3372-3397.
[23] J. Qian, C.K. Law, Regimes of coalescence and separation in droplet collision, Journal of Fluid Mechanics 331 (1997) 59-80.
[24] J. Nijdam, S. Stårner, T. Langrish, An experimental investigation of droplet evaporation and coalescence in a simple jet flow, Experiments in Fluids 37 (2004) 504-517.
[25] M. Ruger, S. Hohmann, M. Sommerfeld, G. Kohnen, EULER/LAGRANGE CALCULATIONS OF TURBULENT SPRAYS: THE EFFECT OF DROPLET COLLISIONS AND COALESCENCE, 10 (2000) 35.
[26] J.C. Lasheras, E. Hopfinger, Liquid jet instability and atomization in a coaxial gas stream, Annual review of fluid mechanics 32 (2000) 275-308.
[27] J. Jedelsky, M. Jicha, Energy considerations in spraying process of a spill-return pressure-swirl atomizer, Applied Energy 132 (2014) 485-495.
[28] A. Tratnig, G. Brenn, Drop size spectra in sprays from pressure-swirl atomizers, International Journal of Multiphase Flow 36 (2010) 349-363.
[29] J.-H. Im, D. Kim, P. Han, Y. Yoon, V. Bazarov, Self-pulsation characteristics of a gas-liquid swirl coaxial injector, Atomization and Sprays 19 (2009).
[30] A. Radcliffe, Fuel injection, High Speed Aerodynamics, and Jet Propulsion 11 (1960) 84.
[31] A. Jasuja, Atomization of crude and residual fuel oils, Journal of Engineering for Power 101 (1979) 250-258.
[32] A. Lefebvre, Atomization and sprays, combustion: an international series, Hemisphere Pub. Corp (1989).

CHAPTER 4: Investigating the Role of Fuel Atomization on Flame Stability of Liquid Fuels in an Annular Spray Burner[3]

4.1 Summary

When fuels with varying physical properties, e.g., density, viscosity and surface tension, are used in the same fuel injection system, they can exhibit very different atomization, represented by droplet size (SMD) and spray droplet distribution (SDD), which can then potentially influence the flame stability. In the current paper, the effect of the atomization process on flame stability is investigated by using a single nozzle size with three different hydrocarbon fuels, i.e., n-heptane, n-dodecane, and toluene. This study also investigates the flame stability for the same fuels using a unique approach in which nozzle sizes are selectively varied for each fuel to control the atomization process and minimize differences in the spray characteristics between the different fuels and this influence on flame stability. As such, this approach can be used to better understand the sensitivity of the various fuel properties, e.g., the fuel's volatility and chemical reactivity, on global flame behaviors/combustion stability. The results presented here show that the atomization process plays a major role in the flame liftoff heights and blowout limits. Thus, the large droplet and less volatile fuel, e.g., n-dodecane, exhibit higher flame liftoff heights and the most resistance to flame blowout compared to the other tested fuels. When the atomization process controlled by minimizing the differences in the spray properties (e.g., SMD and SDD) of the tested fuels, more similar liftoff heights and blowout limits for the set fuels where observed as compared to the results from the common nozzle approach. The differences in liftoff height was shown to be a result of two-phase flame speed, which accounts for both pre-vaporized fuel reactivity defined by laminar

[3] This chapter is largely based on a submitted manuscript: Alsulami, Radi A., et al. "Investigating the Role of Atomization on Flame Stability of Liquid Fuels in an Annular Spray Burner." *Fuel (2019).*

flame speed (S_L) and time scales associated with droplet evaporation. In addition, the differences in blowout was also largely tied to fuel volatility and droplet size (SMD) (i.e., liquid loading to flame) along with heat release.

4.2 Introduction

The physical and chemical properties of liquid fuels, as well as, the process that liquid fuel goes through, e.g., atomization, vaporization, and fuel/air mixing, in IC engines can influence the combustion process and emissions [2-14]. The first step toward the cleaning and efficient energy conversion is the atomization of liquid fuels into small droplets with large surface area to extract the maximum energy from them. The atomization quality can have a significant impact on the following processes, such as vaporization and mixing, and thus on flame stability and behavior. Therefore, special focus should be implemented on this phenomena. In fact, many previous works have been confined to only mentioning the significant importance of the atomization process on the flame stability but not quantifying it (e.g., [15-20]).

4.2.1 Two-Phase Flame Stability

Lean blowout (LBO) is an important characteristic to evaluate the combustion performance of fuels [21], especially for those which are used in a gas-turbine engine. For a premixed flame, the blowout limit is influenced by the chemical kinetics and transport of heat and mass (i.e., a Damkohler number), as discussed in details by the review work of Shanbhogue et al. [22]. Spray flame stability is influenced by much of the same physics that control gas phase (premixed/non-premixed) flame, but also must include the time scales associated with gas phase mixture formation, which are driven by spray properties and the vapor-liquid equilibrium (VLE) of the fuel.

Many works have studied the LBO phenomena for different fuels and using different combustors, and thus variations in the conclusions have been reached. For example, Burger et al. [23] studied the flame blowout behavior for 16 different fuels (i.e., different blends that comprised a mix of conventional Jet A-1, synthetic paraffinic kerosene, linear paraffinic solvents, aromatic solvents and pure compounds) at an air inlet temperature of 310 K, using laboratory-scale swirl-stabilized spray flame. They found that the easiest fuels to vaporize were the most difficult to reach blowout limit. They tried to correlate the LBO results to a number of variables, such as derived cetane number (DCN) and Sauter mean diameter (SMD), however a weak correlation was found. They concluded that lean blowout limits are potentially influenced by both physical and chemical fuel properties. After that, Grohmann et al. [3] studied the LBO behavior of different single hydrocarbon fuels, including n-hexane, iso-octane, and n-dodecane, in addition to Jet A-1, at two different air preheated temperatures, using a burner with a pressure-swirl atomizer to form a hollow spray cone surrounded by swirling airflows. At a temperature of 323 K, in contrast to Burger at al. observation, they found that the differences in the atomization (droplet sizes) and vaporization of the different tested fuels, especially n-hexane and n-dodecane, were important parameters in the LBOs with the fuels forming bigger droplets and exhibiting lower volatility (e.g., n-dodecane) being the most difficult fuel to blowout. At higher temperature (e.g., 423 K), no clear conclusion was listed.

A number of previous studies, e.g., [24-26], have shown that the LBO correlates best with the derived cetane number (DCN), especially at higher flow temperatures. This makes sense as the DCN effectively describes the ability of a fuel to undergo two-phase ignition, which is driven by many of the same physical processes important in spray flame stability including atomization, vaporization, ignition chemistry, and molecular/thermal diffusion. Notably, the DCN is measured

using techniques which do not control for the atomization, thus, the DCN is also sensitive to atomization/spray properties when fuels with significant differences in physical properties, e.g., density, viscosity and surface tension, are compared. As such, the DCN does well at providing a measure of how different fuels will perform for a given fuel delivery system. However, further studies are needed to clearly understand the influence of atomization relative to other influences to ultimately support both fuel selection as well as engine hardware design.

A number of works have attempted to correlate flame LBO to the combustor geometry and/or the fuel properties. Lefebvre [27] correlated the LBO to the combustor volume and the amount of air entering the primary combustion zone, the temperature and pressure of inlet gas, and the fuel's physical/chemical properties important in describing mean droplet sizes, effective evaporation, and heat of combustion. Lefebvre's theory has been used to quantify the effect of fuel properties on the LBO limit in several studies, including [21, 28, 29].

Flame liftoff height is another important flame stability behavior, which can be influenced by the two-phase spray process. The majority of previous literature, which has attempted to understand the mechanism that controls lifted flame stability, has been performed with gaseous fuels, as reviewed by [30, 31]. The edge-flame concept first proposed by Buckmaster [32], has been used to explain lifted flame behavior in non-premixed gaseous flames and considers the leading edge to be a partially premixed flame (where the mixture is at near stoichiometric mixture fraction) located where the flame burning velocity is at a balance with the incoming flow velocity. Because of the complexity of heterogeneous spray flame phenomena, which arises from the interconnection of a number of processes such as atomization, vaporization, and chemical kinetics, none of the previous work has developed correlations for spray flame liftoff heights and the fuel's physical and chemical properties. Thus, the present research seeks to address a gap in the

literature by defining the mechanism which control liftoff height for spray flames surrounded by an annular air co-flow.

It is clear that previous work led to a variety of conclusions, and thus more investigation is needed to understand the mechanism of LBO and flame liftoff height, especially for heterogeneous combustion systems. To achieve this, a range of questions thus arise: (1) What are the factors that can affect the atomization of different fuels, (2) how do differences in the atomization process influence flame stability, and (3) can differences in spray properties, such as, SMD and SDD of different fuels be minimized to isolate and better understand the role of the evaporation phenomenon and/or reactivity on observed flame dynamics and stability? For these questions to be answered, carefully controlled experiments are required, which can regulate the atomization process while observing differences in flame behaviors for different fuels.

The current work aims to investigate the role of the atomization process, quantified by a number of spray properties (e.g., SMD and SDD) on flame stability using three single liquid hydrocarbon fuels: n-heptane, n-dodecane, and toluene. The impact of the atomization process on flame stability is determined by comparing the different fuels' spray properties and their flame liftoff heights and blowout limits with results using identical injectors for all three fuels. The relationship between the fuels' properties, e.g. volatility and reactivity, on the combustion/flame stability is examined by controlling the spray performance using a unique variable nozzle approach. The spray droplet sizes, i.e., SMD, for the different fuels and conditions are predicted using three previously reported correlations and verified using Phase Doppler Particle Analyzer/Laser Doppler Velocimetry (TSI PDPA/LDV).

4.3 Experimental Setup and Conditions

4.3.1 Annular Co-flow Spray Burner

To investigate the role of the atomization process on flame stability of different hydrocarbon fuels, an Annular Co-flow Spray burner (ACS burner) was used. The experimental schematic is illustrated in Fig. 4.1 and it is also described in Chapters 2, and 3. In this chapter, multiple nozzle injectors with varying size (Delavan 80 ° B solid nozzle) were used to control the spray properties of the different selected fuels. The orifice diameters for the nozzles used in this study are provided

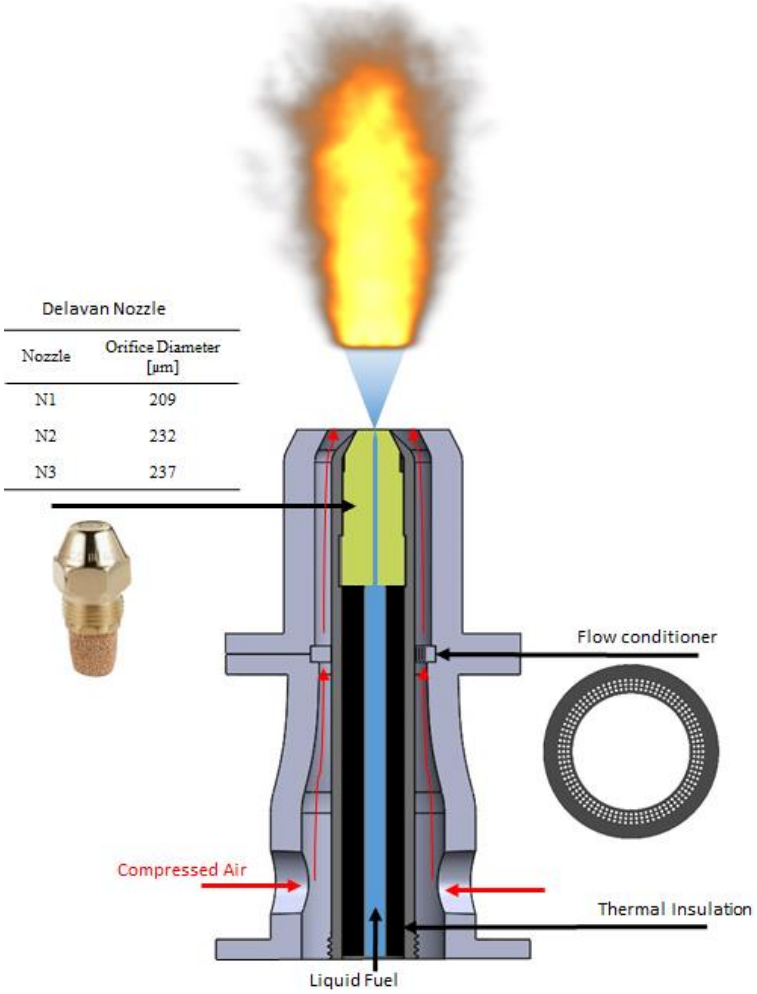

Figure 4.1. Schematic of the turbulent spray burner setup and a list of the nozzle sizes which are used in this work.

in Fig. 4.1. The fuel and the air are delivered to the spray burner at a room temperature of 298 K and at laboratory pressure of 0.84 atm.

4.3.2 Fuel Properties

Three hydrocarbon fuels with a wide range of physical properties (provided in Table 4.1) were used in this study: n-heptane, n-dodecane, and toluene. The physical property differences, such as density, viscosity, and surface tension influence the atomization (i.e., SMD) while the differences in the vapor pressure (P_v) and the normal boiling temperature (NBT) listed in Table 4.1 impact the vaporization of the fuel. n-Heptane is the most volatile fuel, followed closely by toluene and then n-dodecane, which has a normal boiling point that is more than a 100 °C higher than the other fuels. The reactivity of the fuel is marked by the laminar flame speed (S_L), which is a main factor that can influence the flame stability, especially flame liftoff. Here both n-heptane and n-dodecane have similar S_L values whereas toluene exhibits a lower flame speed than the n-alkanes. The fuels were carefully chosen to exhibit large differences in volatility and reactivity so that the influence of vaporization and chemistry on flame stability could be better understood once atomization was controlled.

Table 4.1. Physical and chemical properties of the fuels in this study. All the properties were taken from DIPPR database at standard temperature and pressure [1], laminar flame values were measured by previous works at 400 K, at atmospheric pressure, and stoichiometric equivalence ratio [5, 6].

Test fuel	**NBT [K]**	**P_V [kPa]**	**ρ_F [kg/m^3]**	**μ_l [kg/m.s]**	**σ_l [N/m]**	**S_L [m/s]**	**HOV [kJ/kg]**	**ΔH_C [MJ/kg]**
n-Heptane	371.58	6.021	681.66	0.00039	0.0198	0.6413	365.54	44.6
n-Dodecane	489.473	0.018	746.39	0.0014	0.0249	0.6405	362.05	44.1
Toluene	383.78	3.775	864.05	0.00056	0.0279	0.5434	411.77	40.5

4.3.3 Droplet/Spray Characterization

A Laser Doppler Velocimeter (LDV) and Phase Doppler Particle Analyzer (PDPA) system was used in this study to characterize the fuel spray. The system consists of a TSI Powersight laser (Model No. TR-SS-1D-532) and a receiver (Model No. 450300). One single 300-mW, 532 nm laser beam is split using a Bragg Cell into two crossing beams that form an intersection and sample volume in the vertical plane where droplets pass and are analyzed. The receiver was placed 40 degrees off axis of the laser. The receiver is equipped with two lenses, front and back, with focal lengths of 300 mm and 250 mm, respectively. Signals coming out of the receiver feed into the Photo-detector Module PDM1000-1PSS through photomultiplier tubes (PMTs). Signals are then transferred to a Flow and Size Analyzer (FSA3500-1P) which communicates with a PC using the FlowSizer64 software and provides measurements of size and velocity. For all measurements the detection limits in terms of diameter range from 0.5 μm to 161.1 μm.

The PDPA system was used to measure the SMD at axial locations of 20 and 40 mm and at nine radial locations (0, 2.5, 5, 7.5, 10, 12.5, 15, 17.5, and 20 mm). Since the location close to the injector tip is dense spray region, the axial location of 20 mm was chosen to measure the SMD. The SDD were also noted from the droplet size measurements at the axial location of 20 mm and different radial locations. The PDPA/LDV system was setup to collect data for 1 second at each location/condition. This sample time was confirmed to be sufficient by comparing results for a 1 second and a 5 second collection period, which provided statistically identical results. The uncertainty for the PDPA measurements is investigated in many previous works by calculating the ratio of one standard deviation to the mean of multiple repeated measurements at the same condition [33-35]. The measurement uncertainty is estimated to be 1.3% for the SMD [33-35].

The spray is characterized by the SMD and SDD in this work. For the sake of comparison between the measured and calculated SMD results, a global Sauter Mean Diameter (SMD_{global}) is defined as a single parameter to represent the overall spray droplet size and considers the variation in the SDD. In other words, the SMD_{global} represents the radial weighted SMD, thus it counts for the radial SDD (droplets number at different radial location). Note that previous studies may use the same term, while others refer to the SMD_{global} as the integral or overall SMD [9, 36, 37]. The simplified equation for the calculation of SMD_{global} over the complete radial cross section at a set axial location (i.e. 20 mm from the nozzle tip in this study) is given as the following:

$$\mathrm{SMD_{global}} = \sum_{i=2}^{m}(r_i D_{30,i}^3 N_i) / \sum_{i=2}^{m}(r_i D_{20,i}^2 N_i) \tag{4.1}$$

where $D_{30,i}$ and $D_{20,i}$ are the volumetric and surface diameters of the fuel droplets measured at the radial position r_i and N_i represents the number of droplets detected at the radial position r_i.

The measured SMD_{global} using PDPA is then compared to the SMD calculated by three well-known correlations: Radcliffe [38], Jasuja [39], and Lefebvre [10], listed in order as the following:

$$\mathrm{SMD}_{Radcliffe} = 7.3\sigma_l^{0.6}\nu_l^{0.2}\dot{m}_l^{0.25}\Delta P^{-0.4} \tag{4.2}$$

$$\mathrm{SMD}_{Jasuja} = 4.4\sigma_l^{0.6}\nu_l^{0.16}\dot{m}_l^{0.22}\Delta P^{-0.43} \tag{4.3}$$

$$\mathrm{SMD}_{Lefebvre} = 2.25\sigma_l^{0.25}\mu_l^{0.25}\dot{m}_l^{0.25}\Delta P^{-0.5}\rho_{air}^{-0.25} \tag{4.4}$$

where σ_l is the liquid surface tension, μ_l and ν_l are the dynamic and kinematic liquid viscosities, respectively, $\dot{m}_l$ is the liquid mass flow rate, ΔP is the pressure drop across the spray nozzle and ρ_{air} is the surrounding air density. All properties used in the SMD calculations are provided in Table 4.1. The pressure drop (ΔP) across the nozzle was taken to be the pressure difference from

ambient reported by the fuel pump minus the pressure drop measured over the plumbing connecting the pump and the nozzle.

4.3.4 Flame Stability Measurements

The flame stability, quantified by liftoff height and blowout limit, of the selected fuels were measured and compared using a single common nozzle and using different nozzle sizes selected to maintain similar spray parameters. The flame stability experiments were carried out at the laboratory environment, e.g. T = 298K ± 5 K & P = 0.84 atm (the local ambient pressure of Fort Collins, CO).

Flame liftoff heights were measured for a single fuel flow rate (e.g., 50 mL/min) at different air flow rates (e.g., 200, 300, 400, 500, and 600 SLPM). The flame liftoff heights were determined by calculating the average luminosity intensity of 50 images for each experimental condition. The average image was then processed by plotting the average intensity along the horizontal center of the flame as a function of axial distance from the fuel injector nozzle. The flame location was then determined at the point of maximum luminosity gradient after applying calibration factor to convert pixel height to distance. For all tested fuels, the maximum relative standard deviation from the mean liftoff height was 3.6%. Liftoff heights were measured along the centerline and at consistent co-flow conditions for all fuels. As such, we do not expect there to be any influence of the surrounding air on the differences in liftoff height observed between the fuels.

Flame blowout limits were determined by slowly increasing the air flow rate while keeping the fuel flow rate constant until the flame extinguished. The air flow rate at the blowout limit is then recorded and the global equivalence ratio is calculated. The measurements were repeated at least twice for each of the fuel flow rates, i.e., 45, 50, 55, 60, and 65 mL/min with good repeatability; maximum relative standard deviation from the mean was equal to 3.4%. For the blowout

measurements, the air co-flow rates used in this work are significantly high (e.g. 600-1090 SLPM), thus, we expect the influence of the surrounding quiescent air on the global equivalence ratio to be negligible.

4.4 Results and Discussion

4.4.1 Common Nozzle Testing

In this section, a single nozzle (size N1) is used in the ACS burner for all fuels to explore the influence of the fuels' physical properties (e.g., density, viscosity and surface tension) on the atomization process (i.e., SMD) and flame stability.

4.4.1.1 Spray Characterization

Figure 4.2 shows the predicted, according to Eqs. (2-4), and measured SMDs for the three fuels. Despite the mean value of the measurements being consistently larger than the predicted diameters, the predicted SMD does follow the same trends seen in the measurements. It is worth noting that the error bars on the measured SMD data in Fig. 4.2 represents the measured droplet size distribution from the PDPA system and it is not the mean value measurement uncertainty. The uncertainty for the PDPA measurements is investigated in many previous works by calculating the ratio of one standard deviation to the mean of multiple repeated measurements at the same condition [33-35]. The measurement uncertainty is estimated to be 5.9% for mean droplet diameter [33]. A previous work by the authors has more detailed analysis of the spray characterizations [40]. As illustrated in Fig. 4.2, when a single constant fuel injector is used (N1), the SMDs of n-heptane and toluene are similar and the measured SMD of n-dodecane differs from n-heptane by ~21%. This is due to the differences in physical properties, specifically differences in density, viscosity and surface tension, as well as differences in pressure drop across the nozzle, as explained by Eqs. (2-4). Amongst the fuels, the viscosity varied more than any of the other properties. Since n-

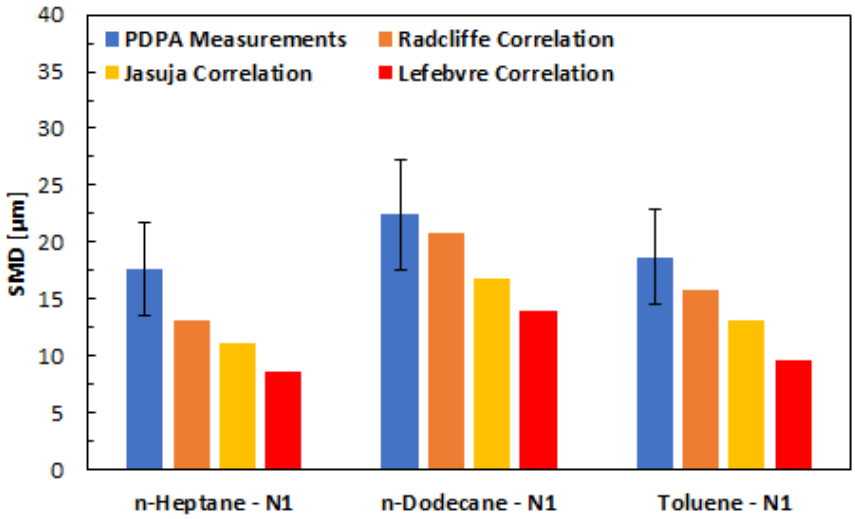

Figure 4.2. Measured and predicted SMDs in µm unite for the tested fuels at same nozzle sizes (N1) and at fuel flow rate of 50 mL/min.

dodecane has the highest viscosity (Table 4.1), compared to n-heptane and toluene, it exhibits the largest droplet size.

The measured radial spray droplet distributions (SDD) are shown in Fig. 4.3 for the three fuels at an axial distance of 20 mm above the nozzle exit at radial locations of 0, 2.5, 5, 7.5, 10, 12.5,

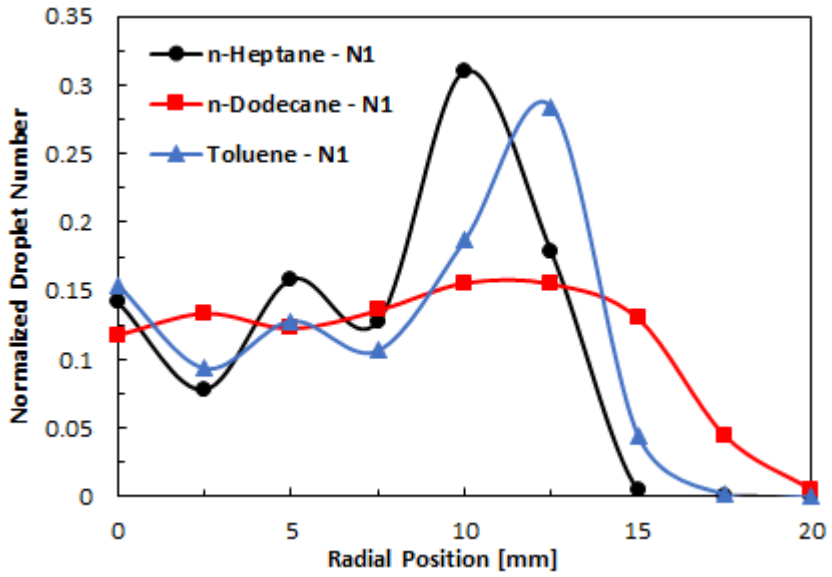

Figure 4.3. The number of droplets detected by the PDPA system at an axial location of 20 mm at multiple radial positions normalized by the total number of droplets in each profile for each of the tested fuels. All data here was collected using the same nozzle size (N1), fuel flow rate of 50 mL/min, and air co-flow rate of 200 SLPM.

15, 17.5, and 20 mm. The SDD values reported in Fig. 4.3 represent the number of droplets counted at each location by the PDPA normalized by the total number of droplets detected. Distinct gradients in the radially dependent SDD for n-heptane and toluene compared to n-dodecane fuels can be seen when the same nozzle size is used. The reason for this can be again attributed to the differences in the fuels' physical properties, which can influence the droplets breakup and the spatial droplet distributions (e.g. spray angle).

4.4.1.2 Flame Behavior and Stability

Differences in spray characteristics can impact subsequent vaporization rates and air-fuel mixing time scales, and thus influence flame behaviors (e.g. liftoff heights and blowout limits). In general, larger droplet sizes and less volatile fuels, e.g., as seen with n-dodecane when a constant nozzle size is used (Figs. 4.2-4.3), exhibit higher liftoff height as shown in Fig. 4.4a. This is because the fuel needs more time to evaporate and generate enough vapor to stabilize the flame against the incoming reactant stream. Opposite trends are observed in blowout limits, where the least volatile fuel and the fuel with largest droplet sizes are more difficult to blowout (Fig. 4.4b). In both liftoff height and blowout results, n-heptane experiences a sharp increase compared to the other fuels as the air and/or fuel flow rates increased. This is believed to be caused by the higher volatility of n-heptane and its smaller droplet sizes, which enhances the fuel/air mixing, leading to pre-mixed local fuel lean regions [14]. As a result, n-heptane reaches its blowout limit at an air co-flow rate of ~600 SLPM, preventing the measurement of the flame liftoff height at this air flow rate condition. The influence of increasing fuel and/or air flow rates on the spray characteristics (e.g., SMD) and flame stability were discussed in more details in previous works [40, 41].

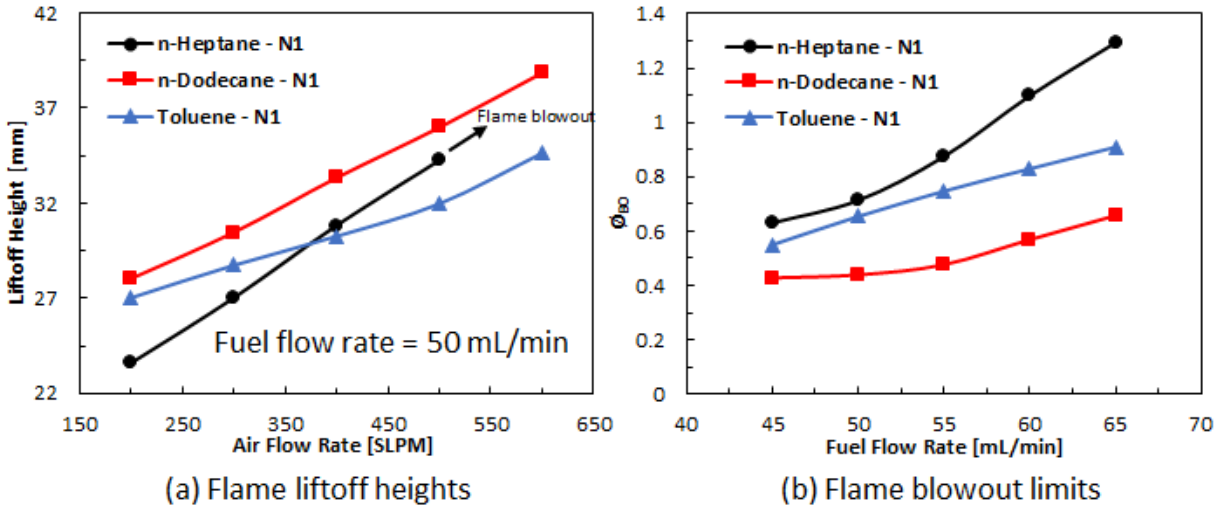

Figure 4.4. Flame liftoff heights with a maximum relative standard deviation from the mean value equals to 3.6% (a), and blowout limits with a maximum relative standard deviation from the mean equals to 3.4% (b), using the same nozzle sizes (N1) with all tested fuels.

4.4.2 Variable Nozzle Testing

In this section, the influence of the atomization process is controlled by reducing the differences in the SMD and SDD for the tested fuels. This is accomplished by using different nozzle sizes with tested fuels selected based on the SMD correlations in Eqs. (4.2-4.4). Using this unique approach allows one to more closely study the influence of varying fuel volatility and reactivity on the flame stability.

4.4.2.1 Spray Characterization

Figure 4.5 shows the predicted, Eqs. (4.2-4.4), and measured SMDs for the selected fuels using different nozzle sizes, N3, N1, and N2, for n-heptane, n-dodecane, and toluene, respectively. The differences in the SMD amongst the three different fuels can be minimized, with less than 10% difference achieved in both the measured and predicted SMDs, noting that ~21% difference in SMD between the three fuels were observed when a common nozzle size was used (Fig. 4.2). Despite the mean value of the measurements being consistently larger than the predicted SMD, the predicted SMD do follow similar trends. Similar to Fig. 4.2, the SMD predicted by Radcliffe's

correlation when using different nozzle sizes is closest to the measured values, follow by Jasuja's correlation and then Lefebvre's.

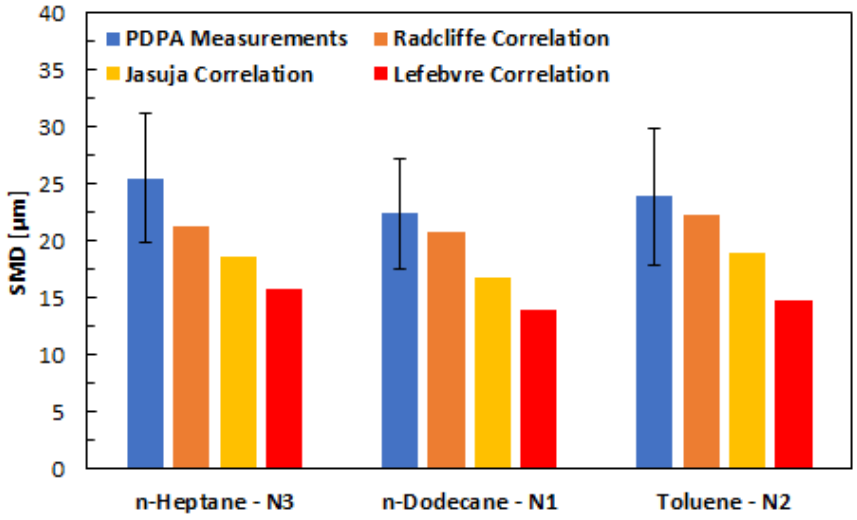

Figure 4.5. Measured and predicted SMDs for the tested fuels at different nozzle sizes: N3, N1, and N2 used with n-heptane, n-dodecane, and toluene, respectively. All measurements were taken at a fuel flow rate of 50 mL/min. The error bars for the measurements represent the droplet size distribution detected by the PDPA system.

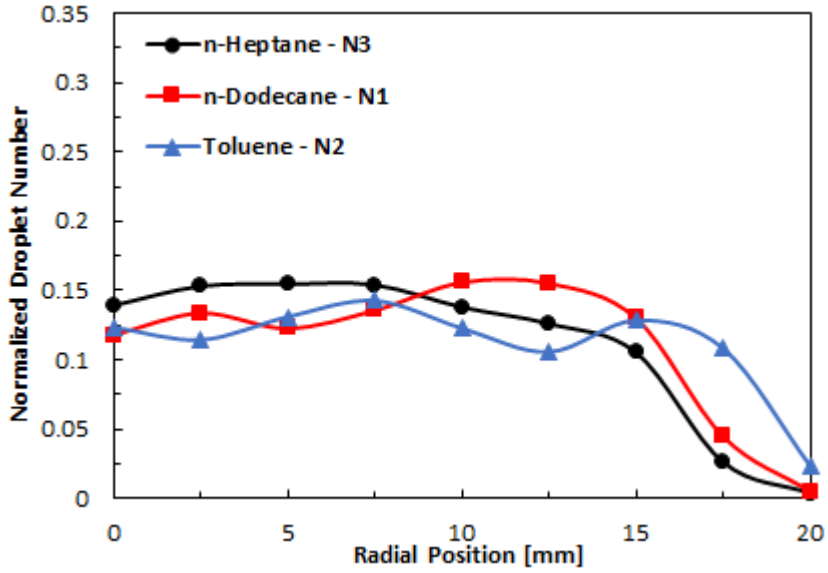

Figure 4.6. The number of droplets collected by PDPA system at an axial location of 20 mm at multiple radial positions normalized by the total number of droplets in each profile for each of the tested fuels. The data here was collected using different nozzle sizes (e.g., N3, N1, and N2 used with n-heptane, n-dodecane, and toluene fuels, respectively), and for the same fuel flow rate of 50 mL/min, and air co-flow rate of 200 SLPM.

The spray droplet distributions (SDDs) for the tested fuels using different nozzle sizes were measured and are shown in Fig. 4.6. Interestingly, all tested fuels show similar radial SDD profiles, in contrast to Fig. 4.3. These data illustrate the effectiveness of varying nozzle sizes to control the atomization process of hydrocarbon fuels.

4.4.2.2 Flame Behavior and Stability

The appropriate nozzle orifice size was selected for each fuel to minimize the spray characterization differences (especially droplet diameter) across all fuels, as shown in Fig. 4.5 and 6. When controlling the atomization process, the liftoff heights (Fig. 4.7a) and blowout limits (Fig. 4.7b) for the set of fuels become more similar in value compared to the constant nozzle flame liftoff heights and blowout limits (Fig. 4.4a and 4.4b). When the atomization effect is eliminated, toluene experiences the highest liftoff as shown in Fig 4.7a, which is believed to be caused by the lower reactivity of toluene compared to the n-alkane fuels. The lower reactivity (i.e., low flame speed as listed in Table 4.1) of toluene causes the flame to stabilize further downstream (where flow velocities are lower) compared to that of n-alkane flames. It was noticed that when the SMD

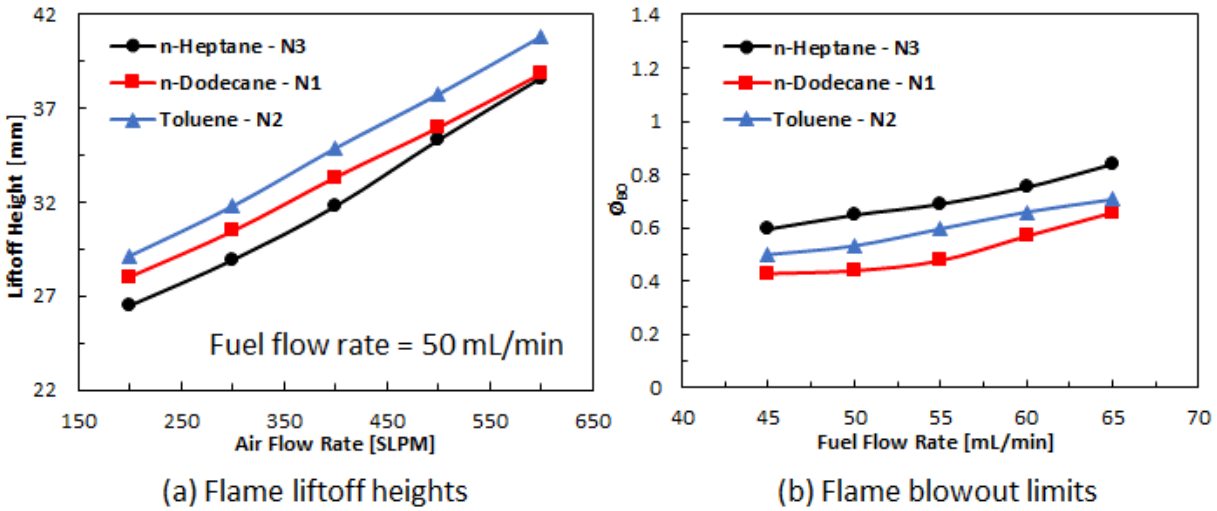

Figure 4.7. Flame liftoff heights, with a maximum relative standard deviation from the mean value equals to 2.8% (a), and blowout limits, with a maximum relative standard deviation from the mean value equals to 3.14% (b), using multiple nozzle sizes with tested fuels.

(and SDD) of n-heptane and toluene were increased to provide a better match to that of n-dodecane, the two fuels become harder to blowout as illustrated in Fig. 4.7b. Despite becoming closer in value, the blowout limits follow the same trend as before with n-dodecane experiencing the most resistance to blowout, followed by toluene, then n-heptane. Despite more closely matching the spray characteristics (e.g., SMD and SDD), blowout follows inversely to the fuel's vapor pressure, signifying that evaporation dynamics play a significant role in blowout behavior.

4.4.2.3 Flame Liftoff Height Stability Mechanism

To understand the influence of fuel properties on flame liftoff height, the data collected using the two approaches (Figs. 4.4a & 4.7a) are used in this section. As a first attempt to explain differences in flame liftoff between the fuels, the gas phase laminar flame speed (S_L) was used, as suggested by many previous works [42, 43]. Thus, the liftoff height (LOH) is plotted with ($V_{co\text{-}flow}/S_L$) in Fig. 4.8. $V_{co\text{-}flow}$ is the air co-flow velocity at the exit of the burner claculated (5.24, 7.86, 10.48, 13.1, and 15.72 m/s) for the different air flow rates, e.g., 200, 300, 400, 500, and 600 SLPM,

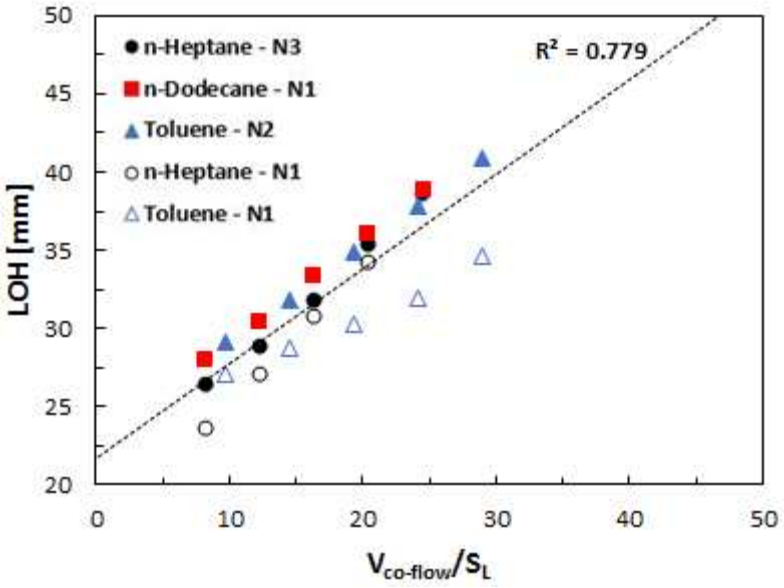

Figure 4.8. Flame liftoff heights (LOH) plotted against $V_{co\text{-}flow}/S_L$ for the different fuels. Open symbols represent results using consistent nozzle approach (nozzle N1). Filled symbols represent data collected using variable nozzles to minimize atomization differences.

respectively. The laminar flame speeds used in this work (listed in Table 4.1) are for stoichiometric fuel-air mixtures and were measured at atmospheric pressure and a temperature of 400 K using the counterflow flame approach [44, 45]. As seen in Fig. 4.8, normalizing by the laminar flame speed of the fuels resulted in a linear fit correlation coefficient of 0.78. This indicates the need to include time scales associated with vaporization in concert with the gas phase flame speed. Lefebvre et al. [42] derived a correlation to predict the rate of flame propagation through quiescent multi-droplet mists:

$$S_{spray} = \alpha_g \left[\frac{(1-f_v)\rho_F D^2}{8\rho_g ln(1+B)} + \frac{\alpha_g^2}{S_L^2}\right]^{-0.5} \quad (4.5)$$

In Eq. (4.5), S_{spray} is the two-phase flow (spray) flame speed, α_g and ρ_g are the thermal diffusivity and density of the air, respectively, at an average temperature ~1200 K, which was suggested in Lefebvre et al. and in the work of Neophytou and Mastorakos [42, 43], f_v is the fuel vapor mass fraction entering the preheat zone and *D* is the droplet diameter at the preheated zone

Table 4.2. Values of parameters used in Eq. (4.5) to calculate the spray flame speed.

Fuels - Nozzle	n-Heptane - N3	n-Dodecane - N1	Toluene - N2	n-Heptane - N1	Toluene - N1
Measured droplet diameter at nozzle exit ($D_{initial}$) [µm]	25.5	22.4	23.9	17.7	18.7
Predicted droplet diameter at preheated zone (D) [µm]	24.1	22.4	23.1	16.	17.7
Predicted vapor volume fraction entering the flame (f_v)	0.156	0.0012	0.10	0.254	0.143
Specific heat (C_P) [kJ/kg.K] at average temperature ($\overline{T}$)	3.37	3.46	2.53	3.37	2.53
Air density (ρ_{air}) at 1200 K [kg/m^3]	0.2902				
Air thermal diffusively (α_{air}) at 1200 K [m^2/s]	2.24E-04				

(just before entering the flame), both calculated using a 0D droplet evaporation model based on the d^2 law. The initial droplets, which was plugged in the droplet model was measured using the PDPA/LDV system and listed in Table 4.2. The approximate residence time (from injector to flame preheat zone) used to predict f_v and D, was estimated based on the averaged measured droplet velocity (~6 m/s using PDPA) and the average location of the primary zone (~30 mm) feom the nozzle exit and was calculated to be ~5 ms. ρ_F is the liquid fuel density at 298 K, and B is the heat transfer number (Spalding number), calculated using the following formula:

$$B = \frac{c_{pg}(T_\infty - T_{boil})}{h_{fg}} \tag{4.6}$$

In Eq. (4.6), c_{pg} is the specific heat of the fuel at average temperature (e.g. $\overline{T} = \frac{T_\infty + T_{boil}}{2}$) and was taken from DIPPR database [1]. T_∞ and T_{boil} are the environment temperature of the preheated zone (~1200 K) and fuel boiling temperature, respectively, and h_{fg} is the fuel heat of vaporization (HOV). All of the parameters used in Eq. (4.5) and (4.6) are listed in Table 4.1 and 4.2. As seen in

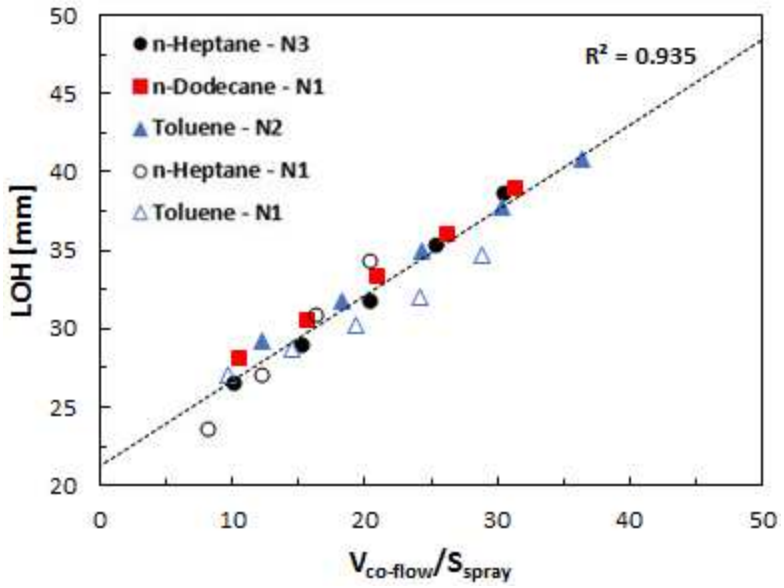

Figure 4.9. Flame liftoff heights (LOH) plotted against $V_{co\text{-}flow}/S_{spray}$ for the different fuels. Open symbols represent results using consistent nozzle approach (nozzle N1). Filled symbols represent data collected using variable nozzles to minimize atomization differences.

Fig. 4.9, normalizing the LOH measurements by the two-phase flame speed, calculated from Eq. (4.5), resulted in a linear correlation with $R^2 = 0.94$. These results (comparing Fig. 4.8 and Fig. 4.9) demonstrates that the LOH is influenced by both the evaporation rate (first term in Eq. (4.5)), as well as, the chemical reaction rate (last term in Eq. (4.5)). Thus, the spray flame speed is enhance by increases in fuel volatility, vapor concentration, normal burning velocity, and reduction in droplet diameter.

4.4.2.4 Flame Blowout Mechanism

The influence of fuel properties on blowout limit is evaluated by analyzing the data collect for both approaches (Fig. 4.4b & 4.7b). First, the empirical correlation developed by Lefebvre [27] is used:

$$q_{LBO} \propto \left[\frac{f_{pz}}{V_{pz}}\right]\left[\frac{\dot{m}_{air}}{P_3^{1.3}\exp(T_3/300)}\right]\left[\frac{D_o^2}{\lambda_{eff}\,\Delta H_c}\right] \tag{4.7}$$

In Eq. (4.7), q_{LBO} is the fuel-air ratio at the lean blowout limit, f_{pz} and V_{pz} represent the fraction of airflow entering the primary combustion zone (PCZ) and the volume of the PCZ, respectively, $\dot{m}_{air}$ is the air mass flow rate, P_3 and T_3 are the pressure and temperature of inlet gas, D_o is the mean droplet size and listed in Table 4.2, λ_{eff} is the effective evaporation, and ΔH_c is the heat of combustion. A 0D droplet evaporation model based on the d^2 law is used to calculate the effective evaporation ($\lambda_{eff} = \frac{D_o^2}{evaporation\ time}$) for a droplet initially at 298 K and in an environment at 0.84 atm (the local ambient pressure of Fort Collins, CO where the experiments were conducted) and 750 K, corresponding approximately to the average temperature of the environment that the droplet travels through between the nozzle tip (~300 K) and the primary zone (~1200 K). The first and second term on the right-hand side of Eq. (4.7) are independent of the fuel properties and represent the combustor design and operation conditions, respectively. The third term embodies the effect

Table 4.3. Fuels properties relative to n-dodecane and they are used in Eq. (4.8) and (4.9) to predict the equivalence ratio at LBO.

Fuel	n-Heptane - N3	Toluene - N2	n-Heptane - N1	Toluene - N1
$D_{o,r}$	1.136364	1.064617	0.786988	0.832442
$\lambda_{eff,r}$	1.361209	1.073811	1.361328	1.07383
$dH_{c,r}$	1.01013	0.918724	1.01013	0.918724

of fuel properties. Since the combustor parameters are kept constant, the blowout limit depends only on the fuel properties and is calculated relative to that of n-dodecane (nc12), as the following:

$$q_{LBO} \propto \left[\frac{D_{o,r}^2 \dot{V}_{F,r}}{\lambda_{eff,r} \Delta H_{c,r}}\right] \tag{4.8}$$

where subscript *r* represents quantities relative to that of n-dodecane. Notice that fuel flow rate term relative to 50 mL/min ($\dot{V}_{F,r}$) was added to Eq. (4.8), since the blowout limits were tested at different fuel flow rates. The relative properties in Eq. (4.8) are calculated and are listed in Table

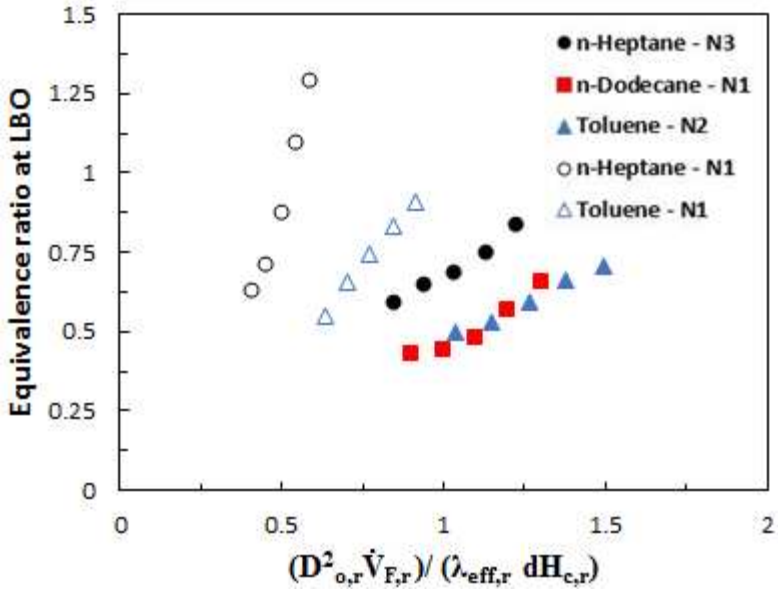

Figure 4.10. Equivalence ratios at LBO as a function of Eq. (4.8) for the different fuels. Open symbols represent results using consistent nozzle approach (nozzle N1). Filled symbols represent data collected using variable nozzles to minimize atomization differences.

4.3. The measured LBO results are plotted against Eq. (4.8) the results of which are shown in Fig. 4.10. Interestingly, despite normalizing by terms that have been shown to account for differences in atomization, vaporization, and the energy content of the fuel, the data still remain disparate, especially for data taken using the same nozzle size. The lack of convergence following the normalization of the data with the well-known Lefebvre correlation is likely due to differences in the flame regime experienced in the current burner compared to the combustors used in the derivation of Eq. (4.7). Also, the set of fuels tested here exhibit a wider range in properties important in the fuel atomization, vaporization, and chemical reactivity than the set of fuels use to derive Eq. (4.7), which consisted of petroleum-derived jet fuels (JP-4, JP-8, and No. 2 Diesel).

The Lefebvre correlation (Eq. (4.8)) was modified by way of a re-regression to explain the differences in the blowout results of the tested fuels for the spray burner used here. The re-regression of Eq. (4.8) resulted in the collapse of all LBO data with a linear fit correlation coefficient of 0.94. The resulting correlation can be seen in Eq. (4.9):

$$q_{LBO} \propto \left[\frac{\lambda_{eff,r}^{1.35}\,\dot{V}_{F,r}^{1.29}}{D_{o,r}^{0.71}\,\Delta H_{c,r}^{1.42}}\right] \tag{4.9}$$

Figure 4.11 shows the measured LBO plotted against the modified correlation in Eq. (4.9). Eq. (4.9) suggests that the volatility and the droplet sizes (SMD), which enhance the liquid loading into the flame, as well as the chemical reactivity of the fuel, represented by the heat of combustion, are the dominate properties promoting flame stability for the current set of fuels and spray burner. Interestingly, Eq. (4.9) demonstrates an opposite dependency of the atomization (i.e., droplet size) and the droplet evaporation (λ_{eff}) on LBO from Eq. (4.8). As previously noted, this is likely due

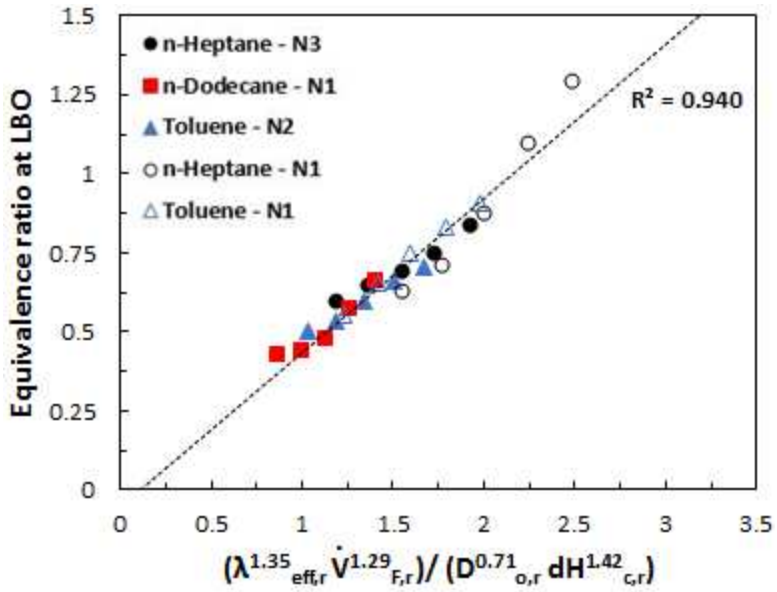

Figure 4.11. Equivalence ratios at LBO as a function of Eq. (4.9) for the different fuels. Open symbols represent results using consistent nozzle approach (nozzle N1). Filled symbols represent data collected using variable nozzles to minimize atomization differences.

to differences in the flame regime, where larger droplets, which slow the vaporization, can create local fuel rich regions and elevated temperature which stabilize the flame [27].

The time averaged (1 second duration) liquid volumes at an axial location of 40 mm from the burner tip (representing the approximate flame LOH) are calculated from the radially dependent PDPA measurements while matching at the same air and fuel flow rates. The measurements were implemented on a cold spray (i.e., without a flame) to eliminate the impact of the varying flame location (relative to the detection location) on the droplet evaporation. At a fuel flow rate of 50 mL/min, n-dodecane delivers the highest averaged liquid volume per second, followed by toluene and n-heptane, as seen in Fig. 4.12. These results follow the same trend of the lean blowout results in Figs. 4.4a & 4.7a (i.e., n-dodecane being the most difficult to blowout and n-heptane being the easiest), supporting the notion that liquid loading enhances the flame resistance to blowout. A similar trend is observed for the LBO cases experienced with a fuel flow rate of 65 mL/min. Although the global equivalence ratio increases with the increase in fuel flow rate, the liquid

volume measured at 40 mm decreases. This behavior is due to the reduced droplet sizes at higher fuel flow rates, which leads to more rapid droplet vaporization and leaner local regions. Following the same hypothesis, this explains why the flames experience LBO at higher equivalence ratios (i.e., easier to blowout) when higher fuel flow rates are provided (as seen in Fig. 4.4a and 4.7a).

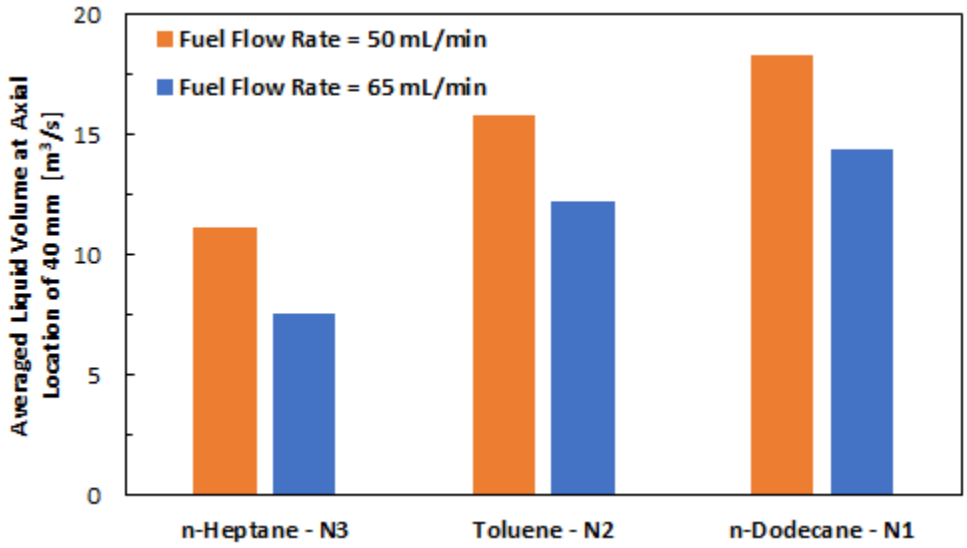

Figure 4.12. Averaged liquid volume detected by the PDPA system at axial location of 40 mm for cold spray. The averaged volumes are calculated considering the number of droplets and their sizes over the radial positions (0, 2.5, 5, 7.5, 10, 12.5, 15, 17.5, and 20 mm).

4.5 Conclusions

In this work, the tested fuels, e.g., n-heptane, n-dodecane, and toluene, have a wide range of physical properties which impact the atomization/spray process. The influence of the atomization process on flame stability was investigated for the three single component hydrocarbon fuels by using a single fuel injection nozzle. In addition, to minimize the role of the spray process, e.g. SMD, SDD, and spray angle, on the flame stability, different fuel injector nozzle sizes that were carefully selected to account for differences in the fuel's physical properties (e.g., density, viscosity and surface tension) were used. This unique approach of controlling the atomization

process, permitted a more systematic study of the fuels' volatility and reactivity on flame behavior. The following conclusions are drawn from the current work:

1) The SMD and SDD are solely affected by the fuel's physical properties when the same injection system and flow conditions are used. Subsequently, the flame stability (e.g. flame liftoff heights and blowout limits) is influenced. The larger droplet size and less volatile fuel, e.g. n-dodecane, demonstrated higher liftoff heights, while opposite trends were observed in blowout limits, where the least volatile fuels, which also produce the largest droplet sizes, were more difficult to blowout.
2) Although the absolute SMD values predicted by the correlations consistently under predicted the measured SMD, the correlations did closely predict the relative differences in the measured SMD of the different fuels and different nozzles and thus were appropriate to use when selecting nozzle sizes to minimize atomization differences.
3) After controlling for the atomization process (i.e., similar SMD and SDD achieved for the different tested fuels) by using different nozzle sizes more similar liftoff heights and blowout limits for the set fuels where observed as compared to the results from the common nozzle approach. The differences in liftoff height was shown to be a result of two-phase flame speed, which accounts for both pre-vaporized fuel reactivity (SL) and time scales associated with droplet evaporation. In addition, differences in blowout were also found to be largely tied to fuel volatility and droplet size (SMD), indicating the significance of the liquid fuel loading into the flame preheat zone on flame stability, along with heat release.

The comparison of the flame stability results of the single and multiple nozzle size approaches indicate the positive effectiveness of this unique approach on controlling the atomization process of the different fuels. This was clear as the role of evaporation and reactivity on flame liftoff

heights and blowout limits were determined, when the atomization process was controlled. These conclusions highlight the importance of considering both the physical properties, which can influence the atomization, vaporization, and mixing processes, in concert with the fuel's chemical/reactivity when projecting the performance of a fuel. The sensitivity of physical properties on flame stability illustrated here suggests the need to consider these key physical properties when formulating surrogate fuels.

References

[1] R. Rowley, W. Wilding, J. Oscarson, Y. Yang, N. Zundel, T. Daubert, R. Danner, DIPPR information and data evaluation manager for the design institute for physical properties, AIChE, New York, Version 5 (2011).

[2] J. Grohmann, W. O'Loughlin, W. Meier, M. Aigner. Comparison of the Combustion Characteristics of Liquid Single-Component Fuels in a Gas Turbine Model Combustor. In: editor^editors. ASME Turbo Expo 2016: Turbomachinery Technical Conference and Exposition; 2016: American Society of Mechanical Engineers. p. V04AT04A010-V004AT004A010.

[3] J. Grohmann, B. Rauch, T. Kathrotia, W. Meier, M. Aigner, Influence of Single-Component Fuels on Gas-Turbine Model Combustor Lean Blowout, Journal of Propulsion and Power (2017) 1-11.

[4] N. Rock, I. Chterev, T. Smith, H. Ek, B. Emerson, D. Noble, J. Seitzman, T. Lieuwen. Reacting Pressurized Spray Combustor Dynamics: Part 1—Fuel Sensitivities and Blowoff Characterization. In: editor^editors. ASME Turbo Expo 2016: Turbomachinery Technical Conference and Exposition; 2016: American Society of Mechanical Engineers. p. V04AT04A021-V004AT004A021.

[5] K. Kumar, J. Freeh, C. Sung, Y. Huang, Laminar flame speeds of preheated iso-octane/O2/N2 and n-heptane/O2/N2 mixtures, Journal of propulsion and power 23 (2007) 428-436.

[6] X. Hui, C.-J. Sung, Laminar flame speeds of transportation-relevant hydrocarbons and jet fuels at elevated temperatures and pressures, Fuel 109 (2013) 191-200.

[7] J.-S. Gong, W.-B. Fu, The experimental study on the flow characteristics for a swirling gas–liquid spray atomizer, Applied Thermal Engineering 27 (2007) 2886-2892.

[8] H.G. Wagner, Soot formation in combustion, Symposium (International) on Combustion 17 (1979) 3-19.

[9] J. Jedelsky, M. Jicha, Energy considerations in spraying process of a spill-return pressure-swirl atomizer, Applied Energy 132 (2014) 485-495.

[10] A. Lefebvre, Atomization and sprays, combustion: an international series, Hemisphere Pub. Corp (1989).

[11] A.H. Lefebvre, Gas turbine combustion: alternative fuels and emissions, CRC press2010.

[12] B. Williams, J. Fleming, DETERMINATION OF THE STRAIN IN COUNTERFLOW DIFFUSION FLAMES FROM FLOW CONDITIONS.

[13] Y. Lin, Y. Lin, C. Zhang, Q. Xu, C.-J. Sung, G. Liu, Evaluation of Combustion Performance of a Coal-Derived Synthetic Jet Fuel, (2012) 569-576.

[14] J.A. Bossard, R.E. Peck, Droplet sie distribution effects in spray combustion, Symposium (International) on Combustion 26 (1996) 1671-1677.

[15] A. Agosta, N.P. Cernansky, D.L. Miller, T. Faravelli, E. Ranzi, Reference components of jet fuels: kinetic modeling and experimental results, Experimental Thermal and Fluid Science 28 (2004) 701-708.

[16] S. Humer, A. Frassoldati, S. Granata, T. Faravelli, E. Ranzi, R. Seiser, K. Seshadri, Experimental and kinetic modeling study of combustion of JP-8, its surrogates and reference components in laminar nonpremixed flows, Proceedings of the Combustion Institute 31 (2007) 393-400.

[17] S. Dooley, S.H. Won, M. Chaos, J. Heyne, Y. Ju, F.L. Dryer, K. Kumar, C.-J. Sung, H. Wang, M.A. Oehlschlaeger, A jet fuel surrogate formulated by real fuel properties, Combustion and Flame 157 (2010) 2333-2339.
[18] S. Dooley, S.H. Won, J. Heyne, T.I. Farouk, Y. Ju, F.L. Dryer, K. Kumar, X. Hui, C.-J. Sung, H. Wang, The experimental evaluation of a methodology for surrogate fuel formulation to emulate gas phase combustion kinetic phenomena, Combustion and Flame 159 (2012) 1444-1466.
[19] S. Dooley, S.H. Won, S. Jahangirian, Y. Ju, F.L. Dryer, H. Wang, M.A. Oehlschlaeger, The combustion kinetics of a synthetic paraffinic jet aviation fuel and a fundamentally formulated, experimentally validated surrogate fuel, Combustion and Flame 159 (2012) 3014-3020.
[20] P. Dagaut, F. Karsenty, G. Dayma, P. Diévart, K. Hadj-Ali, A. Mzé-Ahmed, M. Braun-Unkhoff, J. Herzler, T. Kathrotia, T. Kick, C. Naumann, U. Riedel, L. Thomas, Experimental and detailed kinetic model for the oxidation of a Gas to Liquid (GtL) jet fuel, Combustion and Flame 161 (2014) 835-847.
[21] Z. Zhang, L. Chen, Y. Lu, A.P. Roskilly, X. Yu, A. Smallbone, Y. Wang, Lean ignition and blow-off behaviour of butyl butyrate and ethanol blends in a gas turbine combustor, Fuel 239 (2019) 1351-1362.
[22] S.J. Shanbhogue, S. Husain, T. Lieuwen, Lean blowoff of bluff body stabilized flames: Scaling and dynamics, Progress in Energy and Combustion Science 35 (2009) 98-120.
[23] V. Burger, A. Yates, C. Viljoen. Influence of fuel physical properties and reaction rate on threshold heterogeneous gas turbine combustion. In: editor^editors. ASME Turbo Expo 2012: Turbine Technical Conference and Exposition; 2012: American Society of Mechanical Engineers. p. 63-71.
[24] S. Stouffer, T. Hendershott, J.R. Monfort, J. Diemer, E. Corporan, P. Wrzesinski, A.W. Caswell. Lean Blowout and Ignition Characteristics of Conventional and Surrogate Fuels Measured in a Swirl Stabilized Combustor. In: editor^editors. 55th AIAA Aerospace Sciences Meeting; 2017. p. 1954.
[25] D.C. Bell, J.S. Heyne, S.H. Won, F.L. Dryer. The Impact of Preferential Vaporization on Lean Blowout in a Referee Combustor at Figure of Merit Conditions. In: editor^editors. ASME 2018 Power Conference collocated with the ASME 2018 12th International Conference on Energy Sustainability and the ASME 2018 Nuclear Forum; 2018: American Society of Mechanical Engineers. p. V001T001A011-V001T001A011.
[26] N. Rock, I. Chterev, B. Emerson, S.H. Won, J. Seitzman, T. Lieuwen, Liquid Fuel Property Effects on Lean Blowout in an Aircraft Relevant Combustor, Journal of Engineering for Gas Turbines and Power 141 (2019) 071005-071005-071013.
[27] A. Lefebvre, Fuel effects on gas turbine combustion—ignition, stability, and combustion efficiency, Journal of engineering for gas turbines and power 107 (1985) 24-37.
[28] L. Esclapez, P.C. Ma, E. Mayhew, R. Xu, S. Stouffer, T. Lee, H. Wang, M. Ihme, Fuel effects on lean blow-out in a realistic gas turbine combustor, Combustion and Flame 181 (2017) 82-99.
[29] L. Zheng, J. Cronly, E. Ubogu, I. Ahmed, Y. Zhang, B. Khandelwal, Experimental investigation on alternative fuel combustion performance using a gas turbine combustor, Applied Energy 238 (2019) 1530-1542.
[30] S. Karami, E.R. Hawkes, M. Talei, J.H. Chen, Edge flame structure in a turbulent lifted flame: A direct numerical simulation study, Combustion and Flame 169 (2016) 110-128.
[31] C. Lawn, Lifted flames on fuel jets in co-flowing air, Progress in Energy and Combustion Science 35 (2009) 1-30.

[32] J. Buckmaster, Edge-flames and their stability, Combustion Science and Technology 115 (1996) 41-68.
[33] N.S. Rodrigues, V. Kulkarni, J. Gao, J. Chen, P.E. Sojka, An experimental and theoretical investigation of spray characteristics of impinging jets in impact wave regime, Experiments in Fluids 56 (2015) 50.
[34] N.S. Rodrigues, P.E. Sojka. A parametric investigation of gelled propellant spray characteristics utilizing impinging jet geometry. In: editor^editors. 52nd Aerospace Sciences Meeting; 2014. p. 1184.
[35] S.J. Kline, Describing uncertainty in single sample experiments, Mech. Engineering 75 (1953) 3-8.
[36] A. Tratnig, G. Brenn, Drop size spectra in sprays from pressure-swirl atomizers, International Journal of Multiphase Flow 36 (2010) 349-363.
[37] J.-H. Im, D. Kim, P. Han, Y. Yoon, V. Bazarov, Self-pulsation characteristics of a gas-liquid swirl coaxial injector, Atomization and Sprays 19 (2009).
[38] A. Radcliffe, Fuel injection, High Speed Aerodynamics, and Jet Propulsion 11 (1960) 84.
[39] A. Jasuja, Atomization of crude and residual fuel oils, Journal of Engineering for Power 101 (1979) 250-258.
[40] R. Alsulami, S. Nates, W. Wang, H.W. Won, B. Windom. Effects of varying liquid fuel and air co-flow rates on spray characterisation of an annular co-flow spray burner, Proceedings of the ASME Turbo Expo 2019: Turbomachinery Technical Conference and Exposition GT2019; 2019; Phoenix, Arizona, USA.
[41] R.A. Alsulami, B. Windell, D. Bartholet, B. Windom, Exploring the Role of Physical and Chemical Properties on the Ignition and Flame Stability of Liquid Fuels with a Spray Burner and Fuel Ignition Tester (FIT), 2018 AIAA Aerospace Sciences Meeting, American Institute of Aeronautics and Astronautics2018.
[42] G.D. Myers, A.H. Lefebvre, Flame propagation in heterogeneous mixtures of fuel drops and air, Combustion and Flame 66 (1986) 193-210.
[43] A. Neophytou, E. Mastorakos, Simulations of laminar flame propagation in droplet mists, Combustion and Flame 156 (2009) 1627-1640.
[44] C. Ji, E. Dames, H. Wang, F.N. Egolfopoulos, Propagation and extinction of benzene and alkylated benzene flames, Combustion and Flame 159 (2012) 1070-1081.
[45] C. Ji, E. Dames, Y.L. Wang, H. Wang, F.N. Egolfopoulos, Propagation and extinction of premixed C5–C12 n-alkane flames, Combustion and Flame 157 (2010) 277-287.

CHAPTER 5: Investigating the Role of Fuel Droplet Vaporization and Atomization on Spray Flame Stability and Dynamics of Single and Two Simple Mixture Fuels[4]

5.1 Summary

The focus of this study is to investigate the role of atomization and vaporization, processes which control spray dynamics and reactant mixing in the majority of our transportation power systems, on flame stability. Single component fuels, including n-heptane, n-dodecane, toluene, and 1,2,4-trimethylbenzene, carefully selected to cover a wide range of physical and chemical properties, as well as, two binary fuel mixtures were tested in a spray burner in which flame liftoff heights and blowout limits were measured. Using a derived correlation capable of predicting the gas phase global extinction behavior of simple hydrocarbon blends, the mixture compositions were formulated to match gas phase extinction performance with differences in the relative volatility of the reactive species. Despite having similar gas phase extinction limits, when utilized in the spray burner while maintaining a constant droplet size, the mixtures exhibited different stability behaviors marked by variation in flame liftoff height and blowout limits. It was found that flame liftoff heights were primarily influenced by the flame speed of the vaporized fuel entering the flame and to a lesser extent the overall volatility of the fuel. In the case of Mixture 1 (55% n-heptane/45% 1,2,4-trimethylbenzene), preferential vaporization of the lighter species provided a more reactive gas phase mixture contributing to a shorter lifted flame than Mixture 2 (63% toluene/37% n-dodecane). Spray flame blowout was largely influenced by the amount of liquid

[4] This chapter is largely based on a manuscript that will be submitted soon: Alsulami, Radi A., et al. "Investigating the Role of Fuel Droplet Vaporization and Atomization on Flame Stability and Dynamics." *Combustion and Flame (2020).*

fuel penetrating the flame and the reactivity of the liquid fuel within the droplet. In Mixture 2, preferential evaporation promoted the reactivity of the liquid fuel droplet entering the flame enhancing its stability relative to Mixture 1. The results herein suggest that atomization/vaporization dynamics can influence flame stability in liquid fueled applications and should be carefully considered in surrogate fuel development activities.

5.2 Introduction

The majority of previous work has studied the combustion behavior and stability of flames fed by gaseous or pre-vaporized fuels, e.g. [4-6]. As such, surrogate formulation efforts have primarily focused on emulating the gas phase combustion characteristics of the real liquid fuel, e.g. [7-9]. This methodology eliminates the effect of significant physical phenomena on the energy conversion process, namely atomization and vaporization, and presents a pitfall in the form of potential preferential vaporization for multicomponent fuels which may prevent the surrogate fuel from emulating the target fuel in a real combustion application. There have been a limited number of studies which have targeted both physical (e.g. density, viscosity, surface tension, volatility) and chemical properties in the development of surrogate fuels, e.g. [10, 11], and even fewer that have used two phase combustion phenomena to aid in surrogate fuel development, e.g. [12, 13].

Recent numerical work have shown that in relevant conditions for internal combustion engines preferential evaporation phenomena can occur resulting in a transient vapor composition which differs from that of the liquid fuel droplet [14, 15]. This preferential droplet evaporation can affect the fuel composition distribution within the engine, and can influence the ignition timing, flame phenomenon, and sooting tendency of the fuel (or surrogate fuel) [14-18]. Other works have studied the influence of the complex interaction between the atomization, vaporization, and turbulent fuel/air mixing on spray flame stability, though these activities have primarily focused

on the behaviors of single component liquid fuels [19-22]. For many of these studies, conclusions were drawn that the processes of atomization, mixing, turbulence, evaporation, and flame chemistry could influence flame stability limits, and that the effect of different physical and chemical properties of the fuel, such as boiling temperature, enthalpy of vaporization and ignition temperature influence flame liftoff height.

A spray burner was developed to investigate the role of atomization and evaporation processes on the stability of liquid-fueled flames. Experiments were carried out with carefully selected single component fuels and operating conditions to explore the role of fuel volatility, droplet size, and reactivity on the flame stability marked by blowout limits and flame liftoff heights. Differing from previous work, experiments were carried out with select fuels of varying volatility and reactivity, as well as carefully design fuel mixtures while maintaining a consistent droplet size to remove the influence of atomization on observations related to flame stability. The mixtures studied in the spray flame were selected to exhibit identical gas phase flame extinction behavior, confirmed by counterflow flame experiments, while varying the volatility of the reactive and unreactive species to explore the role of preferential vaporization on the spray flame behavior.

5.3 Experimental Design and Procedures

Similar to the previous chapter, four single hydrocarbon components were chosen, including n-heptane, n-dodecane, toluene, and 1,2,4-trimethylbenzene (TMB). The single fuels covered a wide range of physical properties and reactivity represented by gas phase diffusion flame extinction limits [6]. The n-alkane fuels were chosen to eliminate the chemical kinetic effect on the flame stability and rather focus on the influence from differences in their physical properties. The aromatic fuels were chosen to match as closely as possible the volatility of the n-alkane species allowing for the influence of chemical reactivity on the two-phase flame stability to be studied. In

addition, two binary mixtures were formed using the four fuels, each containing an n-alkane and aromatic species, but with opposed volatility. Selection of the mixture composition is described later. The properties of the fuels used in this study are listed in Table 5.1 [23].

Table 5.1. Physical and chemical properties of the fuels used in this study. All properties at 298 K, excluding the normal boiling temperature (NBT).

Fuel	MW [kg/kmol]	ρ_L [kg/m^3]	μ_L [kg/m.s]	σ_L [N/m]	NBT [K]	P_V [kPa]	Ri	ΔH_c [MJ/kg]
Mixture 1	109.2	764.38	0.000566	0.02358	-	-	0.75	42.918
Mixture 2	121.07	799.07	0.02624	0.02624	-	-	0.72	41.905
n-Heptane	100.2	681.66	0.000391	0.01984	371.58	6.021	1	44.5
n-Dodecane	170.33	746.39	0.00136	0.025	489.473	0.018	1	44.147
Toluene	92.14	864.05	0.00056	0.028	383.78	3.775	0.56	40.589
1,2,4-TMB	120.19	872.31	0.00089	0.03	442.53	0.284	0.44	40.984

5.3.1 Counterflow Burner

The counterflow burner was used to derive a predictive correlation to aid in the selection of fuel mixtures which exhibited identical gas phase diffusion flame extinction limits. The burner consists of two opposing converging nozzles with an inner exit diameter of 10 mm that have been aerodynamically designed to generate a radially uniform velocity at the nozzle exit. The separation distance between the two nozzles is set at 9 mm. The fuel is pre-vaporized and blended with nitrogen to control the fuel mass fraction. Figure 5.1 illustrates the burner configuration. Measurements were carried out at fuel mole fractions between 6-25% with air as the oxidizer. A fuel exit temperature of 500 K (±10 K) for all the experiments was used. A syringe pump was used to control the liquid fuel flow rate, and the flow rates of the nitrogen and air were controlled by

calibrated sonic nozzles. The temperature of the oxidizer was kept at 298 K. A nitrogen co-flow was applied to shield the flame from the ambient air.

To calculate the extinction strain rates, the fuel and air flow rates are increased simultaneously while maintaining a momentum balance until the flame extinguishes. Once the flame extinguishes,

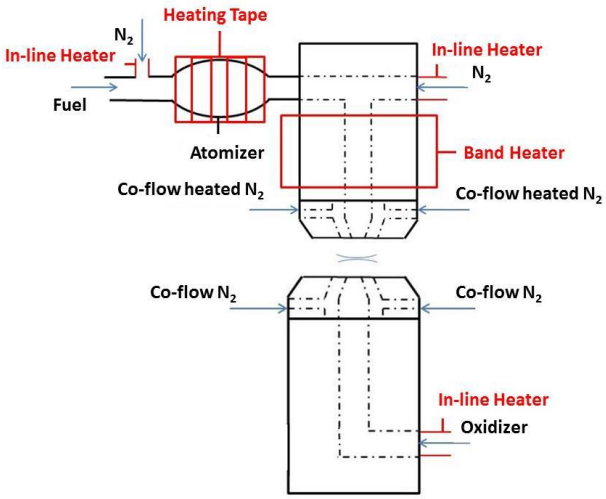

Figure 5.1. Counterflow burner configuration [1].

the fuel and oxidizer nozzle exit velocities are recorded and the global strain rate is calculated using the established formula from [24].

$$a = \frac{2U_O}{L}\left(1 + \frac{U_F}{U_O}\left(\sqrt{\frac{\rho_F}{\rho_O}}\right)\right) \tag{5.1}$$

where U_O is the velocity of oxidizer, U_F is the velocity of fuel, L is the axial distance, ρ_F is the density of vapor fuel, and ρ_O is the density of oxidizer. The fuel mole fraction is adjusted, and the experiment is repeated at least twice for each fuel and the results showed promising repeatability [22, 23]. With the measured global extinction strain rates, the radical index approach was applied to determine a correlation to predict the extinction strain rate of a mixture [6].

5.3.2 Annular Co-flow Spray Burner

The ACS Burner is used and its schematic is illustrated in Fig. 5.2. More description of the burner can be found in Chapter 2. Similar to the study in Chapter 4, multiple exchangeable spray injectors (listed in Fig. 5.2) were used with different orifice sizes to control droplet size. The fuel and air temperatures used in the spray burner experiment were kept at 298 K.

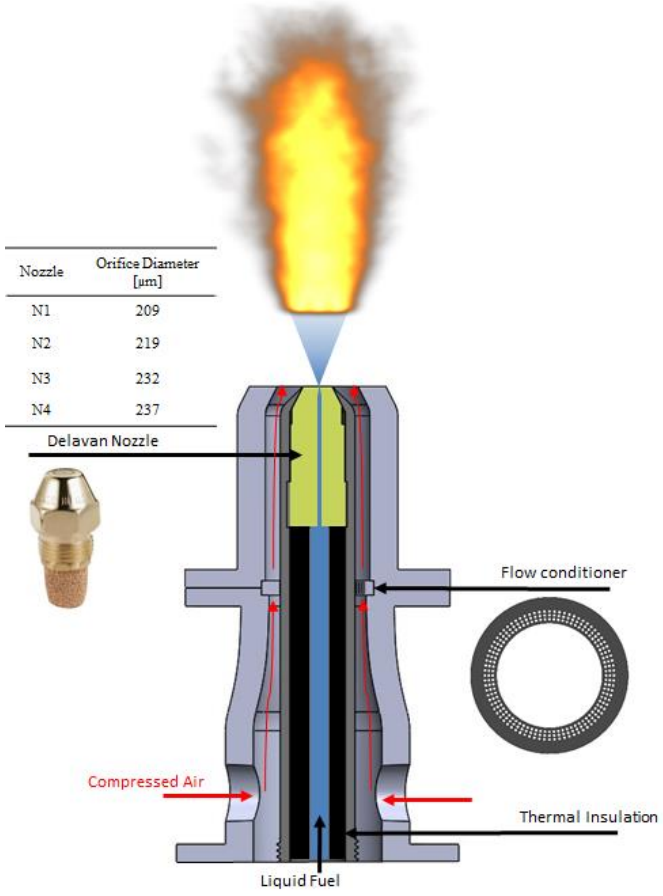

Figure 5.2. Schematic of the turbulent spray burner setup.

Stemming from the differences in physical properties between the fuels, seen in Table 5.1, the spray atomization process can result in different droplet sizes for each fuel. The Sauter Mean Diameter is calculated using the commonly employed correlation of Lefebvre [26, 27]:

$$d_{SMD} = 2.25\sigma_l^{0.25}\mu_l^{0.25}\dot{m}_l^{0.25}\Delta P^{-0.5}\rho_{air}^{-0.25} \tag{5.2}$$

where σ_l is the liquid surface tension, μ_l is the liquid viscosity, $\dot{m}_l$ is the liquid mass flow rate, ΔP is the pressure drop across the spray nozzle orifice, and ρ_{air} is the surrounding air density. The droplet size was calculated for all the fuels using the properties listed in Table 5.1. The ΔP term was taken as the difference between the pressure reading by the syringe pump and the ambient pressure. The Lefebvre correlation (Eq. (5.2)) provides an insight into the relative differences in the droplet sizes of the different tested fuels, as a result of the variation in their physical properties, such as viscosity, surface tension, and density, and was verified to predict relative difference in droplet sizes for different fuels using ACS burner [28]. In addition, it was used in several related works, e.g., [27, 29].

In the spray burner, the role of the physical and chemical properties of all selected fuels on flame stability were investigated by measuring the liftoff heights (LOH) and lean blowout (LBO) limits for a range of fuel and air flow rates. Flame liftoff height is measured by collecting 50 images of the turbulent stabilized spray flame for each condition. The set of images are averaged, and the liftoff height is defined as the distance between the nozzle tip and the base of the flame, identified by the location of the maximum intensity gradient in the image. Liftoff heights were measured along the centerline and at consistent co-flow conditions for all fuels. As such, we do not expect there to be any influence of the surrounding air on the differences in liftoff height observed between the fuels. Liftoff heights are reported for the set of fuels at a single fuel flow rate, $\dot{V}_F = 50$ mL/min, and a range of air flow rates, $\dot{V}_{air} = 200$, 300, 400, 500, and 600 SLPM, corresponding to Reynolds numbers spanning from 5760 to 17300.

Blowout limits were determined by slowly increasing the air flow rate while keeping the selected fuel flow rate constant until the flame is extinguished. The fuel and air flow rates along with the global equivalence ratios at the time of blowout are identified. The blowout measurements

were repeated at least twice for each of the selected fuels. The measurements were carried out for multiple fuel flow rates, $\dot{V}_F$ = 45, 50, 55, 60, and 65 mL/min. Measurement repeatability was observed with a relative standard deviation from the mean value between 0.5-4.5% for all of the fuels tested. For the blowout measurements, the air co-flow rates used in this work are significantly high (e.g. 700-1080 SLPM), thus, we expect the influence of the surrounding quiescent air on the global equivalence ratio to be negligible. The LBO and LOH experiments were carried out at the laboratory environment, e.g., T= 298 K ± 5 K and P= 0.84 atm.

5.4 Results and Discussion

5.4.1 Gas Phase Flame Extinction

Using the previously published radical index approach, the following correlation was derived from the experimental measurement to predict the extinction behavior of a pre-vaporized diffusion flame:

$$a_E = 144.18 \times Ri \times [Fuel] \times \Delta H_C \times \left(\frac{MW_F}{MW_{N2}}\right)^{-0.5} + 5.5184 \quad (5.3)$$

where Ri is the fuel radical index, a measure of the fuel's reactivity or ability to produce radicals, $[Fuel]$ is the fuel concentration, ΔH_C is the fuel's enthalpy of combustion, and MW_F, and MW_{N2} are the fuel and nitrogen molecular weights, the ratio of which describe the transport dynamics of the reactants. The Ri, derived in [6], along with the ΔH_C for each single component fuel are provided in Table 1. It should be noted that this correlation, derived from experiments taken in Fort Collins, CO at reduced pressure (0.84 atm), differed from the correlation previously reported. Though beyond the scope of this study, it is possible that this stems from the differences in the pressure from which the measurements were taken, 0.84 atm vs. 1 atm. Using the correlation in Eq. (5.3) two mixtures were selected to have similar extinction strain rates with the following

molar composition: Mixture 1: 55/45% n-heptane/TMB and Mixture 2: 63/37% toluene/n-dodecane.

The extinction strain rate measurements for each of the single component fuels and the selected mixtures along with the correlation derived from the radical index approach, both current and previous, are provided in Fig. 5.3. Clearly, the gas phase flame extinction limits are dependent on the molecular structure of the fuel, with n-dodecane producing the most robust flame and toluene the weakest of those that were measured. Flame extinction data for TMB are not presented in Fig. 5.3 as its flame at the local ambient pressure was unstable and did not allow for repeatable extinction measurements. Previous work showed that the TMB flames were weaker than that of toluene [6]. It should also be pointed out that the extinction strain rates for the mixtures fall between the extinction strain rates of the components. The current correlation (solid lines) predicts the experimental measurements for the two mixtures within a maximum uncertainty level of ~10% from the experiment, whereas the correlation from previous work (dashed lines) [6] over

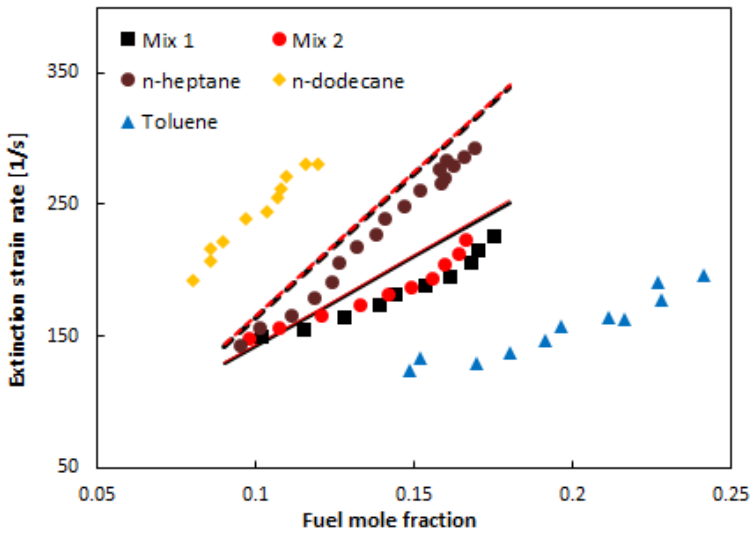

Figure 5.3. Extinction strain rates for measured (symbols) and predicted from the radical index, enthalpy of combustion, and average molecular weight; correlation from previous work (dashed lines) and the current work (lines).

predicts the experimental results. The good agreement between the correlation and the experiments for the mixtures suggests that the radical index approach, once normalized to the current conditions, can be used to predict extinction behavior of fuel mixtures without measurements for each individual species (TMB in this case).

5.4.2 Spray Flame Stability

The spray flame stability was predicted by measuring the liftoff heights and the blowout limits for each fuel at different spray, co-flow, and fuel flow rates. Consistent with previous work, it was noticed that n-alkane fuels have a double flame structure, blue (partially premixed) flame upstream near the burner tip followed by a soot rich yellow flame [30]. The two aromatic species, toluene and TMB, exhibit an entirely sooty yellow flame with very high luminosity. Interestingly, the two mixtures resemble more closely the aromatic flames than those from the n-alkanes. For the heavier/less volatile fuels, such as n-dodecane and TMB, unburned droplets can be seen passing through the flame.

Since the hydrocarbon species used in this study possess very different physical properties, the atomization process and the resulting droplet size can be affected. Variation in droplet size will influence the droplet lifetimes and the amount of liquid which penetrates the flame. The Sauter mean diameter (SMD) for n-heptane was calculated using Eq. (5.2) for different spray injector orifice sizes as a function of fuel flow rate and is illustrated in Fig. 5.4a. As the fuel droplet size increases, the flame liftoff height rises as shown in Fig. 5.4b and the flame becomes more difficult to blowout, as seen in Fig. 5.4c, the reasons for which stem from reduced vaporization as the droplet size is increased [21]. To remove this influence from flame lift and blowout measurements, each fuel was tested with a selected nozzle orifice size (based on Eq. (5.2)) to maintain a similar

droplet diameter across all fuels, as seen in Fig. 5.5. This approach was described in detail in Chapter 4.

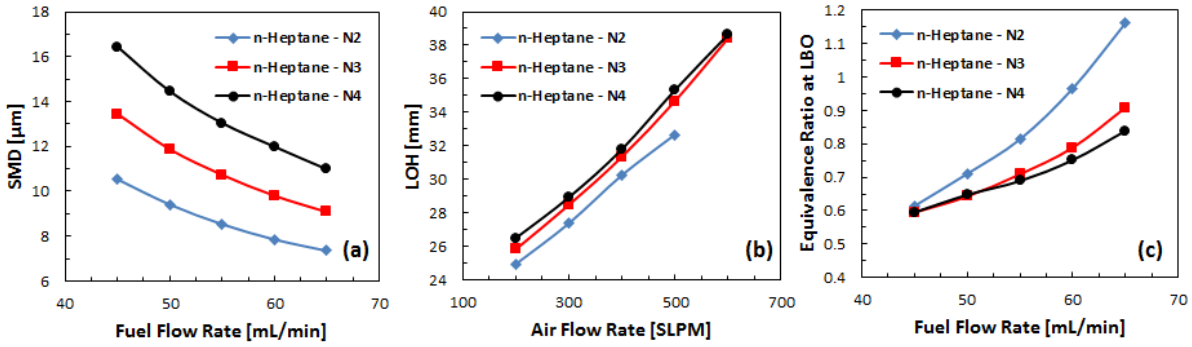

Figure 5.4. (a) Droplet diameters for n-heptane for different nozzle sizes. The effect of droplet size on (b) flame liftoff height, and (c) on flame blowout limit.

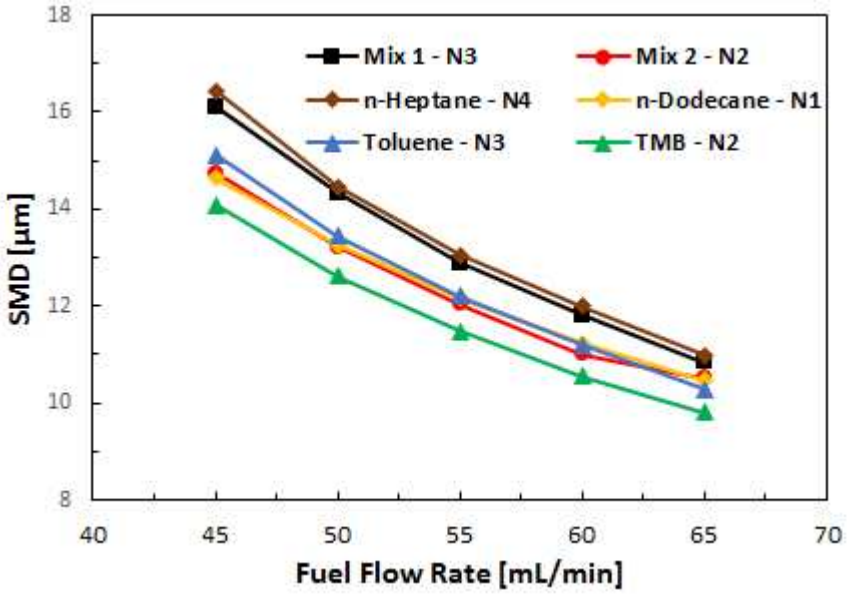

Figure 5.5. The calculated Sauter mean droplet diameter for all selected fuels using Eq. (5.2) at different fuel flow rates, using nozzle N1 with n-dodecane, N2 with TMB and Mix 2, N3 with toluene and Mix 1, and N4 with n-heptane.

5.4.3 Liftoff Height Results

Figure 5.6 shows the liftoff height for all the fuels at $\dot{V}_F = 50$ mL/min as a function of air flow rate while maintaining similar droplet diameters for all tested fuels. In general, the liftoff height

increases with increased air flow rate due to the leaning of the mixture, resulting in moving the stoichiometric mixture and that of the maximum burning velocity (spray flame speed) downstream before it can stabilize against the coming fuel and air flow. The role of volatility and diffusivity on flame lift can be observed in the case of n-heptane and n-dodecane, which have similar gas phase reactivity but very different vapor pressures and molecular weights. The flame lift is higher for n-dodecane than n-heptane, however the difference is minimal compared to the other species suggesting that the effect of vaporization on flame liftoff is minor in this case. 1,2,4-trimethylbenzene demonstrates the highest liftoff despite having a higher vapor pressure than n-dodecane, as it is the least reactive of the single component fuels (marked by the laminar flame speed as listed in Table 5.2). Furthermore, it was noticed that the liftoff height for toluene was larger than n-dodecane (Fig. 5.6), although toluene is significantly more volatile, again, indicating that the reactivity of the fuel has a stronger impact on the liftoff height than the volatility. The

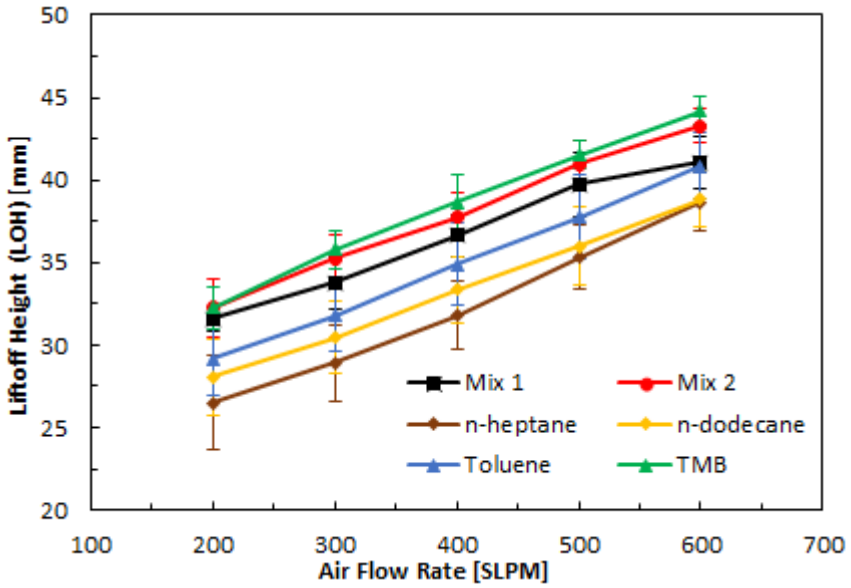

Figure 5.6. Liftoff heights for all selected fuels at fuel flow rate of 50 mL/min as a function of air flow rate.

Table 5.2. Laminar flame speeds for the single fuels from previous works and they were measured at 400 K, at atmospheric pressure, and stoichiometric equivalence ratio [2, 3]. The flame speed of the mixtures are calculated based on the mass fraction of their individual components.

Fuel	S_L [cm/s]
Mix 1	56.84
Mix 2	59.39
n-Heptane	64.13
n-Dodecane	64.05
Toluene	54.34
TMB	49.42

flame of Mixture 2 is lifted higher than that of Mixture 1 and interestingly higher than the two components which comprise the mixture.

To better understand the trends, the measured liftoff heights in Fig. 5.6 were plotted against the co-flow velocity ($V_{co\text{-}flow}$) in Fig. 5.7a. $V_{co\text{-}flow}$ is the air co-flow velocity at the exit of the burner and was estimated as (5.24, 7.86, 10.48, 13.1, and 15.72 m/s) for the different air flow rates, e.g., 200, 300, 400, 500, and 600 SLPM, respectively. As a first attempt to explain differences in flame liftoff between the fuels, the gas phase laminar flame speed (S_L) was used, as suggested by many previous works [31, 32]. Thus, the liftoff height (LOH) is plotted against ($V_{co\text{-}flow}/S_L$) in Fig. 5.7b. The laminar flame speeds used in this work (listed in Table 5.2) are for stoichiometric fuel-air mixtures and were measured at atmospheric pressure and a temperature of 400 K using the counterflow flame approach [2, 3]. As seen in Fig. 5.7b, the liftoff height shows good correlation with the flow velocity and the inverse of gaseous flame speed ($V_{co\text{-}flow}/S_L$) with a correlation coefficient of 0.88. Differences were still observed for the different fuels. This indicates the need to include time scales associated with vaporization in concert with the gas phase flame speed as

shown previously by Lefebvre et al. [31], when he proposed a model to predicted the rate of flame propagation through quiescent multi-droplet mists as the following:

$$S_{spray} = \alpha_g \left[\frac{(1-f_v)\rho_F D^2}{8\rho_g ln(1+B)} + \frac{\alpha_g^2}{S_L^2} \right]^{-0.5} \quad (5.4)$$

In Eq. (5.4), S_{spray} is the two-phase flow (spray) flame speed, α_g and ρ_g are the thermal diffusivity and density of the air, respectively, at an average temperature ~1200 K, which was suggested in Lefebvre et al. and in the work of Neophytou and Mastorakos [31, 32], f_v is the fuel vapor mass fraction and *D* is the droplet diameter at the preheated zone (just before entering the flame), both calculated using a 0D droplet evaporation model based on the d^2 law. The vapor fraction (f_v) and the droplet diameter (*D*) were specified for all the fuels at the time when n-heptane was completely

Table 5.3. Values of parameters used in Eq. (5.4) to calculate the spray flame speed.

Fuels - Nozzle	n-Heptane	n-Dodecane	Toluene	TMB	Mix 1	Mix2
Predicted droplet diameter at nozzle exit (D_o) [µm]	14.46	13.26	13.46	12.63	13.58	12.53
Predicted droplet diameter at preheated zone (*D*) [µm]	0.67	13.2	8.14	11.98	9.81	10.3
Predicted vapor volume fraction entering the flame (f_v)	0.999	0.0128	0.778	0.146	0.623	0.445
Specific heat (C_P) [kJ/kg.K] at average temperature ($\overline{T}$)	3.37	3.46	2.53	2.74	3.06	3.01
Heat of Vaporization (HOV)at 298 K [kJ/kg]	365.54	362.05	411.77	397.59	381.42	385.89
Air density (ρ_{air}) at 1200 K [kg/m^3]	0.2902					
Air thermal diffusively (α_{air}) at 1200 K [m^2/s]	2.24E-04					

vaporized, since it is the most volatile fuel in this work and they are listed in Table 5.3. The initial droplets (D_o), which was plugged in the droplet model are shown in Fig. 5.4. ρ_F is the liquid fuel density at 298 K, and B is the heat transfer number (Spalding number), calculated using the following formula:

$$B = \frac{c_{pg}(T_\infty - T_{boil})}{h_{fg}} \tag{5.5}$$

where c_{pg} is the specific heat of the fuel at average temperature and was taken from DIPPER database [33]. T_∞ and T_{boil} are the environment temperature of the preheated zone (~ 1200 K) and fuel boiling temperature, respectively. h_{fg} is the fuel heat of vaporization, which is provided in Table 5.3.

Plotting the liftoff height (LOH) with the co-flow velocity and the inverse of the spray burning velocity predicted by Eq. (5.4) improved the results and explains the differences in measured liftoff heights amongst single component fuels, as seen in Fig. 5.7c. In addition, when the change of the compositions, as a result of preferential vaporization, was accounted for to predict the spray burning velocity for the mixtures, the results of Mixtures 1 and 2 improved, and thus overall correlation coefficient of 0.91 was achieved.

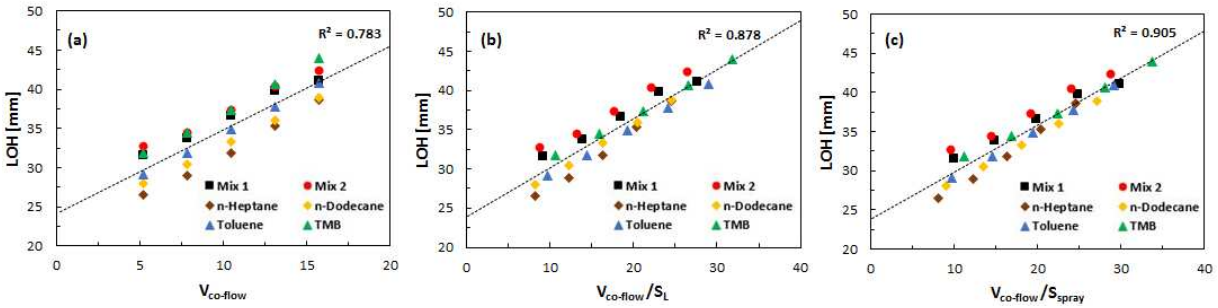

Figure 5.7. Liftoff heights (LOH) for all fuels (from Fig 5.6) (a), LOH correlated to the air co-flow velocity over the gaseous flame speed ($V_{co\text{-}flow}/S_L$) (b), and LOH as a function of the co-flow velocity and the inverse the spray burning speed ($V_{co\text{-}flow}/S_{spray}$) (c).

5.4.4 Blowout Limit Results

The flame stability of the fuels was also investigated by measuring the blowout limits, the results of which are presented in Fig. 5.8. In general, the heavier/less volatile fuels (e.g. n-dodecane) were the most difficult to blowout. This result is explained by the heavier fuels requiring more time to evaporate and delivering more liquid fuel into the flame, causing a local enrichment supporting similar observations from [21, 34]. In contrast, the n-heptane flame was the easiest to blowout, as it is the most volatile fuel in this study. However, volatility is not the sole driving mechanism for spray flame stability, as seen in the opposite trends between the aromatic species. The toluene flame is more difficult to extinguish than the TMB despite being significantly more volatile. This will be discussed in more detail later and is a result of differences between the fuel's reactivity as well as differences in density and molecular weight, which influence the amount of liquid moles, which enter the flame. It should also be pointed out that Mixture 1 behaves similarly to the TMB, the heavy component of the Mixture 1.

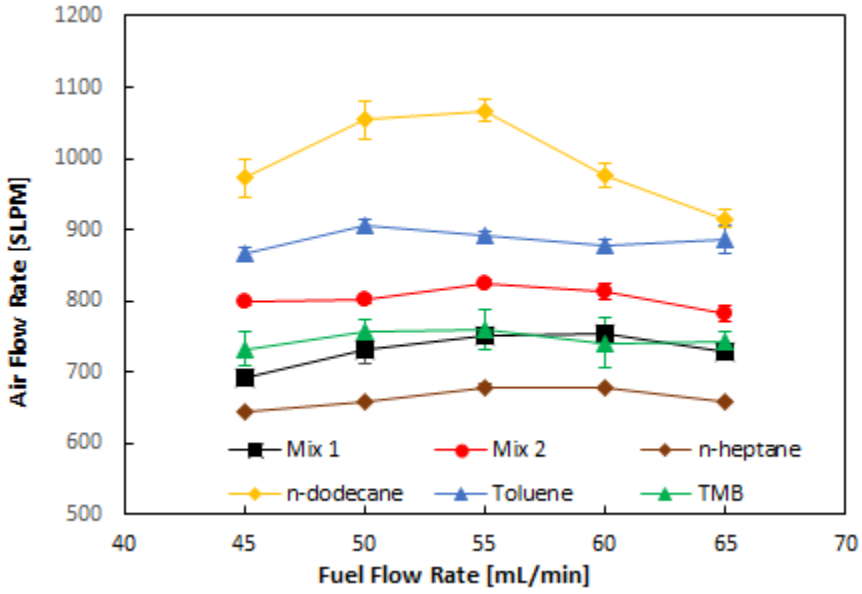

Figure 5.8. Blowout limits for all selected fuels.

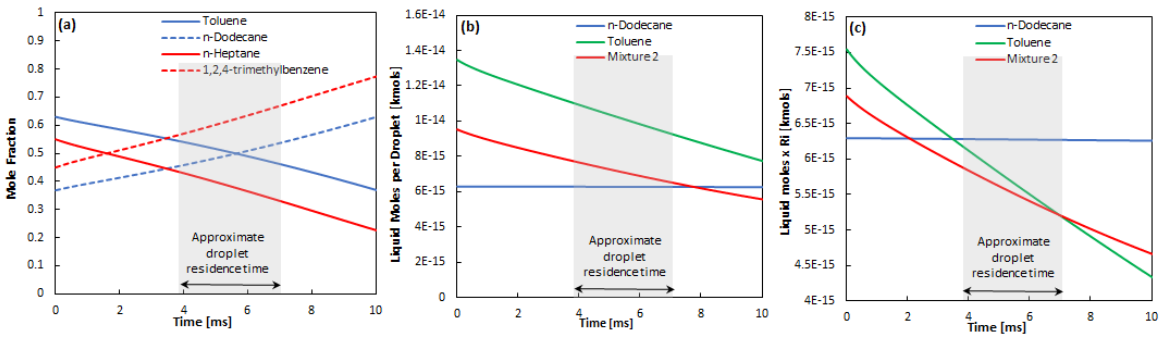

Figure 5.9. (a) Transient liquid droplet composition for mixture 1 (red) and mixture 2 (blue), (b) time dependent liquid moles per droplet and (c) the liquid moles per droplet normalized by the transient radical index for the toluene, n-dodecane, and fuel Mixture 2 flames.

Utilizing results from the droplet evaporation model, the transient droplet composition of the two mixtures were predicted. Plotting the moles of each species remaining in the liquid droplet as a function of time, Fig. 5.9a, it can be seen that the number of moles of TMB is nearly double that of the n-heptane at approximate times corresponding to the residence time of the droplet needed to travel from the burner exit to the flame, measured by PDPA system in previous chapter. Given that, the number of moles of TMB is twice that of n-heptane it makes sense that the flame stability of Mixture 1 follows closely that of TMB, further highlighting the significance of the liquid portion of the fuel on spray flame stability.

Mixture 2 exhibits an unexpected behavior as its flame is easier to blowout than the two components, which comprise the mixture: toluene and n-dodecane. Looking at the transient composition (Fig. 5.9a, blue curves), it is seen that the number of moles of each species in the liquid phase at the time the droplet reaches the flame are nearly identical. This results from a combined effect of the mixture VLE but also the significant density and molecular weight differences between the two components. Comparing the time dependent number of liquid moles which enter the flame for Mixture 2 to the single fuel cases of its two components, it can be seen that the toluene spray actually has many more liquid moles entering the flame than either n-

dodecane or Mixture 2 (Fig. 5.9b). Accounting for reactivity by normalizing by the radical index, the three fuels now follow the same trend observed in the blowout experiments (Fig. 5.9c). This analysis signifies that the localized flame surrounding the fuel droplet plays a dominant role in a spray stabilized flame and that the amount of fuel remaining in the liquid, along with the reactivity potential of the liquid species, plays a significant role in defining the robustness of the flame.

5.5 Conclusion

Flame stability was measured for single component fuels and binary mixtures in a pre-vaporized counterflow and spray burner. A correlation derived to predict the gas phase extinction behavior was used to determine two mixtures with identical gas phase extinction strain rates, but with opposite trends in the volatility of the reactive species. Despite having similar gas phase extinction limits, when utilized in the spray burner experiments while maintaining a constant droplet size, the mixtures exhibited different stability behaviors marked by flame liftoff and blowout limits. For the experiments, it was found that flame liftoff heights were largely influenced by the flame speed of the fuel vaporized prior to entering the flame and to a lesser extent the volatility. In the case of Mixture 1, preferential vaporization of the lighter species provided a more reactive mixture contributing to a shorter lifted flame than Mixture 2. Consistent with previous studies, spray flame blowout was largely influenced by the amount of liquid fuel in the form of droplets penetrating the flame, controlled by the fuel volatility, along with the reactivity of the liquid fuel within the droplet entering the flame. For simple mixtures, as the case herein, preferential evaporation of the fuel can alter the reactivity of the liquid fuel and subsequently affect flame stabilization. The results suggest that VLE and atomization/vaporization dynamics can influence flame stability in liquid fueled applications and should be carefully considered in surrogate fuel development activities.

References

[1] C.W. Curtis, Combustion characteristics of thermally stressed hydrocarbon fuels, University of Colorado at Colorado Springs2016.
[2] K. Kumar, J. Freeh, C. Sung, Y. Huang, Laminar flame speeds of preheated iso-octane/O2/N2 and n-heptane/O2/N2 mixtures, Journal of propulsion and power 23 (2007) 428-436.
[3] X. Hui, C.-J. Sung, Laminar flame speeds of transportation-relevant hydrocarbons and jet fuels at elevated temperatures and pressures, Fuel 109 (2013) 191-200.
[4] B. Windom, S.H. Won, C.B. Reuter, B. Jiang, Y. Ju, S. Hammack, T. Ombrello, C. Carter, Study of ignition chemistry on turbulent premixed flames of n-heptane/air by using a reactor assisted turbulent slot burner, Combustion and Flame 169 (2016) 19-29.
[5] S.H. Won, B. Windom, B. Jiang, Y. Ju, The role of low temperature fuel chemistry on turbulent flame propagation, Combustion and Flame 161 (2014) 475-483.
[6] S.H. Won, S. Dooley, F.L. Dryer, Y. Ju, A radical index for the determination of the chemical kinetic contribution to diffusion flame extinction of large hydrocarbon fuels, Combustion and Flame 159 (2012) 541-551.
[7] A. Agosta, N.P. Cernansky, D.L. Miller, T. Faravelli, E. Ranzi, Reference components of jet fuels: kinetic modeling and experimental results, Experimental Thermal and Fluid Science 28 (2004) 701-708.
[8] S. Honnet, K. Seshadri, U. Niemann, N. Peters, A surrogate fuel for kerosene, Proceedings of the Combustion Institute 32 (2009) 485-492.
[9] S. Dooley, S.H. Won, J. Heyne, T.I. Farouk, Y. Ju, F.L. Dryer, K. Kumar, X. Hui, C.-J. Sung, H. Wang, The experimental evaluation of a methodology for surrogate fuel formulation to emulate gas phase combustion kinetic phenomena, Combustion and Flame 159 (2012) 1444-1466.
[10] T. Edwards, L.Q. Maurice, Surrogate mixtures to represent complex aviation and rocket fuels, Journal of Propulsion and Power 17 (2001) 461-466.
[11] A. Violi, S. Yan, E. Eddings, A. Sarofim, S. Granata, T. Faravelli, E. Ranzi, Experimental formulation and kinetic model for JP-8 surrogate mixtures, Combustion Science and Technology 174 (2002) 399-417.
[12] M. Aye, J. Beeckmann, N. Peters, H. Pitsch, Spray Phenomena of Surrogate Fuels and Oxygenated Blends in a High Pressure Chamber, Fuels From Biomass: An Interdisciplinary Approach, Springer, 2015, pp. 1-17.
[13] H.M. Poon, K.M. Pang, H.K. Ng, S. Gan, J. Schramm, Development of multi-component diesel surrogate fuel models–Part II: Validation of the integrated mechanisms in 0-D kinetic and 2-D CFD spray combustion simulations, Fuel 181 (2016) 120-130.
[14] S.C. Burke, M. Ratcliff, R. McCormick, R. Rhoads, B. Windom, Distillation-based Droplet Modeling of Non-Ideal Oxygenated Gasoline Blends: Investigating the Role of Droplet Evaporation on PM Emissions, SAE International Journal of Fuels and Lubricants 10 (2017) 69-81.
[15] A. Stagni, L. Esclapez, P. Govindaraju, A. Cuoci, T. Faravelli, M. Ihme, The role of preferential evaporation on the ignition of multicomponent fuels in a homogeneous spray/air mixture, Proceedings of the Combustion Institute 36 (2017) 2483-2491.
[16] N. Kurimoto, N. Watanabe, S. Hoshi, S. Sasaki, M. Matsumoto, Numerical Modeling of International Variations in Diesel Spray Combustion with Evaporation Surrogate and Virtual Species Conversion, Report No. 0148-7191, SAE Technical Paper, 2017.

[17] L.M. Itani, G. Bruneaux, A. Di Lella, C. Schulz, Two-tracer LIF imaging of preferential evaporation of multi-component gasoline fuel sprays under engine conditions, Proceedings of the Combustion Institute 35 (2015) 2915-2922.
[18] J.E. Madero, R.L. Axelbaum, Spray breakup and structure of spray flames for low-volatility wet fuels, Combustion and Flame 180 (2017) 102-109.
[19] C. Liu, F. Liu, J. Yang, Y. Mu, G. Xu, Investigations of the effects of spray characteristics on the flame pattern and combustion stability of a swirl-cup combustor, Fuel 139 (2015) 529-536.
[20] I. Düwel, H.W. Ge, H. Kronemayer, R. Dibble, E. Gutheil, C. Schulz, J. Wolfrum, Experimental and numerical characterization of a turbulent spray flame, Proceedings of the Combustion Institute 31 (2007) 2247-2255.
[21] J. Grohmann, B. Rauch, T. Kathrotia, W. Meier, M. Aigner, Influence of Single-Component Fuels on Gas-Turbine Model Combustor Lean Blowout, Journal of Propulsion and Power (2017) 1-11.
[22] W. O'Loughlin, A.R. Masri, A new burner for studying auto-ignition in turbulent dilute sprays, Combustion and Flame 158 (2011) 1577-1590.
[23] The DIPPR Information and Data Evaluation Manager for the Design Institute for Physical Properties, The DIPPR Information and Data Evaluation Manager for the Design Institute for Physical Properties, BYU Thermophysical Properties Laboratory, Provo, Utah, 2014.
[24] H. Chelliah, C. Law, T. Ueda, M. Smooke, F. Williams. An experimental and theoretical investigation of the dilution, pressure and flow-field effects on the extinction condition of methane-air-nitrogen diffusion flames. In: editor^editors. Symposium (International) on Combustion; 1991: Elsevier. p. 503-511.
[25] E. Fisher, B. Williams, J. Fleming, Determination of the strain in counterflow diffusion flames from flow conditions, CHEMICAL AND PHYSICAL PROCESSES IN COMBUSTION (1997) 191-194.
[26] A. Lefebvre, Atomization and sprays, combustion: an international series, Hemisphere Pub. Corp (1989).
[27] L. Esclapez, P.C. Ma, E. Mayhew, R. Xu, S. Stouffer, T. Lee, H. Wang, M. Ihme, Fuel effects on lean blow-out in a realistic gas turbine combustor, Combustion and Flame 181 (2017) 82-99.
[28] R. Alsulami, B. Windell, S. Nates, W. Wang, S.H. Won, B. Windom, Investigating the Role of Atomization on Flame Stability of Liquid Fuels in an Annular Spray Burner, Fuel (2019).
[29] A. Lefebvre, Fuel effects on gas turbine combustion—ignition, stability, and combustion efficiency, Journal of engineering for gas turbines and power 107 (1985) 24-37.
[30] M.S. Mansour, I. Alkhesho, S.H. Chung, Stabilization and structure of n-heptane flame on CWJ-spray burner with kHZ SPIV and OH-PLIF, Experimental Thermal and Fluid Science 73 (2016) 18-26.
[31] G.D. Myers, A.H. Lefebvre, Flame propagation in heterogeneous mixtures of fuel drops and air, Combustion and Flame 66 (1986) 193-210.
[32] A. Neophytou, E. Mastorakos, Simulations of laminar flame propagation in droplet mists, Combustion and Flame 156 (2009) 1627-1640.
[33] J. Rowley, W. Wilding, J. Oscarson, R. Rowley, DIADEM, DIPPR Information and Data Evaluation Manager, Brigham Young University, Provo, UT (2002).
[34] J. Grohmann, W. O'Loughlin, W. Meier, M. Aigner. Comparison of the Combustion Characteristics of Liquid Single-Component Fuels in a Gas Turbine Model Combustor, ASME Turbo Expo 2016: Turbomachinery Technical Conference and Exposition; 2016: American Society of Mechanical Engineers. p. V04AT04A010-V004AT004A010.

CHAPTER 6: Flame Blowout and Liftoff of Jet Fuels with Different Physical and Chemical Properties[5]

6.1 Summary

In this section, the investigation of the influence of fuel properties of different fuels on flame stability is extended to include real jet fuels (alternative and conventional). Thus, three conventional jet fuels, (Jet-A, JP-8, and JP-5), one alternative jet fuel, (Gevo-ATJ), and n-dodecane are studied in a spray burner. The laboratory spray burner provides similar trends in LBO and LOH to those experienced inside a realistic gas turbine combustor, but owing to its simplicity, it can be leveraged toward the understanding of the mechanisms that controls flame LBO and LOH of liquid jet fuels. Results show that as you increase fuel flow rates and decrease Sauter mean diameters, LBO correlate with boiling temperatures further into the distillation curve. This indicates the importance of the atomization process (i.e. droplet size) on the vaporization rate and suggests that the liquid fuel fraction entering the flame plays a dominant role in controlling flame stability. LOH results reveal that flame stabilization is a result of a balance between the local spray burning velocity and the local jet velocity, which is strongly tied to laminar flame speed and the relative amount of liquid/gas fuel entering the flame preheat zone.

6.2 Introduction

As a result of the increasing demand on petroleum, especially from the aviation sector [1], understanding the relative importance of fuel physical and chemical properties on gas turbine combustion performance, e.g., LBO, has been of interest for many researchers, (e.g., [2-12]).

[5] This chapter is largely based on a manuscript that will be submitted to the 38th International Symposium on Combustion: Alsulami, Radi A., et al. "Flame Blowout and Liftoff of Jet Fuels with Different Physical and Chemical Properties." *Proceedings of the Combustion Institute (2020).*

However, contradictory results have been reached, and thus further investigation is needed. The early work by Lefebvre concluded that the fuel air ratio at LBO is influenced by three terms, including combustor geometry (e.g., the combustor volume and the amount of air entering the primary combustion zone), operational conditions (e.g., the temperature and pressure of inlet gas), and the fuel's physical/chemical properties (e.g., mean droplet size, effective evaporation, and heat of combustion) as shown in Eq. (6.1) [3].

$$q_{LBO} \propto \left[\frac{f_{pz}}{V_{pz}}\right]\left[\frac{\dot{m}_{air}}{P_3^{1.3}\exp(T_3/300)}\right]\left[\frac{D_o^2}{\lambda_{eff}\,\Delta \mathrm{H_c}}\right] \tag{6.1}$$

The first and second term on the right-hand side of Eq. (6.1) are independent of the fuel properties and represent the combustor design and operation conditions, respectively. For a given combustor and operation conditions, the last term on the right-hand side, which embodies the effect of fuel properties, is the dominant term in predicting the relative fuel air ratio at LBO of conventional jet fuels. This correlation worked well at that time and the differences that occured in LBO were claimed to be caused mainly by differences in the physical properties of the fuel which influence the quality of atomization and the ensuing rate of evaporation. The minor impact of chemical reactivity that was mentioned in Lefebvre work is a result of using different jet fuels with similar chemical properties. A recent work by Esclapez et al. [4] used the same correlation (Eq. (1)) and suggested the implementation of an extra term which represents the temperature at which the ignition delay time equates the residence time of the fuel in the primary zone was required to provide greater predictability of LBO for different fuels. The addition of this term helps to capture the chemistry effect which was only included through the use of the heat of combustion, as discussed by Esclapez at al.

Burger et al. [5] studied the flame blowout behavior for 16 different fuels at an air inlet temperature of 310 K. They found that the easiest fuels to vaporize were the most difficult to reach

blowout limit. They tried to correlate the LBO results to a number of variables, such as derived cetane number (DCN) and Sauter mean diameter (SMD), however a weak correlation was found. Grohmann et al. [6] similarly studied the LBO behavior of different single hydrocarbon fuels, including n-hexane, iso-octane, and n-dodecane, at two different air preheated temperatures. At a temperature of 323 K, they found that the differences in the atomization (droplet sizes) and vaporization of the different tested fuels, especially n-hexane and n-dodecane, were dominant factors influencing the LBOs. In contrast with Burger et al., it was concluded that less volatile fuels (e.g., n-dodecane) and those with bigger droplets were more difficult to blow out (i.e., exhibited blow out at lower equivalence ratios). At higher temperature (e.g., 423 K), no clear conclusion was defined.

Recent studies have been carried out using statistical analysis to determine the impact of alternative and conventional jet fuel properties and compositions on LBO, such as [7-10]. Rock et al. [9] studied the LBO using a large rig scale model combustor of a realistic gas turbine. At low air inlet temperature (e.g., 300 K), they found that LBO correlates best with the 90 % distilled boiling temperatures, $T_{90,}$ with the most easily vaporized fuels having more resistance to blowout. For the case of high air inlet temperature (e.g., 450 K and 550 K), the DCN showed a good relationship with blowout limits with the fuels with high DCN exhibiting blow out at lower equivalence ratios. Won et al. [10] extended on Rock et al., using only 6 fuels, and claimed that using DCN values for the initial 20% liquid volume cuts significantly improved the linear correlation with LBO, credited to preferential vaporization phenomena. Two statistical analysis approaches, including integrated regression prediction and individual linear regression, were used by Zheng et al. [8] to evaluate the relative importance of fuel properties on combustion performance (e.g., LBO) using a Rolls-Royce Tay single can gas turbine combustor. They showed

that DCN and distillation slope between T10 and T50 have the most significant impact on resistance to blowout. Consistent with studies by Rock et al. [9] and Won et al. [10], they concluded that the fuel with high DCN blows out at a lower equivalence ratio. In contrast with Rock et al. [9] study, however, the distillation slope between T10 and T50 has a negative correlation with LBO, indicating that the fuels with higher boiling temperatures were more resistant to blowout. This again illustrates the importance of liquid loading on LBO, which will be discussed in this work. Peiffere at al. [7] did a similar analysis for LBO results using a Honeywell Auxiliary Power Unit (APU) combustor. It was found that the reference velocity, which is important in describing the mixing process, was the most important feature in predicting LBO (noting that this is a combustor characteristic), followed by distillate boiling temperatures (e.g., T20 and T50) and physical properties (e.g., surface tension, density, and viscosity). Chemical fuel properties (e.g., DCN) were shown to have very little impact on LBO. It is worth noting that DCN is specified by many studies as a fuel chemical property, although the nature of defining it is impacted significantly by the physical properties of the fuel, such as density, viscosity, and surface tension, which play important roles in defining the spray characteristics.

Flame stability limits refer to a broad range of conditions that disturb the steadily behavior of a flame and such effects can range from liftoff from the burner tip to intermittent blowout, to transient fluctuations induced by heat release and unsteady pressure feedback [13]. Lifted flames are found in gas turbines engines, as well as, in practical applications like burners in commercial boilers, where the lifted jet flame is utilized to reduce damage to nozzle material by minimizing contact between the flame and the nozzle [14]. The flame liftoff height (LOH) can also be influenced by the two-phase spray process and the interplay of a fuel's physical and chemical properties. The majority of previous literature, which has attempted to understand the mechanism that controls lifted flame stability, has primarily been performed with gaseous fuels, as reviewed by [15, 16].

Although the liftoff height stabilization mechanism is not fully understood and a number of theories are proposed, the edge-flame is the most supported theory among all of them [15]. The edge-flame concept, first proposed by Buckmaster [17], considers the leading edge to be partially premixed, located where the flame burning velocity is at a balance with the downstream flow and the mixture is at approximately stoichiometric mixture fraction.

Because of the complexity of heterogeneous spray flame phenomena, which arises from the interconnection of a number of processes such as atomization, vaporization, and chemical kinetics, none of the previous work has developed correlations for spray flame liftoff heights and the fuel's physical and chemical properties. Thus, the present research seeks to address a gap in the literature by defining the mechanism which control liftoff height for a spray flame surrounded by an annular air co-flow of different jet fuels.

This work focuses on understanding the mechanisms that control the flame LBO limits and the flame liftoff height for jet fuels using a laboratory spray burner. The results can be used to enhance the theoretical understanding of the flame LBO and liftoff height inside realistic gas turbine engines. The annular spray burner, with its small pressure injector and lack of swirler, is shown to have a relatively similar results to that of GIT combustor. In addition, the results illustrate the capability of using a controlled spray burner as a screening tool to help in identifying the promising alternative jet fuels, before further costly and time consuming full scale tests are carried out.

6.3 Experimental Setup

6.3.1 Facility

An Annular Co-flow Spray Burner (ACS Burner) was used to understand the mechanisms that control the flame LBO limits and the flame LOH for jet fuels. The experimental setup and the

burner description is provided in Chapter 2. The fuel and the air are delivered to the spray burner at room temperature of 298 K.

6.3.2 Fuels

A total of five fuels were used, including three conventional jet fuels, (Jet-A (A-2), JP-8 (A-1), and JP-5 (A-3)), one alternative jet fuel, (Gevo-ATJ (C-1)), and n-dodecane (NC12). These fuels were specifically selected to cover a wide range of physical, volatile, and chemical properties. For example, the differences in physical properties, specifically viscosity (which impacts the SMD) and distillate, between the three conventional fuels allow for insight into how these properties impact LBO and LOH. The nearly similar fuel physical properties of Gevo-ATJ and n-dodecane, but the vast differences in their DCNs, allows the evaluation of the relation between the fuel's chemical reactivity and the combustion performance, in particular, LBO. The properties for the candidate fuels evaluated in this study are shown in Table 6.1. Detailed properties of the conventional and alternative jet fuels are provided by Edwards [18].

6.3.3 Experimental Procedure and Conditions

Flame blowout limits were determined by slowly increasing the air flow rate while keeping the fuel flow rate constant until the flame extinguished. The air flow rate at the blowout limit is then recorded and the global equivalence ratio is calculated. The measurements were repeated at least twice for each of the fuel flow rates, i.e., 50, 55, and 65 mL/min, with good repeatability; maximum relative standard deviation from the mean was equal to 2.9%. The variation in test conditions provides an opportunity to analyze how different fuel flow rates affect LBO and its sensitivity to fuel properties. For the blowout measurements, the air co-flow rates used in this work are

significantly high (e.g. 700-1040 SLPM), thus, we expect the influence of the surrounding quiescent air on the global equivalence ratio to be negligible.

Table 6.1. Physical and chemical properties of candidate fuels.

Fuel name	**(A-1), JP-8 POSF 10264**	**(A-2), Jet-A POSF 10325**	**(A-3), JP-5 POSF 10289**	**(C-1), Gevo-ATJ**	**(NC12), n-dodecane**
Fuel description	Low viscosity	Nominal jet fuel	High viscosity	Low DCN	High DCN
MW [Kg/Kmol]	152	159	166	178	170.33
ΔH_c [MJ/kg]	43.24	43.06	42.88	43.88	44.11
DCN	48.8	48.3	39.2	17.1	72.90
TSI	16.5	25.5	32.5	15.6	7
H/C ratio	1.99	1.91	1.89	2.17	2.17
S_L at 1 atm & 130 °C [m/s]	56.54	56.26	55.71	52.26	59.44
ρ at 25 °C [kg/m^3]	772.14	795.57	819.09	751.74	746.60
μ at 25 °C [kg/m.s]	0.001049	0.001645	0.001924	0.001552	0.001276
σ at 25 °C [N/m]	0.02382	0.02468	0.02436	0.02254	0.024939
ASTM D86 Distillation					
IBP (°C)	145	159	174	173	216.2
10% (°C)	164	176	192	178	216.2
20% (°C)	171	184	199	179	216.2
50% (°C)	189	205	218	182	216.2
90% (°C)	234	244	244	228	216.2
FBP (°C)	256	269	258	263	216.2

Flame liftoff heights were measured for a single fuel flow rate (e.g., 50 mL/min) at different air flow rates (e.g., 200, 400, and 600 SLPM). The flame liftoff heights were determined by calculating the average luminosity intensity of 50 images for each experimental condition. The average image was then processed by plotting the average intensity along the horizontal center of

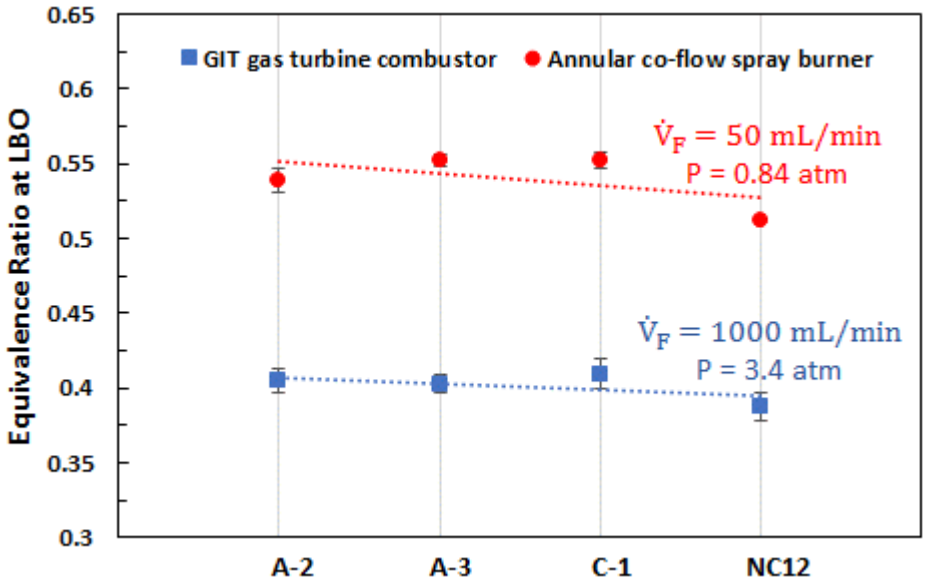

Figure 6.A. Normalized BOL results by Jet A (A-2) fuel for GIT combustor at 300 K and 3.4 atm and spray burner at 300 K and 0.84 atm.

the flame as a function of axial distance from the fuel injector nozzle. The flame location was then determined at the point of maximum luminosity gradient after applying a calibration factor to convert pixel height to distance. For all tested fuels, the maximum relative standard deviation from the mean liftoff height was 3.6%. Liftoff heights were measured along the centerline and at consistent co-flow conditions for all fuels. As such, we do not expect there to be any influence of the surrounding air on the differences in liftoff height observed between the fuels. The LBO and LOH experiments were carried out at the laboratory environment, e.g., T= 298 K ± 5 K and P= 0.84 atm.

6.4 Results and Discussion

6.4.1 LBO Results and Analysis

To demonstrate the effectiveness of using a laboratory spray burner, LBO relative results of two conventional jet fuels, i.e., Jet-A (A-2), and JP-5 (A-3), and one alternative jet fuel, i.e., Gevo-

ATJ (C-1), and one jet fuel surrogate, i.e., n-dodecane using an annular co-flow spray burner are plotted against results from Georgia Institute of Technology (GIT) gas turbine combustor [10], as shown in Fig. 6.1. Regardless of the LBO of the GIT combustor being better than the spray burner with average ~30% differences in their results, as expected, the annular spray burner, with its small pressure injector and lack of swirler, is shown to have a relatively similar results to that of GIT combustor, with less experimental time of operation and cost (i.e., each LBO measurement takes around a minute and ~50 mL of fuel). Although the LBO results of the spray burner were found to be similar to those of GIT combustor, it is necessary to use realistic combustors in the final stage of the testing.

Blowout results are compared for the five fuels at three different fuel flow rates (50, 55, and 65 mL/min) as shown in Fig. 6.2. In general, JP-8 (A-1), blows out at the highest equivalence ratios of all the tested fuels. This can be attributed to the high volatility of A-1 (see Table 1) and its smaller droplet sizes, as illustrated in Fig. 6.3. All the blowout limits of the tested fuels, except n-dodecane (NC12), correlate with the droplet sizes (i.e., larger droplets were harder to blowout),

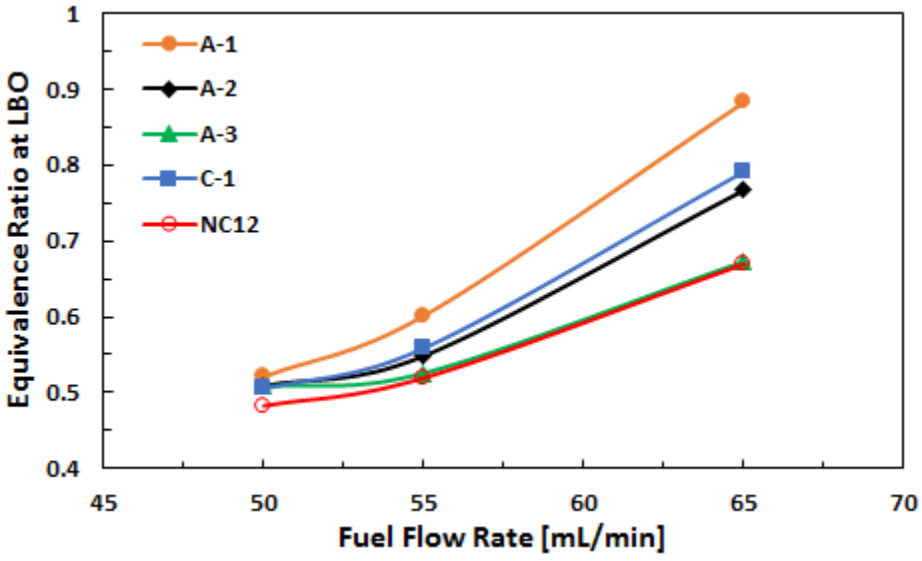

Figure 6.1. Flame BOLs for the tested fuels at different fuel flow rates.

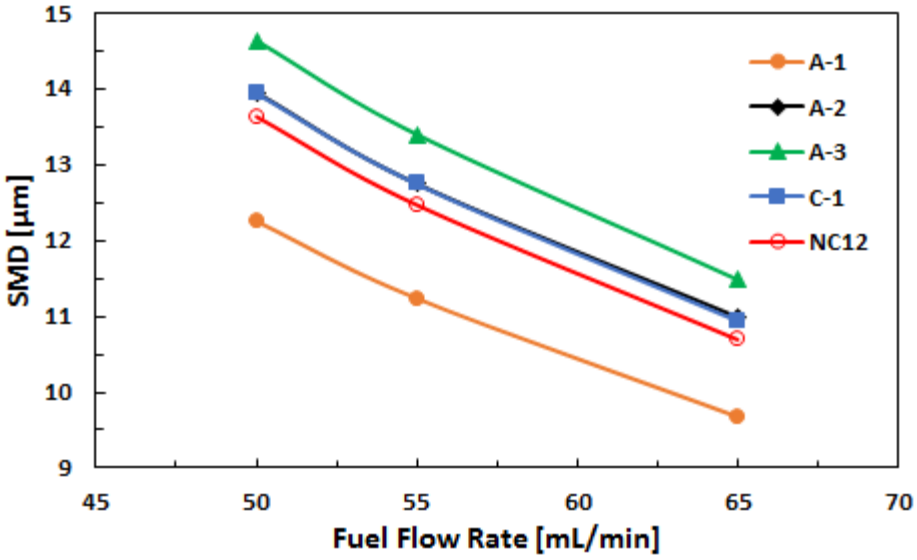

Figure 6.2. Predicted SMDs for the tested fuels using Eq. (1).

suggesting that the liquid fuel loading has a dominant role in controlling the flame blowout. However, NC12 has the best performance, as it features the lowest equivalence ratios. This behavior of NC12 may likely be related to its short ignition delays and low volatility, both of which are important factors for its high DCN, thus the DCN correlates well as noted by Won et al. [10]. To evaluate the influence of the different fuel properties on LBO, a comprehensive analysis is done and will be discussed later in this work. The variation in the slope of the LBO results for the different fuels as the fuel flow rate increases is likely caused by the variation in volatilities and droplet sizes. Thus, it is believed that as the fuel flow rate increases, the droplet sizes, especially for the lighter fuel (easier to evaporate), e.g. A-1, become significantly smaller, resulting in locally and globally fuel lean conditions - as a result, LBO is easier to achieve. In addition, increasing the fuel flow rate can lead to high strain rates, and thus limit the flame stabilization. This behavior was discussed in previous studies, such as [19, 20].

Note that the Sauter mean diameters in Fig. 6.3, which represent the spray droplet sizes, was predicted using a well-known correlation by Lefebvre [21]:

$$\mathrm{SMD}_{Lefebvre} = 2.25\sigma_l^{0.25}\mu_l^{0.25}\dot{m}_l^{0.25}\Delta P^{-0.5}\rho_{air}^{-0.25} \quad (6.2)$$

where σ_l is the liquid surface tension, μ_l is the viscosity, $\dot{m}_l$ is the liquid mass flow rate, ΔP is the pressure drop across the spray nozzle, and ρ_{air} is the surrounding air density. All properties used in the SMD calculations are provided in Table 6.1. The Lefebvre correlation (Eq. (6.2)) provides an insight into the relative differences in the droplet sizes of the different tested fuels, as a result of the variation in their physical properties, such as viscosity, surface tension, and density, and was verified to predict relative difference in droplet sizes for different fuels using ACS burner [22]. In addition, it was used in several related works, e.g., [3, 4].

The influence of each fuel property on the equivalence ratio at LBO is analyzed using individual linear analysis. This approach is inspired by the work of Zheng et al. [8]. The analysis was done for the three different fuel flow rate results, and then the average of the relative importance is taken. This is a helpful way to provide a general perspective of the impacts of fuel

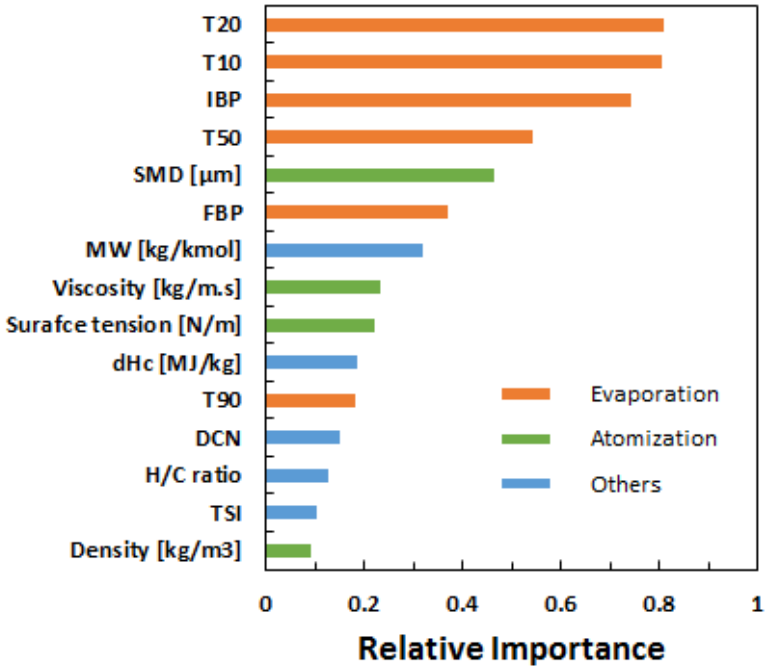

Figure 6.3. Feature importance from the linear individual analysis.

properties and compositions on LBO measured with the ACS burner. Figure 6.4 illustrates the rank of the relative importance of various characteristics, from most significant to least. The results from the analysis suggest that the distillation properties has the highest correlation with the LBO, followed by atomization properties represented by SMD which is influenced by the fuel's physical properties, e.g., viscosity, surface tension, and density, as can be seen in Eq. (6.2).

Multiple regression analysis is then implemented to explain the differences in the blowout results of the tested fuels for the spray burner used here. The regression resulted in the collapse of all LBO data with a linear fit correlation coefficient of 0.94. The resulting correlation can be seen in Eq. (6.3):

$$\emptyset_{\mathrm{LBO}} \propto \frac{\dot{V}_{F,r}^{1.56}}{SMD_r^{0.46}\, T_{50,r}^{0.55}\, \Delta H_{c,r}^{2.3}} \tag{6.3}$$

where subscript r represents quantities relative to the of A-2 (Jet-A), $\dot{V}_{F,r}$ is the fuel flow rate relative to 50 mL/min, SMD is the Sauter mean diameter and was calculated based on Lefebvre correlation (Eq. (6.2)), $T_{50,r}$ is the boiling temperature at 50% distillation curve, and $\Delta H_{c,r}$ is the heat of combustion and both listed in Table 6.2. Figure 6.5 shows the comparison between the measured and predicted LBO based on Eq. (6.3). The predicted correlation (Eq. (6.3)) suggests that the volatility (T_{50}) and droplet sizes (SMD), which enhance the liquid loading into the flame, as well as the chemical reactivity of the fuel, represented by the heat of combustion, are the dominate properties promoting flame stability for the current set of fuels with the ACS burner. As previously noted, this is likely due to differences in the flame regime, where larger droplets, which slow the vaporization, can create local fuel rich regions and elevated temperature which stabilize the flame [3]. Although the results and the analysis of the LBO of ACS burner is consistent with a number of works, such as [3, 4, 6, 7], it is not necessarily true for other combustors (especially

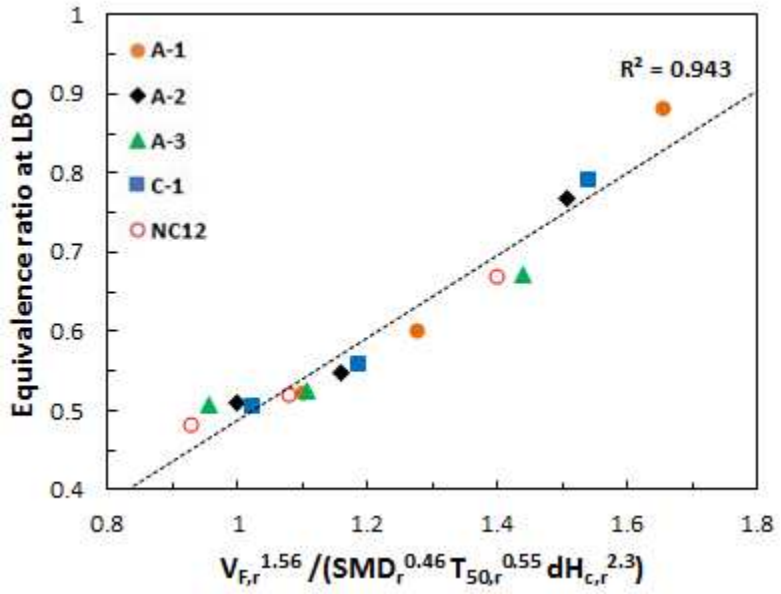

Figure 6.4. Equivalence ratios at LBO as a function of Eq. (6.3) for the different fuels.

ones which use an airblast atomizers, as they are known to be less sensitive to atomization properties relative to pressure atomizers) and test conditions (higher temperature, e.g., 500 K).

6.4.2 LOH Results and Analysis

The flame liftoff height results at three different air flow rates for the five candidates are plotted and shown in Fig. 6.6. In general, larger droplet sizes (as seen in Fig. 6.3) and less volatile fuels (specifically at T50), e.g., A-3, exhibit higher liftoff height. In contrast, A-1 experiences the lowest flame liftoff, which is believed to be caused by its smaller SMD and higher volatility compared to other fuels. This is because the fuels with large droplet sizes and less volatility need more time to evaporate and generate enough vapor to stabilize the flame against the incoming reactant stream. Except for the n-dodecane, the liftoff height behavior of the tested fuels have an opposite trend to the blowout results (Fig. 6.2).

To explain the differences in flame liftoff between the fuels, the data collected (Figs. 6.6) are used in this section. As a first attempt to explain differences in flame liftoff between the fuels, the

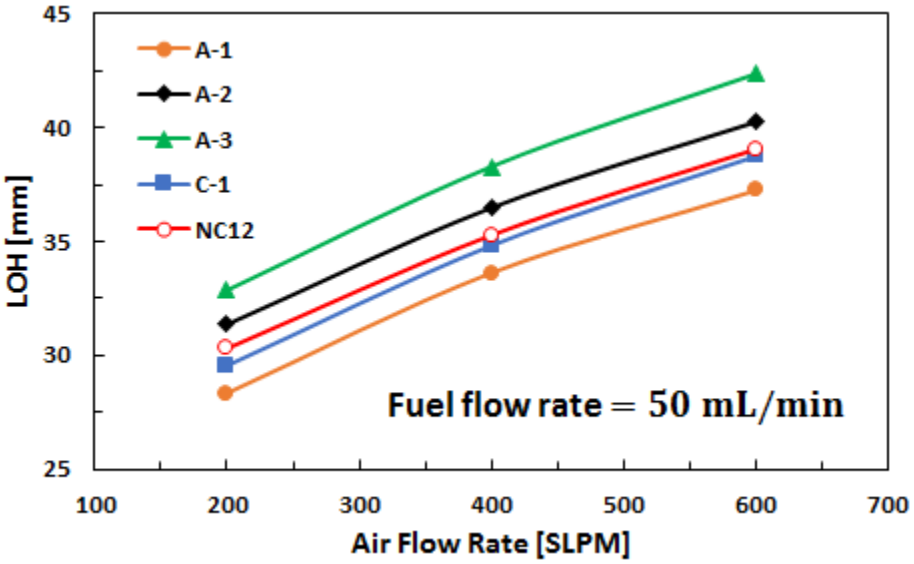

Figure 6.5. LOHs for the tested fuels at constant fuel flow rate and different air flow rates.

gas phase laminar flame speed (S_L) was used, as suggested by many previous works [23, 24]. Thus, the liftoff height (LOH) is plotted with ($V_{co\text{-}flow}/S_L$) in Fig. 6.7. $V_{co\text{-}flow}$ is the air co-flow velocity at the exit of the burner calculated (5.24, 10.48, and 15.72 m/s) for the different air flow rates, e.g., 200, 400, and 600 SLPM, respectively. The laminar flame speeds used in this work are listed in Table 6.1. As seen in Fig. 6.7, normalizing by the laminar flame speed of the fuels resulted in a linear fit correlation coefficient of 0.74. This indicates the need to include time scales associated with vaporization in concert with the gas phase flame speed. Thus, a multiple regression is used and led to a correlation that explains the mechanism which controls the flame liftoff heights of the jet fuels in the ACS burner, as the following:

$$LOH \propto \frac{SMD_r^{0.22}\, T_{50,r}^{0.64}\, V_{coflow,r}^{1.56}}{S_L^{0.44}} \qquad (6.4)$$

where subscript r represents quantities relative to the of A-2 (Jet-A), SMD is the Sauter mean diameter and was calculated based on Lefebvre correlation (Eq. (6.2)), $T_{50,r}$ is the boiling temperature at 50% distillation curve (listed in Table 6.1), $\dot{V}_{co-flow,r}$ is the fuel flow rate relative

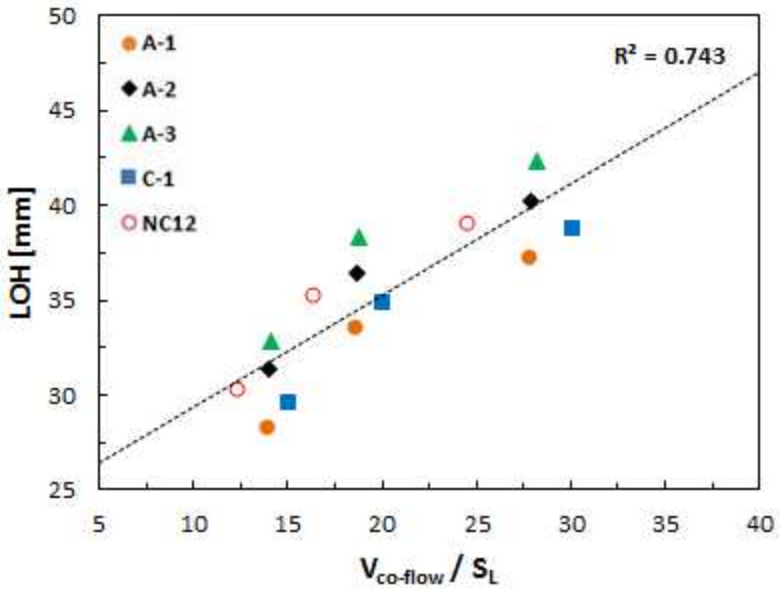

Figure 6.6. Flame liftoff heights (LOH) plotted against Vco-flow/SL for the different fuels.

to 50 mL/min, and $S_{L,r}$ is the laminar flame speed. As seen in Fig. 6.8, normalizing the LOH measurements by Eq. (6.4), which accounts for the two-phase flame speed, resulted in a linear correlation with $R^2 = 0.96$. In fact, the inferred mechanism is similar to the well-known flame-edge mechanism theory, which indicates that the flame stabilizes as a result of a balance between

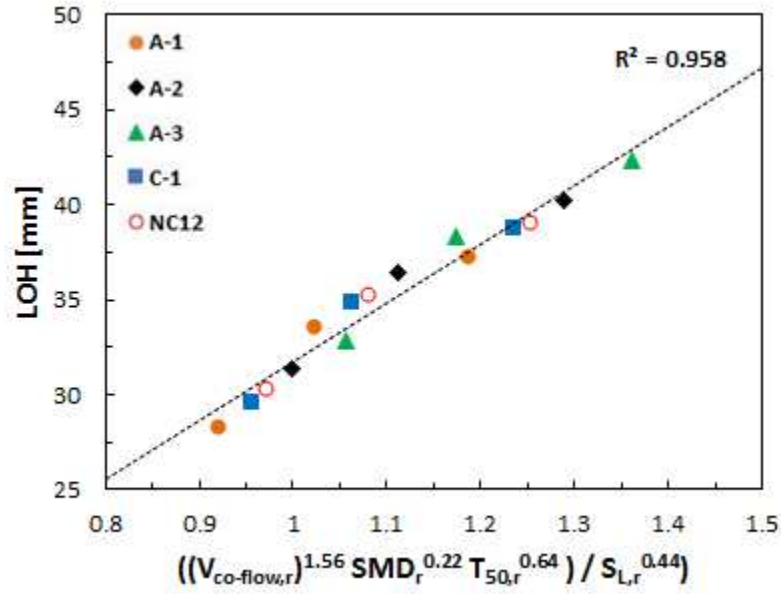

Figure 6.7. Flame liftoff heights (LOH) plotted against Eq. (6.4) for the different fuels.

the local premixed burning velocity and the local jet velocity and at is located where the mixture is at stoichiometric equivalence ratio. In a two-phase spray, however, the flame speed is a function of both the reactivity (S_L) as well as the amount of liquid/gas fuel entering the flame preheat zone.

6.5 Conclusions

An experimental investigation has been carried out to evaluate the influence of jet fuel properties on the flame LBO and LOH using the ACS burner. This is achieved using a comparative statistical analysis to show the relative importance of fuel properties on combustion stability. The results suggest that the LBO of jet fuels in ACS burner is controlled by the fuel liquid loading into the flame. Therefore, a fuel which produces larger droplet sizes and has a lower volatility will achieve flame blowout at lower equivalence ratio. The differences in liftoff height were shown to result from two-phase flame speed, which accounts for both pre-vaporized fuel reactivity (S_L) and time scales associated with droplet evaporation.

The work serves to provide a data foundation, theoretical concepts, and a fair knowledge for the combustion performance of jet fuels. In addition, the ACS burner (or similar platforms) can contribute in the screening of the new alternative jet fuels and aid in their development before the necessary and expensive real engine tests.

References

[1] B. Chèze, P. Gastineau, J. Chevallier, Forecasting world and regional aviation jet fuel demands to the mid-term (2025), Energy Policy 39 (2011) 5147-5158.
[2] M. Colket, J. Heyne, M. Rumizen, M. Gupta, T. Edwards, W.M. Roquemore, G. Andac, R. Boehm, J. Lovett, R. Williams, Overview of the national jet fuels combustion program, AiAA Journal (2017) 1087-1104.
[3] A. Lefebvre, Fuel effects on gas turbine combustion—ignition, stability, and combustion efficiency, Journal of engineering for gas turbines and power 107 (1985) 24-37.
[4] L. Esclapez, P.C. Ma, E. Mayhew, R. Xu, S. Stouffer, T. Lee, H. Wang, M. Ihme, Fuel effects on lean blow-out in a realistic gas turbine combustor, Combustion and Flame 181 (2017) 82-99.
[5] V. Burger, A. Yates, C. Viljoen. Influence of fuel physical properties and reaction rate on threshold heterogeneous gas turbine combustion. In: editor^editors. ASME Turbo Expo 2012: Turbine Technical Conference and Exposition; 2012: American Society of Mechanical Engineers. p. 63-71.
[6] J. Grohmann, B. Rauch, T. Kathrotia, W. Meier, M. Aigner, Influence of Single-Component Fuels on Gas-Turbine Model Combustor Lean Blowout, Journal of Propulsion and Power (2017) 1-11.
[7] E.E. Peiffer, J.S. Heyne, M. Colket, Sustainable Aviation Fuels Approval Streamlining: Auxiliary Power Unit Lean Blowout Testing, AIAA Journal (2019) 1-9.
[8] L. Zheng, J. Cronly, E. Ubogu, I. Ahmed, Y. Zhang, B. Khandelwal, Experimental investigation on alternative fuel combustion performance using a gas turbine combustor, Applied Energy 238 (2019) 1530-1542.
[9] N. Rock, I. Chterev, B. Emerson, S.H. Won, J. Seitzman, T. Lieuwen, Liquid Fuel Property Effects on Lean Blowout in an Aircraft Relevant Combustor, Journal of Engineering for Gas Turbines and Power 141 (2019) 071005-071005-071013.
[10] S.H. Won, N. Rock, S.J. Lim, S. Nates, D. Carpenter, B. Emerson, T. Lieuwen, T. Edwards, F.L. Dryer, Preferential vaporization impacts on lean blow-out of liquid fueled combustors, Combustion and Flame 205 (2019) 295-304.
[11] D.C. Bell, J.S. Heyne, S.H. Won, F.L. Dryer. The Impact of Preferential Vaporization on Lean Blowout in a Referee Combustor at Figure of Merit Conditions. In: editor^editors. ASME 2018 Power Conference collocated with the ASME 2018 12th International Conference on Energy Sustainability and the ASME 2018 Nuclear Forum; 2018: American Society of Mechanical Engineers. p. V001T001A011-V001T001A011.
[12] S. Stouffer, T. Hendershott, J.R. Monfort, J. Diemer, E. Corporan, P. Wrzesinski, A.W. Caswell. Lean Blowout and Ignition Characteristics of Conventional and Surrogate Fuels Measured in a Swirl Stabilized Combustor. In: editor^editors. 55th AIAA Aerospace Sciences Meeting; 2017. p. 1954.
[13] T.F. Guiberti, W.R. Boyette, A.R. Masri, W.L. Roberts, Detachment mechanisms of turbulent non-premixed jet flames at atmospheric and elevated pressures, Combustion and Flame 202 (2019) 219-227.
[14] K.M. Lyons, Toward an understanding of the stabilization mechanisms of lifted turbulent jet flames: experiments, Progress in Energy and Combustion Science 33 (2007) 211-231.
[15] S. Karami, E.R. Hawkes, M. Talei, J.H. Chen, Edge flame structure in a turbulent lifted flame: A direct numerical simulation study, Combustion and Flame 169 (2016) 110-128.

[16] C.J. Lawn, Lifted flames on fuel jets in co-flowing air, Progress in Energy and Combustion Science 35 (2009) 1-30.
[17] J. Buckmaster, Edge-flames and their stability, Combustion Science and Technology 115 (1996) 41-68.
[18] J.T. Edwards. Reference jet fuels for combustion testing. In: editor^editors. 55th AIAA Aerospace Sciences Meeting; 2017. p. 0146.
[19] J. Grohmann, W. O'Loughlin, W. Meier, M. Aigner. Comparison of the Combustion Characteristics of Liquid Single-Component Fuels in a Gas Turbine Model Combustor. In: editor^editors. ASME Turbo Expo 2016: Turbomachinery Technical Conference and Exposition; 2016: American Society of Mechanical Engineers. p. V04AT04A010-V004AT004A010.
[20] R.A. Alsulami, B. Windell, D. Bartholet, B. Windom, Exploring the Role of Physical and Chemical Properties on the Ignition and Flame Stability of Liquid Fuels with a Spray Burner and Fuel Ignition Tester (FIT), 2018 AIAA Aerospace Sciences Meeting, American Institute of Aeronautics and Astronautics2018.
[21] A. Lefebvre, Atomization and sprays, combustion: an international series, Hemisphere Pub. Corp (1989).
[22] R. Alsulami, B. Windell, S. Nates, W. Wang, S.H. Won, B. Windom, Investigating the Role of Atomization on Flame Stability of Liquid Fuels in an Annular Spray Burner, Fuel (2019).
[23] G.D. Myers, A.H. Lefebvre, Flame propagation in heterogeneous mixtures of fuel drops and air, Combustion and Flame 66 (1986) 193-210.
[24] A. Neophytou, E. Mastorakos, Simulations of laminar flame propagation in droplet mists, Combustion and Flame 156 (2009) 1627-1640.

CHAPTER 7: Influence of Physical Properties of Conventional, Alternative, and Surrogate Jet Fuels on Soot Formation in a Spray Flame[6]

7.1 Summary

A Tremendous amount of research has investigated the influence of several parameters, including fuel type, flame strain rate, pressure, and temperature, on soot formation for different gaseous and pre-vaporized fuels. Although these studies have improved understanding regarding the chemical soot formation process, the optimization of the fuels and combustion devices, e.g., liquid-fueled gas turbines, requires the consideration of the two-phase process and the coupling between the complex physical and chemical processes that constitute soot development. The current work investigates the influence of the two-phase spray process, including the atomization and vaporization, on soot volume fraction for three conventional jet fuels (Jet-A, JP-8, and JP-5), an alternative jet fuel (Gevo-ATJ), and n-dodecane. The two-dimensional spatial soot volume fraction is qualitatively measured using Laser-Induced Incandescence (LII). The trends in spray flame soot formation are compared to the gas-phase Yield Sooting Index (YSI). Results indicate differences in planar soot distributions amongst the fuels and suggest a strong correlation between the fuels' boiling behavior (~T50) and Sauter mean diameter (SMD) on the spray flame soot volume fraction pointing to the importance of the atomization and the vaporization processes on mixing and the soot formation.

[6] This chapter is largely based on a manuscript that will be submitted to the 38th International Symposium on Combustion: Alsulami, Radi A., et al. "Influence of Physical Properties of Conventional, Alternative, and Surrogate Jet Fuels on Soot Formation in a Spray Flame." *Proceedings of the Combustion Institute (2020).*

7.2 Introduction

The aviation industry is having to deal with high and volatile fuel costs, increasing emissions regulations, and fuel supply chain insecurity. Soot emissions from commercial and military aircraft have a significant impact on human health and global climate. These issues can be addressed by the development of alternative jet fuels from renewable and cleaner resources [1]. Because the jet fuels have standard ASTM specifications, any alternative fuel is required to have similar properties, chemistry and thus composition to the existing jet fuel.

To reduce soot emissions and to assess the effect of new alternative fuels on combustion and emissions, we need to better understand the mechanisms that control the soot formation inside liquid-fueled gas turbine engines and how the fuel properties, both the physical (including the properties which influence the atomization and vaporization processes) and chemical, can impact the soot development. Some previous works have studied the influence of the distillation curve and spray droplet sizes on the soot development and reached similar conclusions to the current work. For example, Saggese et al. [2] highlighted the influence of distillate fraction of jet fuels and their surrogates on the soot propensity using number of diffusion flames apparatus, such as counter-flow and co-flow flames. They found that the higher boiling distillates produce substantially more soot in nucleation controlled flames. Hayashi et al. [3] conducted detailed experimental and numerical investigations on the influence of the initial droplet size on a spray flame in a laminar counterflow field. They indicated that increasing the SMD of the fuel spray lead to the expanding of the average soot formation area. Many previous works have investigated the influence of the differences in fuel chemical compositions and structures on sooting tendencies, e.g., [4-11]. These studies have mostly been conducted using counterflow or coflow diffusion flames and use gaseous-fuels as a baseline flame with the injection of low concentration of

vaporized liquid fuels. Although these existing experiments have improved understanding regarding the chemical soot formation, the influence of the two-phase process, which is experienced by liquid fuels in realistic combustion systems, e.g., gas turbine engine, is still not fully understood, as a result of the complex multiphase phenomena.

Therefore, the current work aims to highlight the importance of accounting the influence of the two-phase spray process on the soot development by addressing the following questions: (1) What is the role of the two-phase spray process (namely the atomization and vaporization) on the soot formation? and (2) how physical and chemical properties couple to influence soot formation?

To answer these question, the trends in spray flame soot formation are measured for five jet fuels, three conventional jet fuels (Jet-A (A-2), JP-8 (A-1), and JP-5(A-3)), an alternative jet fuel (Gevo-ATJ (C-1)), and n-dodecane (NC12), using Laser-Induced Incandescence (LII). The results from the two-phase combustion system are compared to the gas-phase Yield Sooting Index (YSI) to highlight the influences from the spray/vaporization process on soot formation.

7.3 Experimental Setup

7.3.1 Facility and Measurements Procedure

A schematic of the experimental configuration utilized for this work can be observed in Fig. 7.1. The laboratory apparatus includes an unconfined Annular Co-flow Spray burner (ACS burner), a pressure atomizer (Delavan 80°, 0.4GPH, B solid spray pattern), air supply, and fuel supply. Air is supplied using an Alicat mass flow controller capable of delivering high air flow rates, up to 3000 SLPM, with an accuracy of ±0.8% of reading and 0.2% of full-scale. Fuel is supplied using a high-pressure syringe pump (ISCO, Model 260D). The fuel and the air are

delivered to the spray burner at a room temperature of 298 K and at laboratory pressure of 0.84 atm. More details can also be found in Chapter 2.

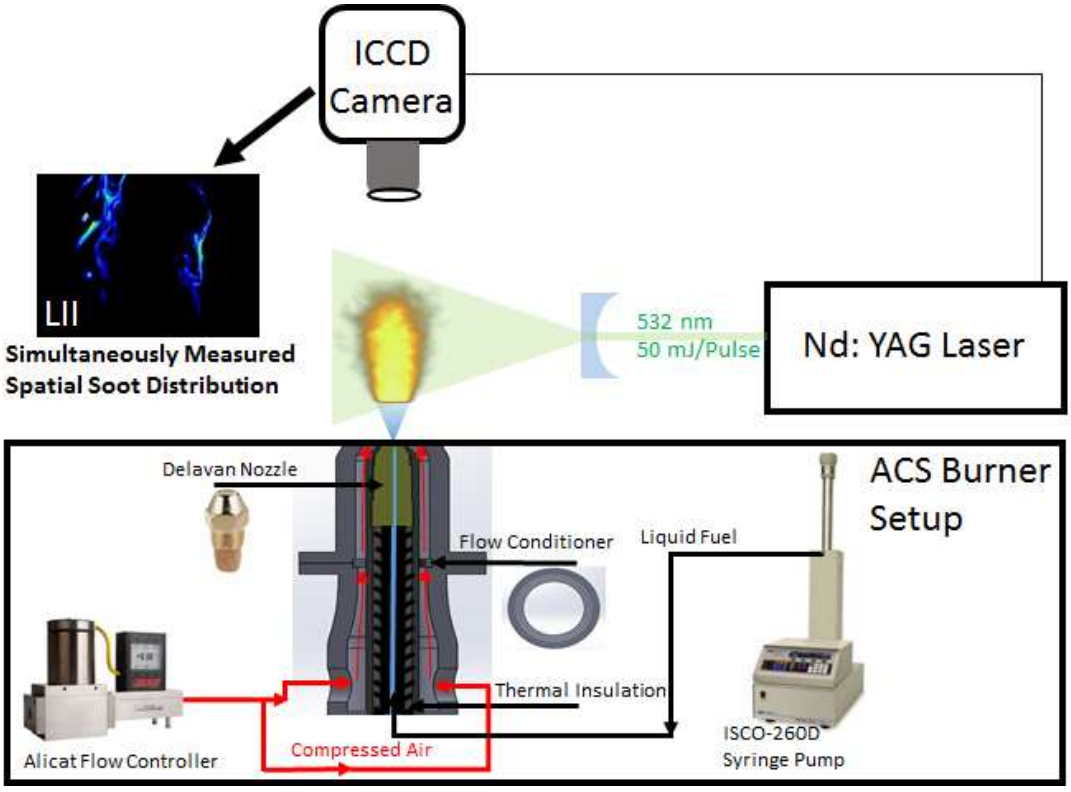

Figure 7.1. Schematic of the laboratory setup and equipment.

The qualitative soot volume fraction (f) was measured using Laser-Induced Incandescence (LII) technique. For these measurements, a pulsed Nd:YAG laser (Continuum Custom laser, @ 532 nm, 50 mJ/pulse, 25 ns pulse width) was used. The signal intensity of the LII is influenced by the energy of laser pulse, as mentioned in Ni et al. [14]. Thus, the energy of 50 mJ/pulse was used with all tested fuels to achieve adequate LII signal intensity without resulting in soot ablation. The laser sheet was formed by expanding the laser beam vertically using a series of cylindrical lenses prior to entering the spray and was aligned in the center of the burner with height of ~160 mm.

The LII signal was detected using an intensified CCD camera orientated 90° from the incoming laser sheet (Andor iCMOS) synchronized with the laser. A delay of 145 ns and a gate width of 10 ns was applied, found to provide optimal signal to noise. These specific times were selected to avoid/minimize the interference of the liquid spray and the flame and were sufficient in providing strong LII signals for all the fuels investigated in this study.

Table 7.1. Physical and chemical properties of candidate fuels.

Fuel name	**(A-1), JP-8 POSF 10264**	**(A-2), Jet-A POSF 10325**	**(A-3), JP-5 POSF 10289**	**(C-1), Gevo-ATJ**	**(NC12), n-dodecane**
Fuel description	Low viscosity	Nominal jet fuel	High viscosity	Low DCN	High DCN
MW [Kg/Kmol]	152	159	166	178	170.33
ΔH_c [MJ/kg]	43.24	43.06	42.88	43.88	44.11
DCN	48.8	48.3	39.2	17.1	72.90
TSI	16.5	25.5	32.5	15.6	7
H/C ratio	1.99	1.91	1.89	2.17	2.17
Smoke point [mm]	28.5	23	20	29	137
Aromatic, vol%	11.2	17	18	1	0
ρ at 25 °C [kg/m^3]	772.14	795.57	819.09	751.74	746.60
μ at 25 °C [kg/m.s]	0.001049	0.001645	0.001924	0.001552	0.001276
σ at 25 °C [N/m]	0.02382	0.02468	0.02436	0.02254	0.024939
ASTM D86 Distillation					
IBP (°C)	145	159	174	173	216.2
10% (°C)	164	176	192	178	216.2
20% (°C)	171	184	199	179	216.2
50% (°C)	189	205	218	182	216.2
90% (°C)	234	244	244	228	216.2
FBP (°C)	256	269	258	263	216.2

To predict the relative soot formation between the different fuels, 150 consecutive images were collected, the background subtracted, and then averaged. Because the background intensities were slightly different for the tested fuels, the mean background intensity was measured for each fuel. The soot volume fractions, which are reported in this work, are the averaged soot value over the entire image.

7.3.2 Fuels

Similar to Chapter 6, total of five fuels were used, including three conventional jet fuels, (Jet-A (A-2), JP-8 (A-1), and JP-5 (A-3)), one alternative jet fuel, (Gevo-ATJ (C-1)), and n-dodecane (NC12). These fuels were specifically selected to cover a wide range of physical, volatility, and chemical properties. For example, the differences in physical properties, specifically viscosity (which impacts the Sauter mean diameter (SMD)) and distillation, between the three conventional fuels allow for insight into how these properties impact soot formation. The Gevo-ATJ provides a means to evaluate the influence of the unusual boiling range on soot, even though previous work has shown this fuel to be cleaner than the A fuel types when it is tested in pre-vaporized diffusion flame burner [15, 16]. In addition, ATJ and n-dodecane are also used in this study to investigate the influence of the absence of aromatics in the fuel on the formation of soot. The properties for the candidate fuels evaluated in this study are shown in Table 7.1. Detailed properties of the conventional and alternative jet fuels are provided by Edwards [17].

The experiments were carried out in a laboratory environment, T= 298 K ± 5 K and P= 0.84 atm. For all tests the fuel flow rate is kept constant at 50 mL/min and the air flow rate at 500 SLPM. The reason for using the same flow rates, and not similar equivalence ratios, is to keep the influence of turbulence and thus the mixing similar for the different fuels. For these conditions, the global equivalence ratio is calculated and are provided in Table. 7.2. Since this study is mainly

focused on investigating the influence of the two-phase spray on soot formation, the Sauter mean diameters (SMD), which represent the spray droplet sizes, were predicted using a well-known correlation by Lefebvre [18]:

$$\mathrm{SMD}_{Lefebvre} = 2.25\sigma_l^{0.25}\mu_l^{0.25}\dot{m}_l^{0.25}\Delta P^{-0.5}\rho_{air}^{-0.25} \quad (7.1)$$

where σ_l is the liquid surface tension, μ_l is the viscosity, $\dot{m}_l$ is the liquid mass flow rate, ΔP is the pressure drop across the spray nozzle, and ρ_{air} is the surrounding air density. All properties used in the SMD calculations are provided in Table 7.1. The Lefebvre correlation (Eq. (7.1)) provides an insight into the relative differences in the droplet sizes of the different tested fuels, as a result of the variation in their physical properties, such as viscosity, surface tension, and density, and was verified to predict relative difference in droplet sizes for different fuels using ACS burner [19]. In addition, it was used in several related works that have studied jet fuels, e.g., [20, 21]. The predicted SMDs of the tested fuels are listed in Table. 7.2.

Table 7.2. Calculated SMD and equivalence ratio of the tested fuels.

Fuel	A-1	A-2	A-3	C-1	NC12
SMD [µm]	12.25	13.95	14.63	13.94	13.63
Equivalence ratio	1.17	1.20	1.23	1.16	1.15

7.4 Results and Discussion

The soot volume fraction for the tested fuels are plotted relative to Jet-A (A-2) fuel, as shown in Fig. 7.2. It is seen that A-3 produces two times more soot than A-2. Comparing to the other fuels, A-1 generates the lowest soot, followed by C-1. Although the threshold sooting index (TSI) of pre-vaporized n-dodecane indicates that it is the cleanest among the tested fuels, the soot formation of the two-phase spray of NC12 shows an opposite trend. This highlights the importance

of considering the atomization, vaporization, and the mixing processes in understanding soot formation.

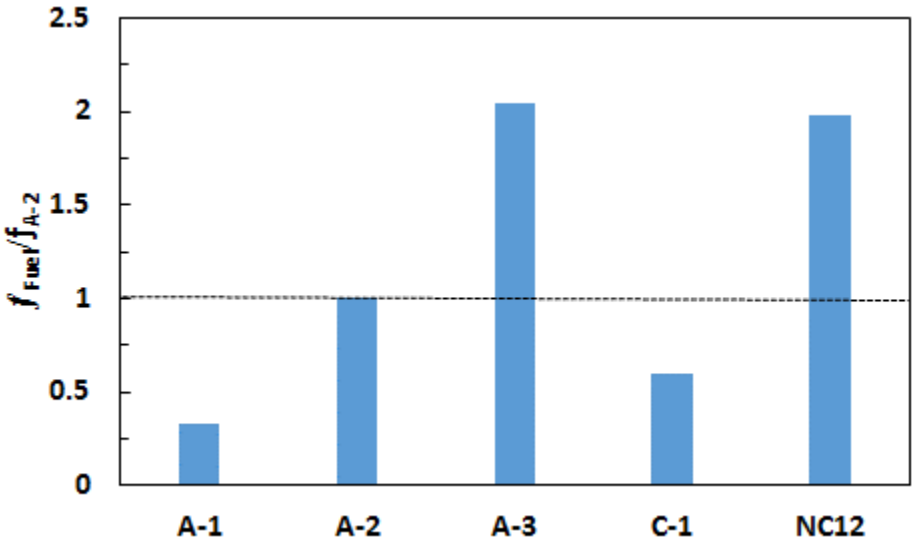

Figure 7.2. Relative soot volume fraction for all tested fuels.

To better evaluate the influence of the spray process on soot emissions, the results of the three conventional fuels have been benchmarked against their results in the gas phase (YSI and TSI), as illustrated in Fig. 7.3. Again, the results are plotted relative to A-1. The YSI and TSI increases as we go from A-1 to A-3, as a result of increasing the aromatic content, as discussed by Dhrubajyoti D. et al. [22]. However, the YSI and TSI growth is much less than that measured in the spray flame experiment. The less volatile and larger fuel, e.g., A-3, produces the highest soot. Opposite result is observed for A-1 as it generates the smallest SMD and it is the most volatile fuel among the reference fuels. This evidence indicates that pre-vaporized measurements, e.g. the YSI and TSI, may not capture all the important phenomenon that control soot formation in a realistic liquid-fueled engine.

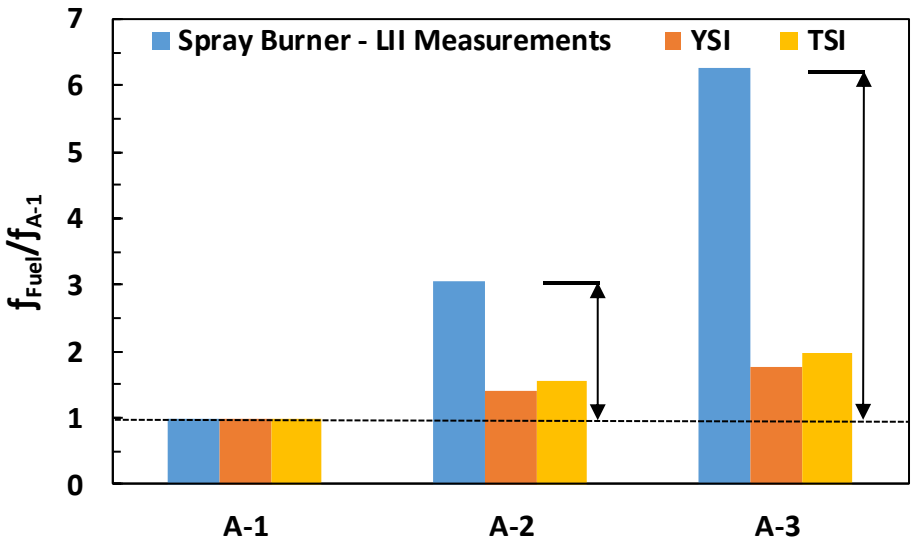

Figure 7.3. Relative soot volume fraction for all conventional jet fuels.

To understand the influence of fuel properties, especially the physical properties, on the soot volume fraction in the spray flame, the data collected for all tested fuels using the ACS burner (Fig. 7.2) were subjected to a multiple regression analysis, which resulted in the identification of a correlation which predicted the relative soot fraction:

$$f = 4.86 \text{ X } 10^{-13} \text{ TSI}^{0.39} \text{ SMD}^{2.1} \text{ T50}^{8.05} \quad (7.2)$$

where TSI is the threshold sooting index, SMD is the Sauter mean diameter, and T50 is the boiling temperature at 50 vol% distilled. All the values of these variables are listed in Tables 7.1 and 7.2. Figure 7.4 shows the comparison between the measured and predicted soot volume fraction and an excellent agreement was achieved. It was noticed that the T20 has significant influence on the soot formation followed by the SMD, and TSI, suggesting that the volatility and the droplet sizes (SMD) are the dominate properties influencing the soot formation in the spray flame. Although the relation between the fuels physical properties were found to be highly influential on the soot formation for the ACS burner, it should be noted that different trends may be present for other combustors with different operation conditions, e.g., high temperature and pressure, and different

atomizer technology, such as an airblast atomizer, which is known to be less sensitive to the atomization property relative to a pressure atomizer used in this work [23].

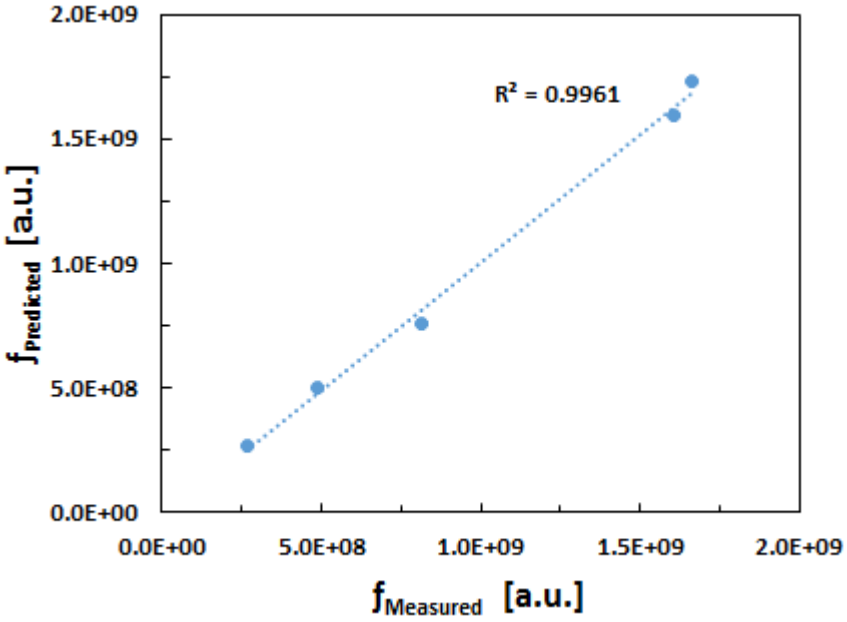

Figure 7.4. Comparison between measured and predicted (using Eq. (3)) soot volume fractions for all tested fuels.

7.5 Conclusions

An experimental investigation has been conducted to investigate the influence of the two-phase spray process, including the atomization and vaporization, on the soot volume fraction for three conventional jet fuels (Jet-A, JP-8, and JP-5), an alternative jet fuel (Gevo-ATJ), and n-dodecane. The two-dimensional spatial soot volume fraction is qualitatively measured using Laser-Induced Incandescence (LII). The results indicate differences in planar soot distributions amongst the fuels and suggest a strong correlation between the fuels' boiling behavior (~T50) and its droplet size (SMD) on the spray flame soot volume fraction. These observations highlight the importance of the atomization and the vaporization processes on mixing and subsequently soot formation and suggest that these properties be included when considering the soot potential of new alternative jet fuels.

References

[1] T.M. Lovestead, J.L. Burger, N. Schneider, T.J. Bruno, Comprehensive assessment of composition and thermochemical variability by high resolution GC/QToF-MS and the advanced distillation-curve method as a basis of comparison for reference fuel development, Energy & Fuels 30 (2016) 10029-10044.
[2] C. Saggese, A.V. Singh, X. Xue, C. Chu, M.R. Kholghy, T. Zhang, J. Camacho, J. Giaccai, J.H. Miller, M.J. Thomson, C.-J. Sung, H. Wang, The distillation curve and sooting propensity of a typical jet fuel, Fuel 235 (2019) 350-362.
[3] J. Hayashi, H. Watanabe, R. Kurose, F. Akamatsu, Effects of fuel droplet size on soot formation in spray flames formed in a laminar counterflow, Combustion and Flame 158 (2011) 2559-2568.
[4] M. Saffaripour, P. Zabeti, M. Kholghy, M.J. Thomson, An experimental comparison of the sooting behavior of synthetic jet fuels, Energy & Fuels 25 (2011) 5584-5593.
[5] M. Saffaripour, A. Veshkini, M. Kholghy, M.J. Thomson, Experimental investigation and detailed modeling of soot aggregate formation and size distribution in laminar coflow diffusion flames of Jet A-1, a synthetic kerosene, and n-decane, Combustion and Flame 161 (2014) 848-863.
[6] M. Saffaripour, M. Kholghy, S. Dworkin, M. Thomson, A numerical and experimental study of soot formation in a laminar coflow diffusion flame of a Jet A-1 surrogate, proceedings of the combustion institute 34 (2013) 1057-1065.
[7] D. Witkowski, K. Kondo, G. Vishwanathan, D. Rothamer, Evaluation of the sooting properties of real fuels and their commonly used surrogates in a laminar co-flow diffusion flame, Combustion and Flame 160 (2013) 1129-1141.
[8] A.G. Mouis, T.A. Litzinger, Y. Wang, V. Iyer, S. Iyer, M. Linevsky, R.J. Santoro, V. Katta, Effects of a JP-8 surrogate and its components on soot in laminar, N2-diluted ethylene co-flow diffusion flames from 1 to 5 atm, Combustion and Flame 162 (2015) 1987-1995.
[9] C.S. McEnally, L.D. Pfefferle, Improved sooting tendency measurements for aromatic hydrocarbons and their implications for naphthalene formation pathways, Combustion and Flame 148 (2007) 210-222.
[10] D.D. Das, C.S. McEnally, L.D. Pfefferle, Sooting tendencies of unsaturated esters in nonpremixed flames, Combustion and Flame 162 (2015) 1489-1497.
[11] M.J. Montgomery, D.D. Das, C.S. McEnally, L.D. Pfefferle, Analyzing the robustness of the yield sooting index as a measure of sooting tendency, Proceedings of the Combustion Institute 37 (2019) 911-918.
[12] R. Alsulami, S. Nates, W. Wang, H.W. Won, B. Windom. Effects of varying liquid fuel and air co-flow rates on spray characterisation of an annular co-flow spray burner. In: Proceedings of the ASME Turbo Expo 2019: Turbomachinery Technical Conference and Exposition GT2019; 2019; Phoenix, Arizona, USA.
[13] R.A. Alsulami, B. Windell, D. Bartholet, B. Windom, Exploring the Role of Physical and Chemical Properties on the Ignition and Flame Stability of Liquid Fuels with a Spray Burner and Fuel Ignition Tester (FIT), 2018 AIAA Aerospace Sciences Meeting, American Institute of Aeronautics and Astronautics2018.
[14] T. Ni, J. Pinson, S. Gupta, R. Santoro, Two-dimensional imaging of soot volume fraction by the use of laser-induced incandescence, Applied Optics 34 (1995) 7083-7091.

[15] X. Xue, X. Hui, P. Vannorsdall, P. Singh, C.-J. Sung, The blending effect on the sooting tendencies of alternative/conventional jet fuel blends in non-premixed flames, Fuel 237 (2019) 648-657.
[16] X. Xue, X. Hui, P. Singh, C.-J. Sung, Soot formation in non-premixed counterflow flames of conventional and alternative jet fuels, Fuel 210 (2017) 343-351.
[17] J.T. Edwards. Reference jet fuels for combustion testing. In: editor^editors. 55th AIAA Aerospace Sciences Meeting; 2017. p. 0146.
[18] A. Lefebvre, Atomization and sprays, combustion: an international series, Hemisphere Pub. Corp (1989).
[19] R. Alsulami, B. Windell, S. Nates, W. Wang, S.H. Won, B. Windom, Investigating the Role of Atomization on Flame Stability of Liquid Fuels in an Annular Spray Burner, Fuel (2019).
[20] A. Lefebvre, Fuel effects on gas turbine combustion—ignition, stability, and combustion efficiency, Journal of engineering for gas turbines and power 107 (1985) 24-37.
[21] L. Esclapez, P.C. Ma, E. Mayhew, R. Xu, S. Stouffer, T. Lee, H. Wang, M. Ihme, Fuel effects on lean blow-out in a realistic gas turbine combustor, Combustion and Flame 181 (2017) 82-99.
[22] D.D. Das, C.S. McEnally, T.A. Kwan, J.B. Zimmerman, W.J. Cannella, C.J. Mueller, L.D. Pfefferle, Sooting tendencies of diesel fuels, jet fuels, and their surrogates in diffusion flames, Fuel 197 (2017) 445-458.
[23] E.E. Peiffer, J.S. Heyne, M. Colket, Sustainable Aviation Fuels Approval Streamlining: Auxiliary Power Unit Lean Blowout Testing, AIAA Journal (2019) 1-9.

CHAPTER 8: Conclusions

The objective of this dissertation was focused on understanding the coupling between the physical and chemical properties of single and multicomponent liquid fuels on flame stability, e.g., flame liftoff height (LOH) and lean blowout limit (LBO), and PM formation. In addition, this work investigates the role of spray processes, including atomization and vaporization (preferential vaporization in multi-component fuels), on flame behaviors and stability. Moreover, this understanding, which uses a fundamental experiment-based approach, will help in the advancement of surrogate fuels formulation, as well as, accelerating the implementation of alternative fuels with smaller carbon footprints. The work in this dissertation has made strong contributions towards understanding the mechanisms which control flame liftoff height and blowout limit of single component, multiple component, alternative jet and conventional jet fuels in a spray flame using laboratory spray burner (ACS Burner). This chapter includes a summary of these contributions, as well as a set of recommendations for future work.

8.1 Summary

As a first step to understand the role of physical and chemical properties of single and multicomponent fuels on spray processes, flame stability, and emissions, the Annular Co-flow Spray Burner (ACS Burner) was designed and manufactured. This laboratory burner, with its small pressure injector and lack of swirler, is shown to have a relatively similar results to that of Georgia Institute of Technology (GIT) gas turbine combustor, with higher data throughput and lower cost. Thus, the ACS Burner (or similar platforms) can contribute in the screening of the new alternative jet fuels and aid in their development before the necessary and expensive real engine tests. The atomization process in this work (similar to previous works) is represented by the Sauter mean

diameter (SMD) which was predicted by three correlations, including the well-known Lefebvre correlation. The predicted SMDs was then verified using measurements from LDV/PDPA along with other spray characterizations, e.g., droplet velocity, turbulence, and distribution.

Because the majority of the previous works have formulated surrogates by emulating the gas-phase combustion stability of the real fuels, the first contribution of this dissertation was to examine the influence of the two-phase spray processes on flame stability. It was shown in this study that the atomization and fuel volatility has a strong influence on flame stability, represented by flame liftoff height (LOH) and lean blowout limit (LBO). The less volatile/heavier fuels have higher liftoff heights, while the fuels with smaller droplet sizes and higher volatility were easier to blowout than less volatile fuels and those which atomize into larger droplets. However, in cases in which there is poor atomization, which produces much larger droplets as a result of decreasing fuel pressure/flow rate, it was observed that the flame would blowout at higher equivalence ratios (i.e., extinguish more easily). In addition, high fuel flow rate, i.e., higher than 65 mL/min for the current burner, generates extremely small droplets, leading to pre-mixed local fuel lean regions, also leading to blowout more easily. Therefore, it was concluded that as a result of the fuels physical properties differences, especially in density, viscosity, and surface tension, each tested fuel has an optimal atomization regime where best performance (i.e., low equivalence ratio at LBO) can be achieved.

Since the hydrocarbon species used in this study possess very different physical properties, the atomization process and the resulting droplet size are affected. Variation in droplet size influences the droplet lifetimes and the amount of liquid, which penetrates the flame, and thus the flame stability. To remove this influence from flame LOH and LBO measurements, each fuel was tested with a selected nozzle orifice size to maintain a consistent spray droplet diameter and distribution

(i.e., SMD and SDD). When the atomization process was controlled, more similar liftoff heights and blowout limits for the set fuels where observed as compared to the results from the common nozzle approach highlighting the importance of the atomization process on the flame stability.

To explore the role of multi-component evaporation on flame stability, measurements were taken for binary fuel mixtures in a pre-vaporized counterflow burner and a spray fueled burner. A correlation derived to predict the gas phase extinction behavior was used to determine two mixtures with identical gas phase extinction strain rates, but with opposite trends in the volatility of the reactive species. Despite having similar gas phase extinction limits, when utilized in the spray burner experiments while maintaining a constant droplet size, the mixtures exhibited different stability behaviors marked by flame liftoff and blowout limits. These results suggest that Vapor-Liquid Equilibrium (VLE) and atomization/vaporization dynamics (and preferential vaporization) can influence flame stability in liquid fueled applications and should be carefully considered in surrogate fuel development activities. Additional future investigation will be needed to more clearly test the hypothesis that preferential vaporization can influence the combustion of liquid multicomponent fuels.

After gaining a clear understanding of the role of physical and chemical properties of single fuels and simple mixtures on spray processes and flame stability, complex fuels (alternative and conventional jet fuels) are used to testify if same conclusions will be achieved. In general, similar results were noticed to that of single fuels - the fuel which produces larger droplet sizes and has a lower volatility (high T_{50}) exhibit higher LOH and blowout at lower equivalence ratios. At low fuel flow rates, e.g., 40 mL/min, the heaver fuel (high T_{50}) can be poorly atomized resulting in blowout at higher equivalence ratios.

Because of the complexity of heterogeneous spray flame phenomena, which arises from the interconnection of a number of processes such as atomization, vaporization, and chemical kinetics, to the best of my knowledge, none of the previous work has developed correlations for spray flame liftoff heights and the fuel's physical and chemical properties. Thus, the present research has addressed a gap in the literature by defining the mechanism which control liftoff height for spray flames surrounded by an annular air co-flow. It was shown that the differences in liftoff height was a result of two-phase flame speed, which accounts for both pre-vaporized fuel reactivity defined by laminar flame speed (S_L) and time scales associated with droplet evaporation. In addition, it was found that the differences in blowout for the current burner and set of fuels was largely tied to fuel volatility and droplet size (SMD) (i.e., liquid loading to flame) along with heat release.

Finally, the influence of the two-phase spray processes, including the atomization and vaporization, on soot volume fraction of the complex fuels is measured using Laser-Induced Incandescence (LII). The results suggest a strong correlation between the fuels' boiling behavior (~T50) and Sauter mean diameter (SMD) on the spray flame soot volume fraction pointing to the importance of the atomization and the vaporization processes on mixing and the soot formation.

This work has shown that the physical and chemical properties of the fuel can influence the two-phase processes, and thus flame stability and emissions. Therefore, these processes should be carefully considered, when alternative and surrogate fuels are tested and developed. In addition, it was concluded that The ACS burner (or similar platforms) can contribute in the screening of the new alternative jet fuels and aid in their development before the necessary and expensive real engine tests. Continued development of these low cost screening platforms should be carried out to aid the development and introduction of renewable jet fuels.

8.2 Recommendations for Future Work

The ACS Burner in its current implementation, with its small pressure injector and lack of swirler, has shown promising potential for studying the effect of liquid fuel properties, as well as, the atomization and vaporization process on flame stability. Thus, adding swirl and using airblast nozzle would be valuable to understand their influence on the flame stability compared to the current flow and pressure nozzle setup. Combustion process in realistic gas turbine occurs at elevated pressure and the flame LBO, which we are interested in, occurs at pressure of ~3 atm, thus pressurizing the burner could provide insights on the influence of pressure on flame stability and if this has an impact on the relative lean blowout of the different tested fuels (e.g., different alternative and conventional jet fuels).

To clearly test the hypothesis that said preferential vaporization can influence the combustion of liquid petroleum fuels, another approach is recommended to be used by designing a set of two multi-component fuels with similar distillation curves, droplet sizes and gas phase ignition characteristics (e.g. similar ignition delays (IDs) when RCM is used over a wide range of pressure, temperature, and equivalence ratios). The RCM gas phase ignition delays will be compared with IDs of FIT at similar conditions. It is expected that the results will show differences in the two-phase ignition delays (in FIT) despite there being little differences in the ignition dynamics of the fuel in gaseous phase (as confirmed by the RCM measurements). Results will also show which conditions increase susceptibility to preferential evaporation effects and will provide a procedure to aid in the selection of fuel surrogates, which account for these previously neglected interactions.

The impact of local enrichment was noticed to have a major effect on the blowout out limit of the tested fuels. More investigation regarding the influence of local enrichment on flame ignition and stability is needed. This can be done by gathering simultaneous Planar Laser Induced

Fluorescence images of the OH radicals (OH-PLIF) and Particle image velocimetry (PIV) data for two different fuel flow rate blowout conditions. The laser technique would provide insight into the local regions flow field and the locations of the radicals' pool, which are responsible for sustaining the flame.

Appendix A: Supplementary material (Chapter 3)

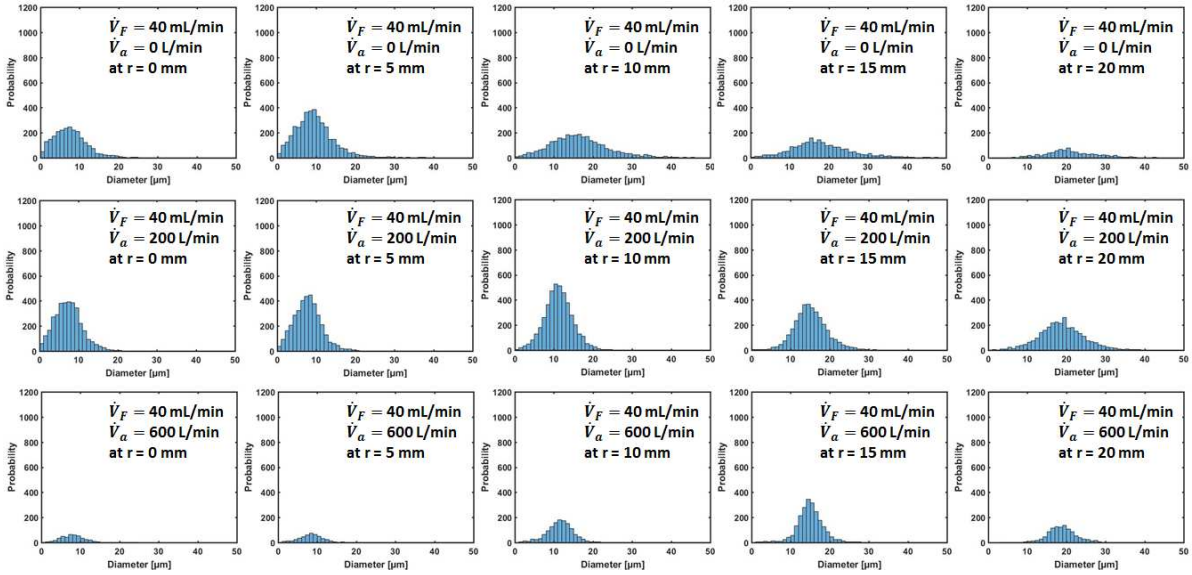

Figure A.1. Histograms of spray droplet size distributions of constant fuel flow rate of 40 mL/min, and at three different air co-flow rates of 0, 200, and 600 L/min, and at axial position of 40 mm. The histograms from left to right represent PDF of different radial positions, i.e., r = 0, 5, 10, 15, and 20 mm.

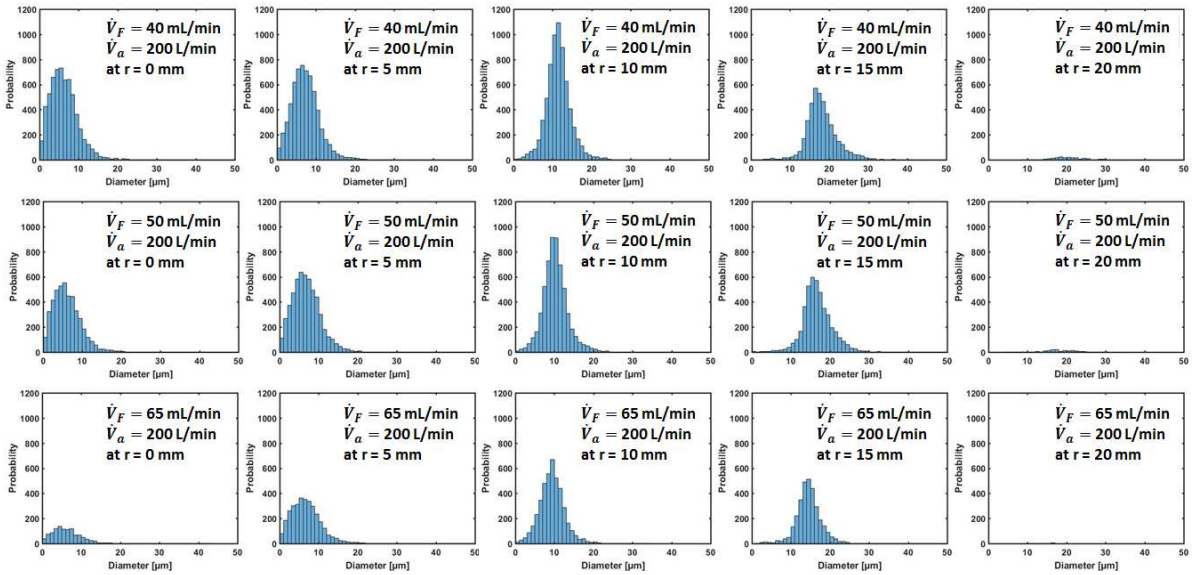

Figure A.2. Histograms of spray droplet size distributions of constant air flow rate of 200 L/min, and at three different fuel flow rates of 40, 50, and 65 mL/min, and at axial position of 20 mm. The histograms from left to right represent PDF of different radial positions, i.e., r = 0, 5, 10, 15, and 20 mm.

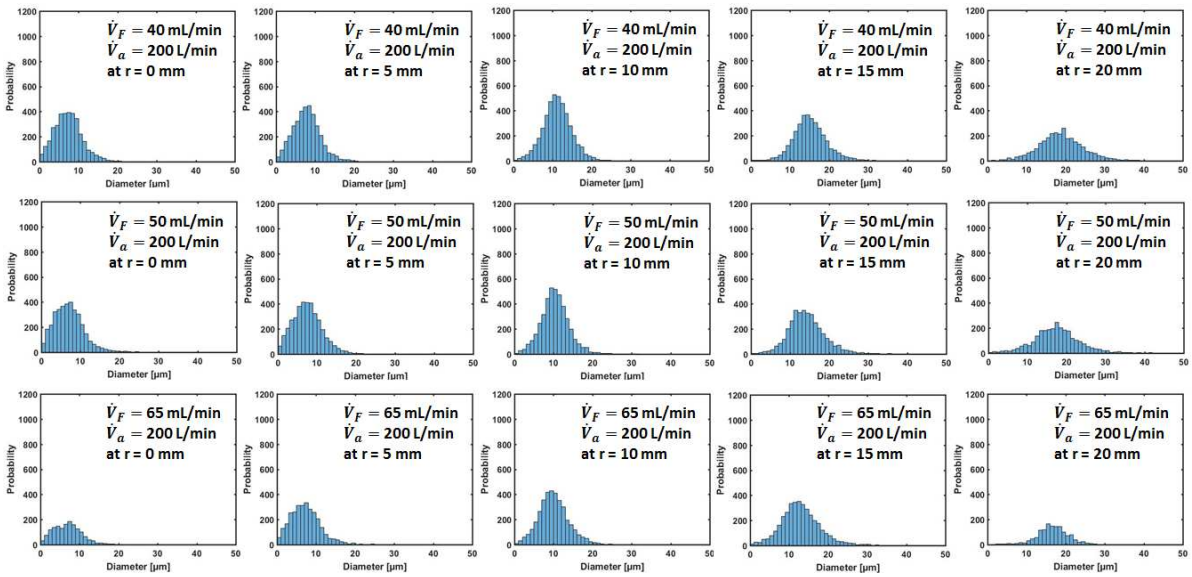

Figure A.3. Histograms of spray droplet size distributions of constant air flow rate of 200 L/min, and at three different fuel flow rates of 40, 50, and 65 mL/min, and at axial position of 20 mm. The histograms from left to right represent PDF of different radial positions, i.e., r = 0, 5, 10, 15, and 20 mm.